



Joining chemically incompatible materials for fused deposition modeling

Master thesis of Klaas Jan van der Vlist

Supervisors: Zjenja Doubrovski and Tim Kuipers
Master program: Integrated Product Design
March 2021

Summary

This report shows the development of a method that joins two chemically incompatible materials during Fused Deposition Modelling (FDM).

Introduction

State of the art FDM printers can extrude more than one material during the printing process. Due to chemical incompatibility of many polymers, the selection for combining materials is limited. This gives the following goal:

“Generate a method to create a dual material object, made of two chemically incompatible materials during the FDM production process”.

Related Work

Studies related to multi-material FDM printing are discussed to find a starting point of this project. The use of a form interlocking shape to join the two chemically incompatible materials is chosen for further investigation.

Proposed Concept

The concept is a form interlocking shape. This shape consists of rows of bridges made of polylactic acid (PLA, rigid material). Thermoplastic urethane (TPU, flexible material) is extruded under and around these bridges to create an interlocking shape. The PLA bridges are created using a non-planar printing approach. As opposed to the regular FDM process (planar), we created a continuous bead across multiple layers (non-planar). A prosthetic hand is created for demonstrating the method. The PLA main body and phalanges are connected with TPU links to allow bending of the fingers.

Design Challenges

This chapter elaborates on the challenges of the concept. We focused on the criteria: strength, applicability and process continuity. Based on these criteria, we made design choices regarding form interlocking shape, printing procedure and sequence, size and geometry and slicing software.

Evaluation

We created specimens for determining the force-displacement relationship and used the peak force as a measure of the interface performance. The proposed concept (bridge pattern) is tested against two benchmarks: the overlapping feature

available in slicer Cura (current industry standard) and an interlocking shape printed using a planar approach. Our proposed concept resulted in a higher peak force than the overlapping feature: 491N compared to 415N, an increase of 18%. The planar interlocking shape resulted in a peak force of 504N, even higher than our proposed concept.

Applications

This production method is relevant for multi-material products manufactured with FDM. Examples are given of products in robotics and prosthetics, compliant mechanisms and wearables. The prosthetic hand was chosen as a demonstrator. A qualitative evaluation was performed on this prosthetic hand: using manual force only, neither the interface bond or the materials (PLA and TPU) could be broken.

Conclusion & Discussion

We have shown a method that creates a stronger bond (vertical interface) between two chemically incompatible materials (PLA and TPU) than the current industry standard.

Glossary

AM – Additive Manufacturing.

CAD – Computer Aided Design.

Cura – A slicer developed by Ultimaker B.V.

FDM – Fused Deposition Modeling. A 3D printing method.

GCode – A file format used by an FDM printer. It contains commands that the printer is able to read in order to create a 3D model.

Interface – The surface where two (chemically incompatible) materials touch.

PLA – Polylactic Acid. A rigid polymer. One of the most commonly used materials in FDM printing.

Slicer – Software that creates GCode. A 3D model is imported. The slicer transforms the 3D model into a toolpath. The user can adjust parameters for the desired performance and production time.

STL – Standard Tessellation Language. A file format imported into slicer software. It contains 3D data of the 3D model.

Toolpath – The path that the printing head follows to create the desired 3D model.

TPU – Thermoplastic Urethane. A flexible polymer.

Table of contents

Summary	2
1: Introduction	9
1.1 – Fused Deposition Modeling	
1.2 – FDM printing workflow	
1.3 – Interlayer vs intralayer bonding	
1.4 – State of the art FDM printing	
1.5 – Compatibility of different polymers	
1.6 – Problem definition	
2: Related Work	15
2.1 – Process parameter optimization	
2.2 – Additional manufacturing technique or hardware	
2.3 – Mechanical interlocking	
2.4 – Interim conclusions	
3: Proposed Concept	19
3.1 – Joining method	
3.2 – Prosthetic hand	
4: Design Challenges	25
4.1 – Criteria	
4.2 – Form interlocking shape	
4.3 – PLA bridge pattern	
4.4 – TPU grids	
4.5 – Bonding strength	
4.6 – Slicing software	
5: Evaluation	35
5.1 – Test method	
5.2 – Benchmarks	
5.3 – Testing	
6: Applications	51
6.1 – Applications	
6.2 – Demonstrator	
7: Conclusion and Discussion	55
8: References	58

Appendix A: Printing parameters of overhanging PLA bridges	62
Appendix B: Ideation phase	63
Appendix C: Literature review	73
Appendix D: Hacksaw concept model	75
Appendix E: Extrusion modes	76
Appendix F: Printing sequence	79
Appendix G: FDM printer	81
Appendix H: Polymer bonding	83
Appendix I: Designing a prosthetic hand	84
Appendix J: Applications brainstorm	86
Appendix K: Original project brief	87

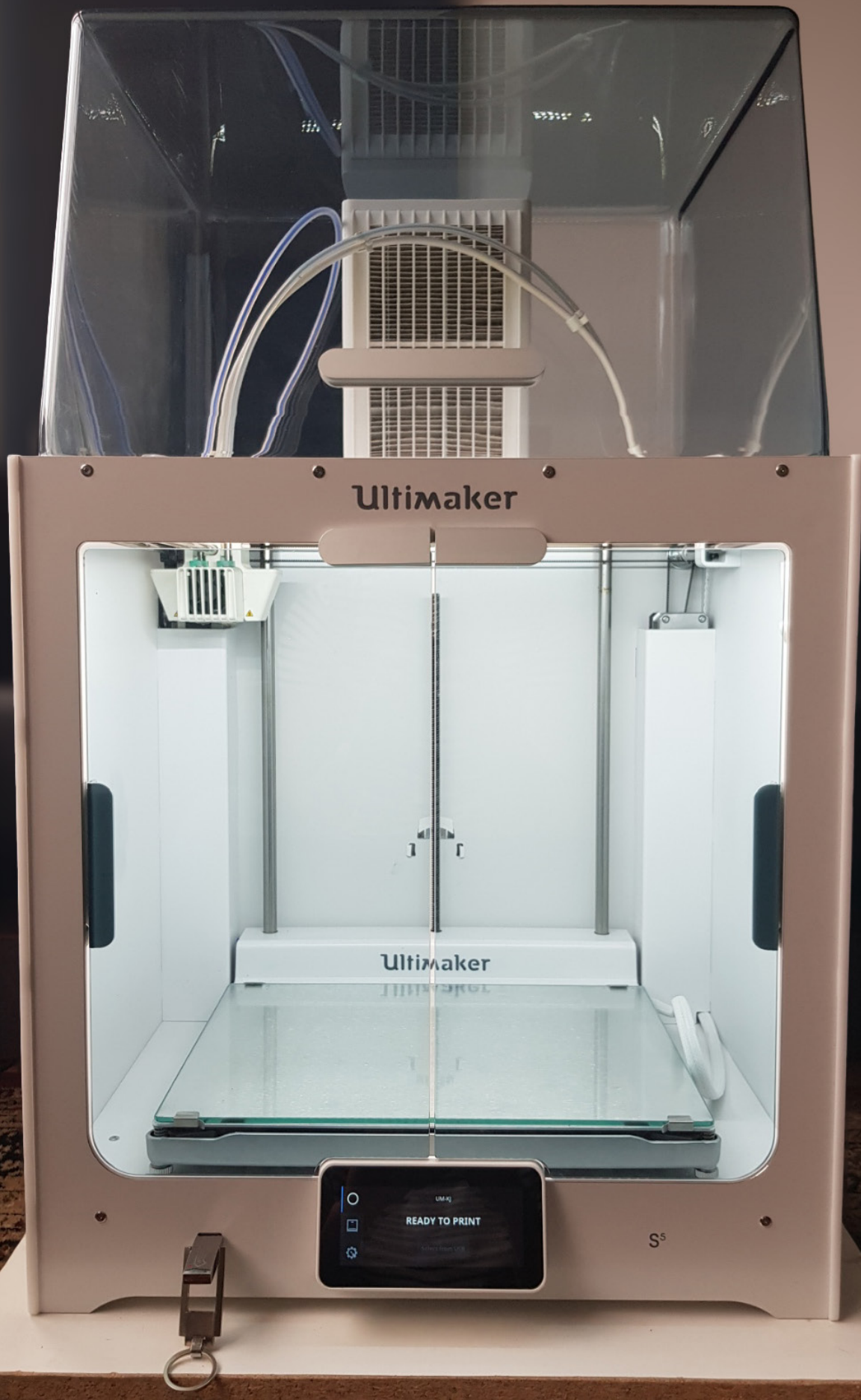
Acknowledgements

I would like to thank my supervisors Zjenja Doubrovski and Tim Kuipers for their support. Your expertise, creativeness and constructive criticism have been vital for this project. You both were involved in every layer of the project: from the overall course and planning of the project until the details like searching a misplaced semicolon in a one-million line code.

Also, thank you to the technical staff of the applied labs of our faculty, Mascha Slingerland and Tessa Essers, for explaining the testing equipment and for allowing me to use it.

Thank you to Ultimaker for lending an FDM printer and for letting me use your materials which allowed me to experiment and try out ideas on a daily basis while working at home.

Last but not least a thanks to my friends and my roommates for discussing ideas and helping me improve my work.



Ultimaker

Ultimaker

READY TO PRINT

S

1: INTRODUCTION

This report is about multi-material additive manufacturing (AM) using the fused deposition modeling (FDM) technique. This first chapter introduces the FDM printing process. Then multi-material FDM printing is explained including information on polymer bonding and the current limitations. From this, the goal is constructed.

1.1 – Fused Deposition Modeling

Fused Deposition Modeling (FDM) is an Additive Manufacturing (AM) technique that is used for producing 3-dimensional parts. An FDM printer melts a thermoplastic polymer filament and deposits this material onto a building plate. By controlling the material flow and the movement of the printing head, we can create a 3D part. The thermoplastic polymer filament is pushed into a nozzle. This nozzle is heated by a heating element to melt the polymer. The nozzle is part of the printing head which can translate in 3 directions (X,Y, Z) relative to the building plate. This particular FDM printer (see Figure 1.2) features a printing head with two nozzles allowing multi-material printing. Quickly after depositing the molten polymer, it solidifies at the desired location. An FDM printer stacks layers of material to create a 3D part. We call this a planar printing approach. A more elaborate explanation of this FDM printer is shown in Appendix G.

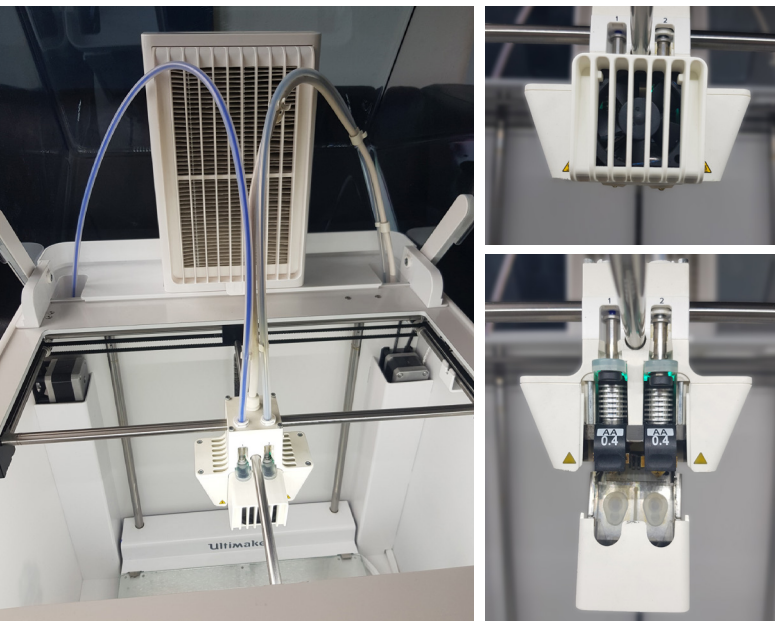


Figure 1.2 Ultimaker S5 printing head

1.2 – FDM printing workflow

In order for the FDM printer to know what to print and how it should print a certain model, some steps are required before turning on the printer (see Figure 1.4). The desired shape is to be modeled with CAD software. This CAD model is then imported into a program called a slicer. This software creates the commands for the FDM printer. To allow all CAD software to be imported into the slicer, a universal format is used called Standard Tessellation Language (.stl). The commands created by the slicing software are compiled in a file format called GCode (.gcode) which holds commands such as nozzle- and

building plate temperature, the coordinates to which the nozzle has to move and the amount of material to be extruded. In the slicer, the user can adapt many variables according to the materials used and the desired quality and structural performance and production time of the print. Variables such as printing speed and nozzle- and building plate temperature are mainly dependent on the type of material and should be tuned accordingly. Variables such as layer height or the amount of infill are mainly a trade-off between print quality and structural performance and production time. Variables such as the addition of support material are mainly determined by the shape of the model.

1.3 – Interlayer vs intralayer bonding

We have just learned that FDM printing is a layer-stacking production method. When printing within a layer, a continuous material flow is generated from the nozzle. We call this type of bonding: intralayer bonding.

When printing the successive layer, we create a bond between already printed material and new material which is extruded from the nozzle. We call this type of bonding: interlayer bonding. See Figure 1.1.

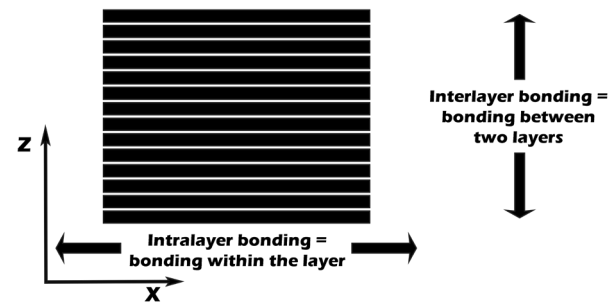


Figure 1.1 intralayer vs interlayer bonding

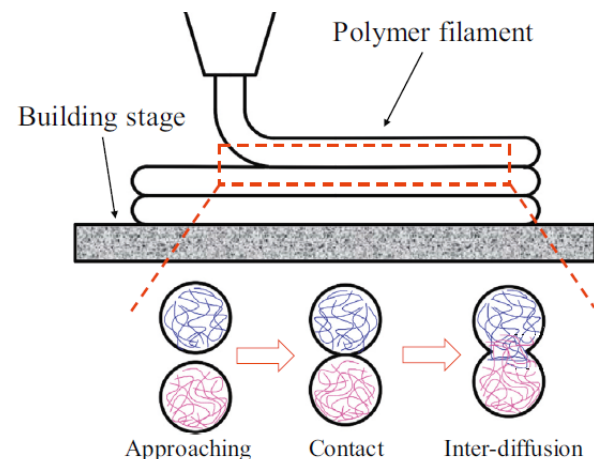


Figure 1.3 polymer fusing (Yin et al., 2018)

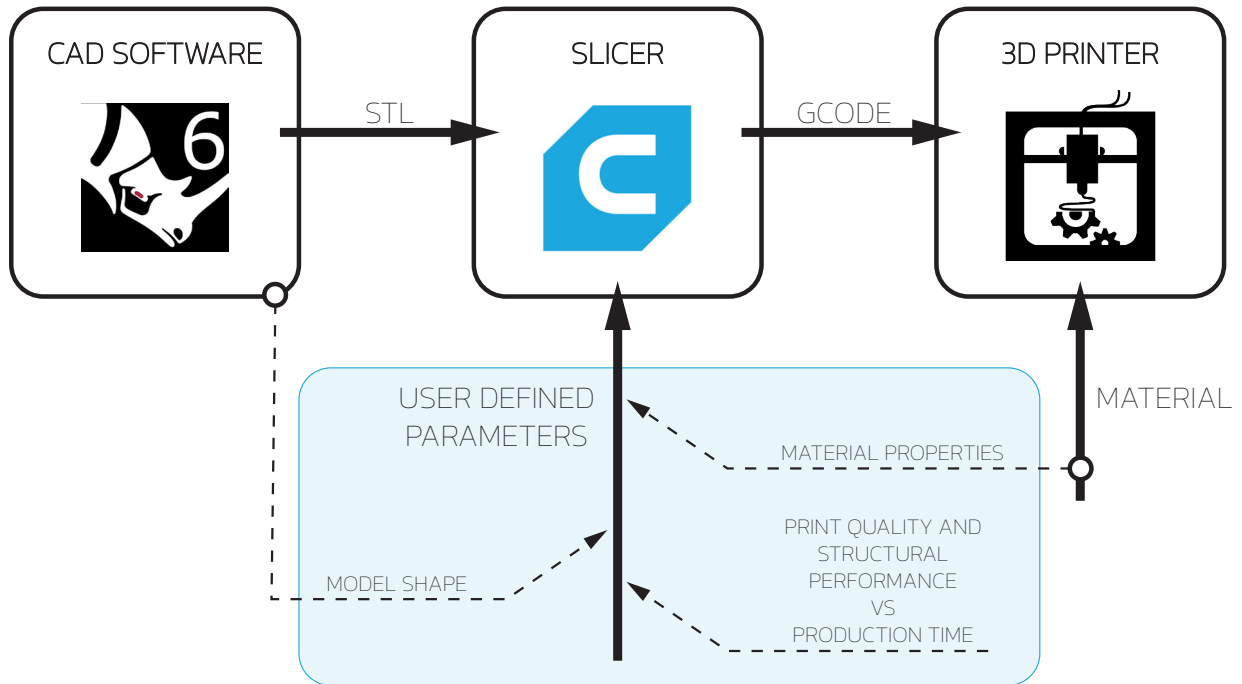
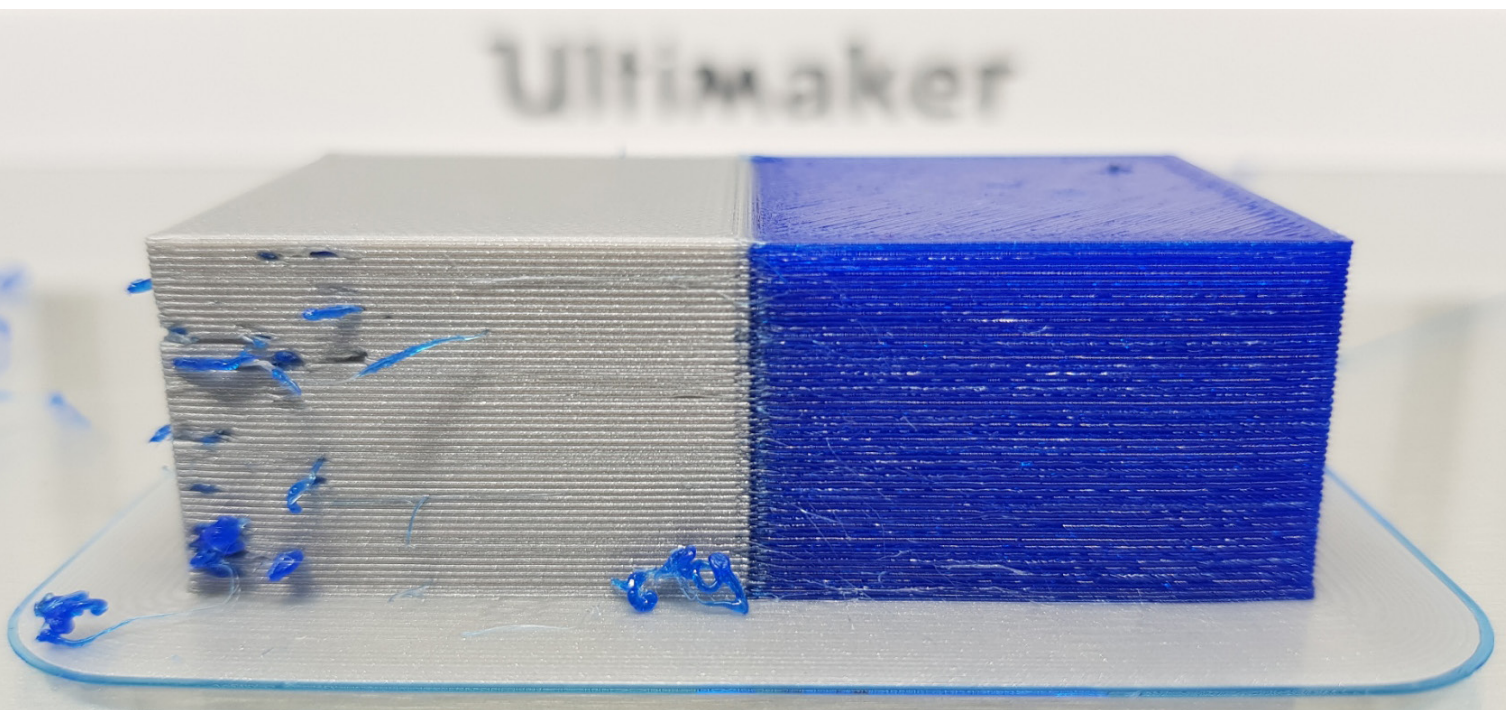


Figure 1.4 FDM printing workflow

The performance difference between intralayer and interlayer bonding is temperature related. As mentioned, during FDM printing a successive layer is only created after finishing the current layer. This means that there is a time delay and thus a certain cooling down period between stacking of the layers. The finished layer has cooled down. Therefore, the new material printed on top only fuses partly to its successive layer (see Figure 1.3). This leads to anisotropic behavior where the strength in Z-direction (interlayer bonding) is lower than in XY-direction (intralayer bonding).

1.4 - State of the art FDM printing

Some FDM printers, like the Ultimaker S3 and S5 feature a dual extrusion printing head (pictures in this report show an Ultimaker S5). This dual extrusion printing head holds two nozzles making it possible to print a model made of two materials. This is called multi-material FDM printing. In theory, this vastly increases the opportunities in prototyping and manufacturing with two different colors or two different materials having different material properties. We could for example create products with flexible and stiff parts. Also, we could create an item with high wear resistant material at its contact points where the rest of the part would be made of another (cheaper or lighter) material. The entire part could be manufactured at once so no need for post-production assembly.



1.5 – Compatibility of different polymers

In practice however, we see a large limitation in combining different polymers. For chemical bonding of two materials, a variety of mechanisms affect the bonding strength. An elaborate explanation of these mechanisms is shown in Appendix H. Here we will list the two most important factors: temperature and chemical nature.

Temperature – energy is required to bond two materials and that can be in the form of heat. The temperature determines the homogeneity and therefore the strength of the bond.

Chemical nature – chemical bonding is based on interatomic and intermolecular forces at the interface of the materials. The magnitude of these forces depends on the chemical composition of the materials because this chemical nature defines what bonds are made and their magnitude (Tamburino, 2019) (Choempff, 2019).

The key take-away is: to create a strong bond between two different materials, the materials must be chemically compatible. Ultimaker provides an overview of which of their FDM printing materials are chemically compatible, see Figure 1.5.

	PLA	ABS	CPE	CPE+	Nylon	PC	TPU 95A	PP	PVA
PLA	✓	×	×	×	×	×	×	×	✓
ABS		✓	×	×	×	×	ⓘ	×	ⓘ
CPE			✓	×	×	×	×	×	✓
CPE+				ⓘ	×	×	×	×	×
Nylon					ⓘ	×	ⓘ	×	✓
PC						ⓘ	ⓘ	×	ⓘ
TPU 95A							ⓘ	×	ⓘ
PP								ⓘ	×
PVA									×

✓ Officially supported ⓘ Experimental × Not supported

Figure 1.5 compatibility of Ultimaker filaments (Ultimaker, 2017)

1.6 - Problem definition

The selection of combining materials during FDM printing is limited because most different polymers do not chemically bond (see Figure 1.5). This is called chemical incompatibility which results in dual material parts that are easily separable (see Figure 1.6), or parts that fail during production already.

Our goal is to generate a method to create a dual material object, made of two chemically incompatible materials during the FDM production process.

Achieving our goal would benefit the FDM community and the end users in two ways. For those that are currently joining the parts post production, it may highly decrease labor time and effort. For those that now confine to current compatible materials it may vastly increase the combination of materials and so the possibilities in prototyping and manufacturing.

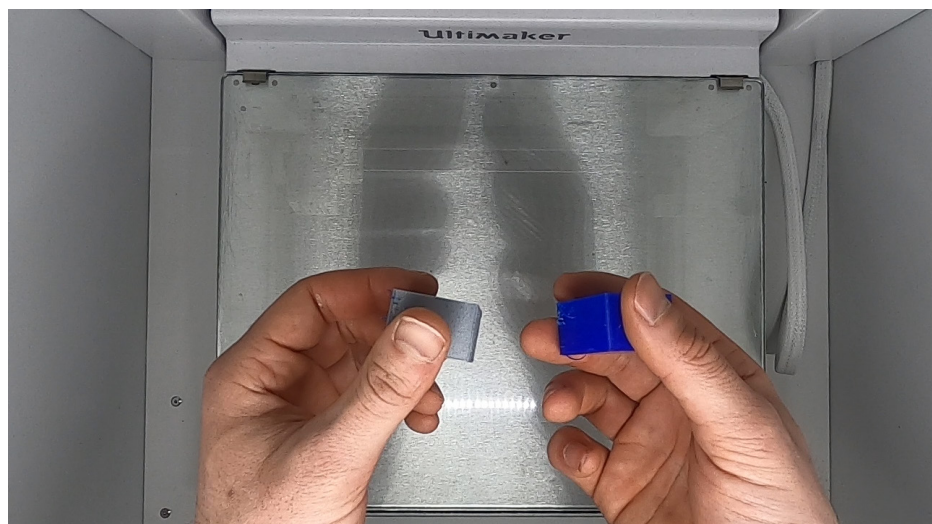
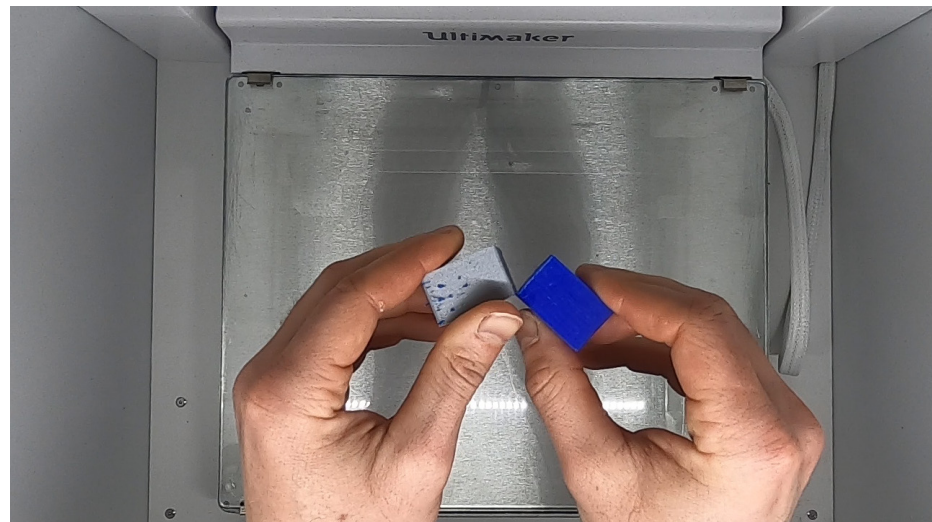
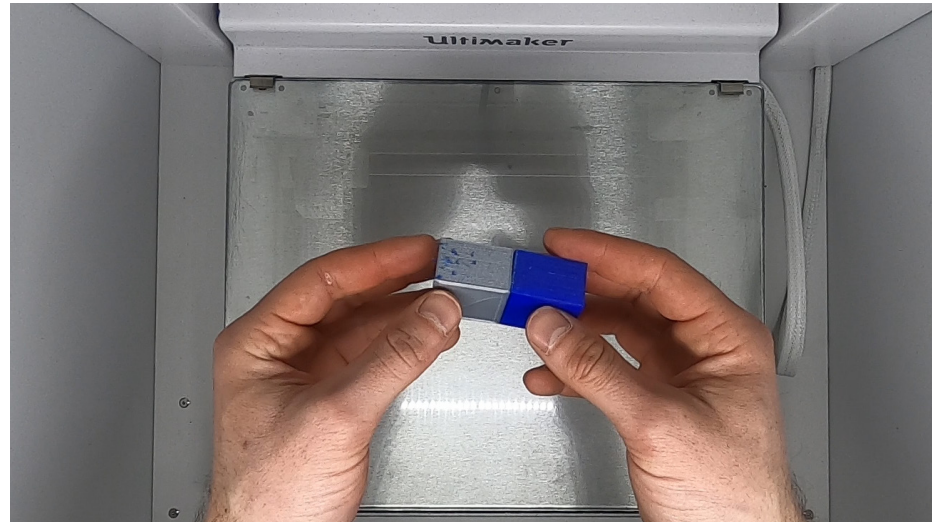


Figure 1.6 PLA and TPU cubes printed face-to-face sideways (vertical interface)

2: RELATED WORK

In order to achieve our goal, we have analyzed related studies about bonding multi-material objects. This provided a starting point for further investigation. This chapter holds the most important take-aways. The full review can be found in Appendix C.

The bonding methods of the reviewed papers can be placed in three categories: process parameter optimization, additional manufacturing technique or hardware and mechanical bonding.

2.1 – Process parameter optimization

Multiple studies show the effects of process parameters (that can be adjusted within the slicer software) on interfacial bonding. The hardware of the particular FDM printer was unchanged. Important process parameters found are:

Nozzle temperature, building stage temperature and printing speed.

The exact temperatures and printing speed depends on the materials used but generally speaking the bonding strength increases by increasing temperature and printing speed, until a certain limit (Yin et al., 2018) (Khan, 2019) (Lin et al., 2018).

Orientation of the interfacial layers and infill density.

The Lines pattern available in Cura created the highest bonding strength when joining PLA, TPU and CPE end-to-end, stacked on top of each other (horizontal interfaces). Increasing the infill density increases the bonding strength (Tamburrino et al., 2019).

2.2 – Additional manufacturing technique or hardware

Another method used to improve interfacial bonding is the addition of a different manufacturing method to the FDM system. In some cases, this approach greatly improved bonding strength of chemically incompatible materials. Rossing (2020) proposed a method of overmolding silicon to a rigid material (PLA). The addition of this overmolding technique together with the use of an FDM printed interlocking structure improved bonding strength between PLA and silicon: up to 5.5 times higher compared to gluing the parts using a primer.

Khondoker (2019) demonstrated a method for bonding a rigid and a soft thermoplastic for the use of soft robotics by introducing a static intermixer just before the nozzle of an FDM system. Mixing SEBS (soft material) and HIPS (hard material) at the interface could increase the adhesion strength by 12 times compared with side-by-side printing (vertical interface).

These approaches requires changes in hardware. Our solution should be backwards compatible and should not require changes in hardware. We therefore exclude the approach of adding hardware to improve bonding of chemically incompatible materials.

2.3 – Mechanical interlocking

Lastly, some studies used mechanical interlocking as a tool to improve multi-material bonding, using an unmodified FDM system. Mechanical interlocking is the creation of a shape at the interface that either enlarges the contact area or creates a form interlocking. When form interlocking two parts, one of the two materials must fail to break the connection.

Several mechanical interlocking features have been developed. Enlarging contact area improves the bonding strength of chemically incompatible materials. Tamburrino et al. (2019) printed two chemically incompatible materials on top of each other (horizontal interface). The interface layer consisted of an outer ring of material A where the remaining part of the layer was made of material B. The larger contact area doubled the peak tensile strength for PLA-TPU combination. Fernandez (2019) tested the effect of material overlap for bonding PLA and TPU sideways (vertical interface). Applying a material overlap of either 1 or 2mm improved the tensile strength by 200% compared to regular side-by-side printing.

Ribeiro et al. (2019) printed specimens of PLA and TPU side-by-side (vertical interface). They tested three different form interlocking shapes: a T-shape, an I-shape and a V-shape. The T-shape resulted in the highest Young's modulus and highest ultimate stress. So creating a form interlocking shape at the interface improves the bonding strength of chemically incompatible materials even more than only enlarging contact area.

Also, a patent and technical disclosure common were found that use mechanical interlocking for joining materials.

A patent of Mosaic Manufacturing Ltd. describes a method for joining multiple materials on top of each other (horizontal interface) during additive manufacturing. The patent includes bulk deposition to form an anchor of material A into a receptacle in a body of material B.

A Technical disclosure common of Kuipers (2020) from Ultimaker describes a method for joining two parts of different materials during FDM by mechanical interlocking. Fingers are printed that overlap into the other volume. These fingers are part of the boundary of the first volume so to make a continuous extrusion flow. The fingers are rotated typically 90° every X-number of layers to interlock the volumes in all directions.

2.4 – Interim conclusions

We have seen different methods for bonding chemically incompatible materials. Firstly, adding different manufacturing techniques or hardware to the FDM system can improve the bonding strength of chemically incompatible materials. This requires changes in hardware. We want to create a joining method that does not require hardware changes to make it backwards compatible for every multi-material FDM printer. We therefore exclude solutions that require extra hardware.

Secondly, optimizing the printing parameters within the slicer software yields improvements for bonding chemically incompatible materials. These improvements are however mild compared with improvements yielded by introducing mechanical interlocking, especially form interlocking shapes. We therefore chose to investigate mechanical interlocking to join chemically incompatible materials.

The next chapter will show the proposed concept using this mechanical interlocking approach. Subsequently, we will show the design challenges and evaluation of it.

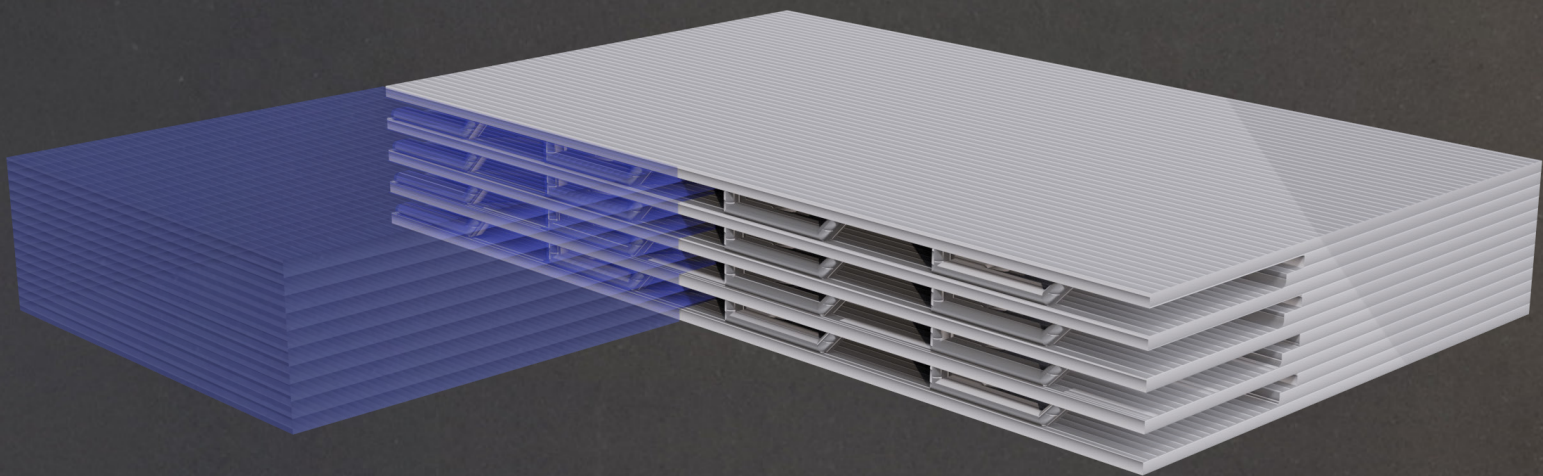
3: PROPOSED CONCEPT

This chapter shows the proposed concept for joining chemically incompatible materials. It explains **what** the proposed concept is and **how** it joins the two materials. The chapter finishes with an example of what can be created using this new joining method for FDM printing: a prosthetic hand made of PLA and TPU, two chemically incompatible materials. Chapter 4 will explain **why** this interlocking pattern and printing procedure is chosen including several design challenges.

3.1 - JOINING METHOD

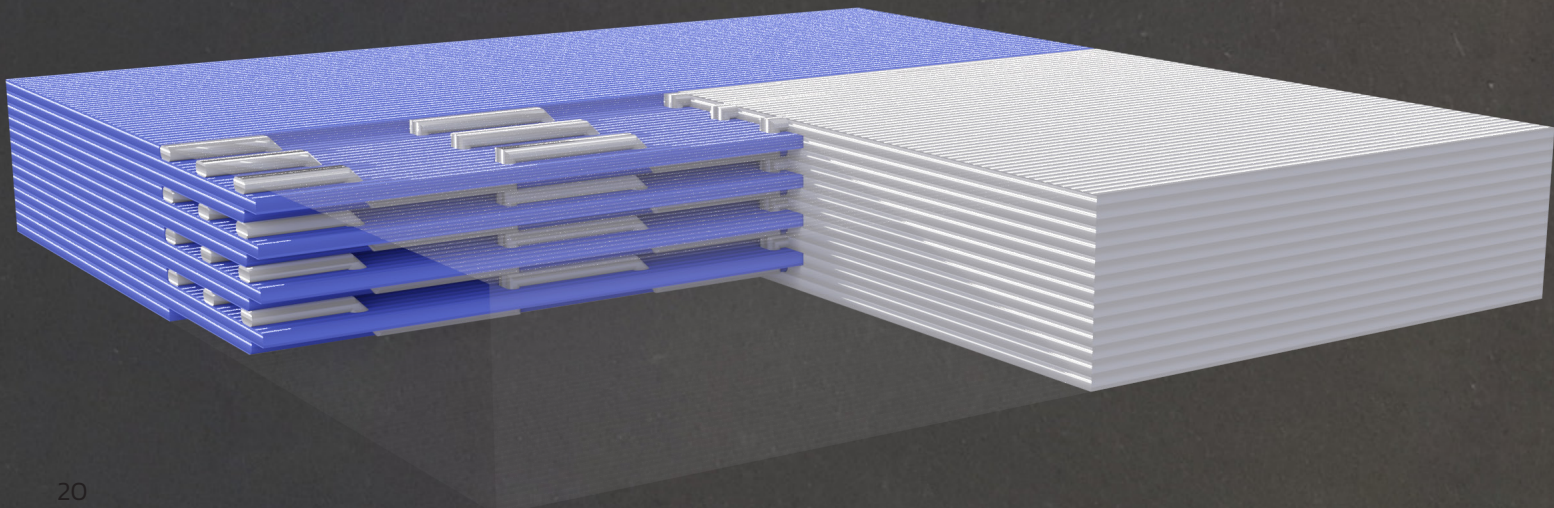
Form interlocking shape

We were able to join chemically incompatible materials by creating a form interlocking shape at the interface which was printed using a non-planar approach. One could imagine the form interlocking shape like shackles interlocked with each other. One of the materials must break to disconnect the parts.



The interface consists of three rows of PLA bridges. The space under and around the bridges and between the rows are filled with TPU. These PLA bridges and TPU grid together create a form interlocking shape which interlocks in three directions (X, Y, Z). The PLA bridge pattern is created using a non-planar approach: as opposed

to the normal FDM printing process (planar approach), this bridge pattern is created in one continuous extrusion across multiple layers. This is made possible by moving the nozzle upwards and downwards (with respect to the building stage) whilst moving forwards. The considerations and tradeoffs of this pattern can be found in chapter 4.



Printing sequence

The interlocking pattern has a height of three layers (excluding a starting plane) and these can be stacked on top of each other. It is created in the following sequence: 1) a TPU grid is printed (see Figure 3.1). This TPU grid is attached to a TPU plane at one end. The main paths of the grid are oriented orthogonal to the interface. 2) Three rows of PLA bridges are printed across the TPU grid (see Figure 3.2). The PLA bridges attach to the PLA plane below it and to each other. They are created in one continuous extrusion by moving the nozzle upwards and downwards (with respect to the building stage) whilst moving forwards. 3) A second TPU grid is printed (see Figure 3.3). Between every row of PLA bridges, TPU is extruded to connect this second TPU grid to the first TPU grid. 4) A PLA top layer is printed to connect the tops of the PLA bridges to each other and to the PLA part (see Figure 3.4). A more elaborate version of this printing sequence can be found in Appendix F. The considerations and tradeoffs of the printing sequence can be found in chapter 4.

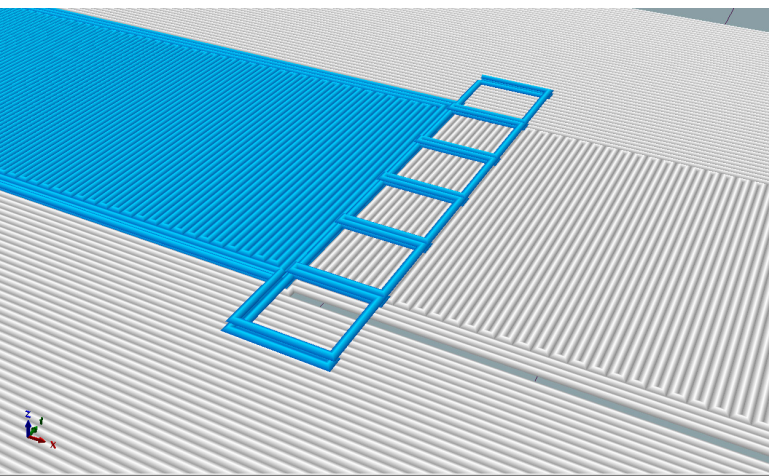


Figure 3.1 TPU grid

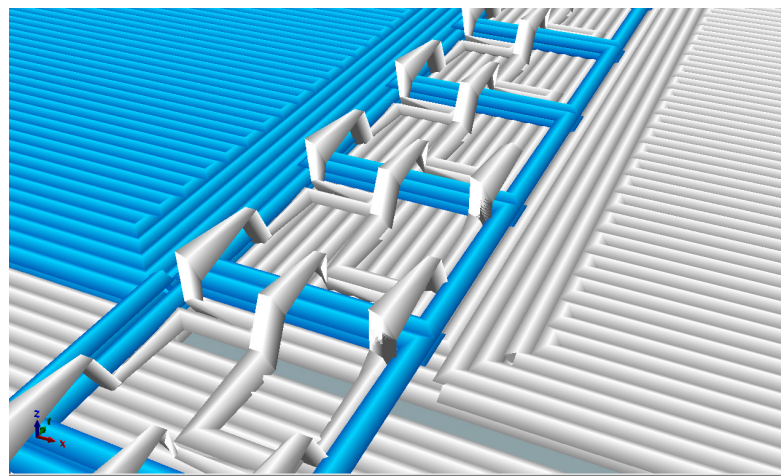


Figure 3.2 PLA bridges

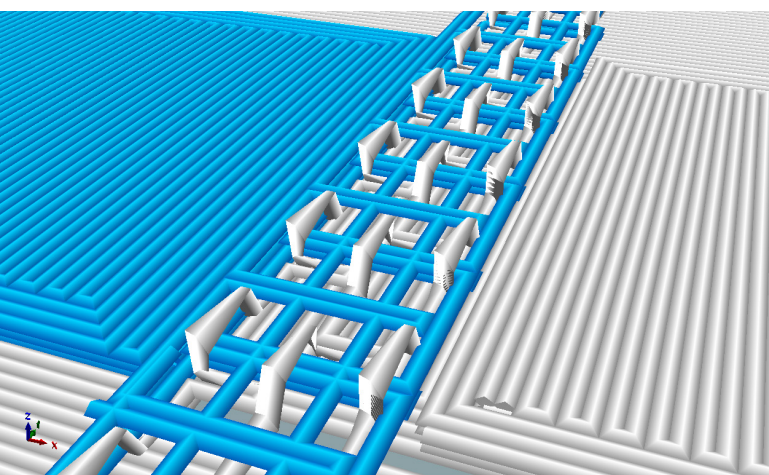


Figure 3.3 TPU extrusion around PLA bridges

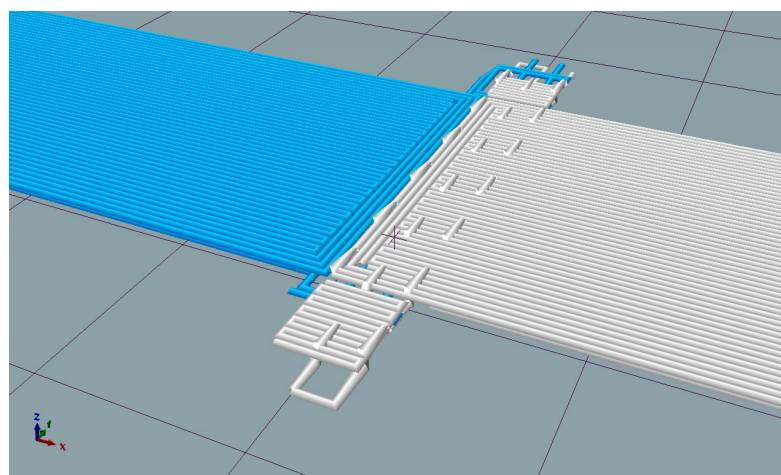
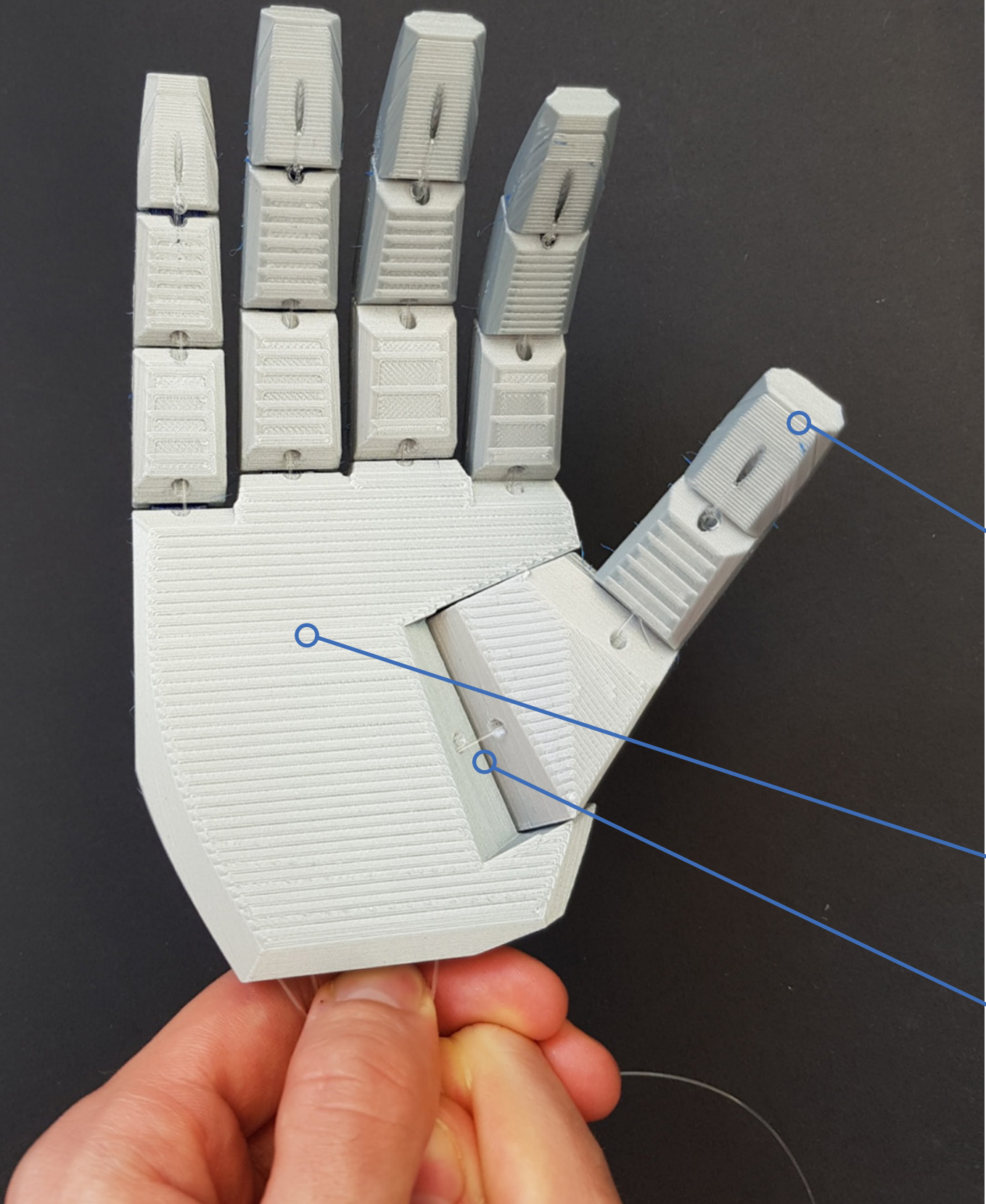


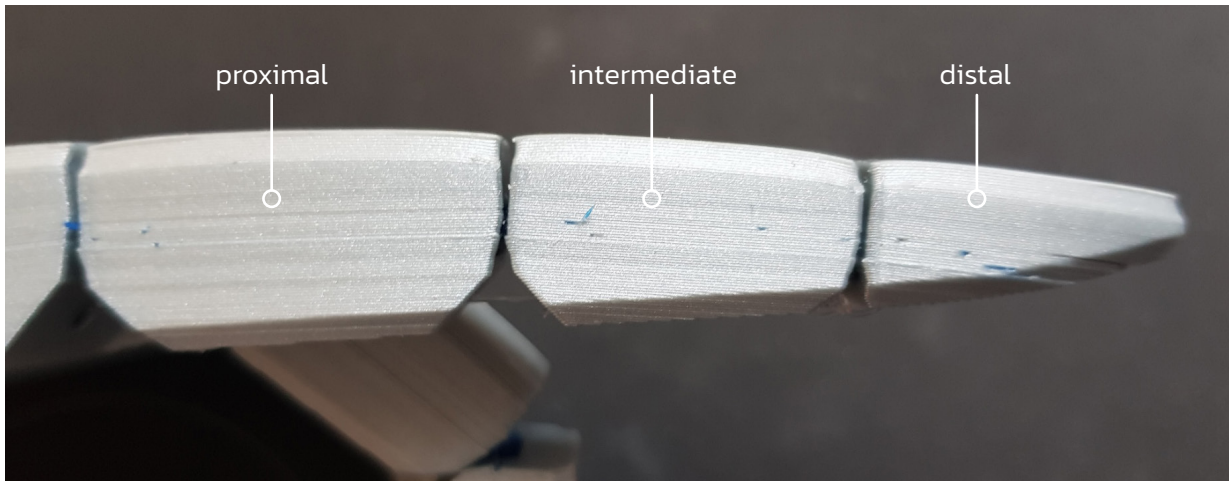
Figure 3.4 PLA plane connecting PLA bridge tops

3.2 - PROSTHETIC HAND

The human hand is a complex part of bones, muscles and ligaments. A prosthetic hand mimics the human hand and is a simplification of it. This prosthetic hand consist of a main body, fingers and actuator cables.

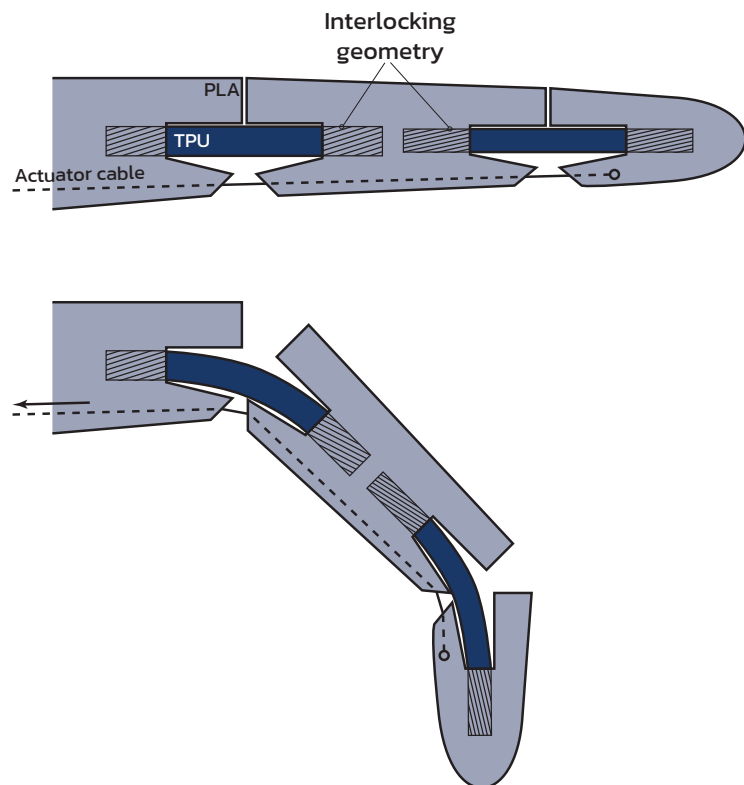
This paragraph shows what the prosthetic hand looks like. A qualitative evaluation of it can be in chapter 6.





Fingers

Human fingers are divided into three phalanges: proximal, intermediate and distal phalange. Each phalange allows rotation between 0° and 90° with respect to its connected phalange. In this prosthetic hand, each phalange is made of PLA, a rigid polymer. To allow rotation of the phalanges, the phalanges are connected with a strip of TPU which is a flexible polymer. The TPU and PLA are only attached on the left and right side of the TPU link (in cross-section view), i.e. a vertical interface. This way, the TPU strip curves when a bending force is applied. Cut-outs in the PLA phalanges are created to allow rotation.



Main body

The human hand consists of carpal and metacarpal bones. These only slightly move with respect to each other. In this prosthetic hand, they are simplified by combining them into one solid piece: the hand main body. It is made of PLA, a rigid polymer.

Actuator cables

Bending is achieved by pulling the actuator cable. This cable runs through canals in the main body of the hand and the proximal and intermediate phalanges. Each actuator cable is attached to a distal phalange.

4: DESIGN CHALLENGES

The previous chapter showed the proposed method and explained how it joins two chemically incompatible materials. This chapter explains **why** this particular interlocking pattern is chosen instead of several alternatives. The criteria for this choice were strength, applicability and process continuity and are explained on the next page. They are followed by the design challenges that were solved during the process. These design challenges are linked with one or more of the criteria.

4.1 - Criteria

For choosing a mechanical interlocking structure, we have composed the following criteria:

Strength

We want to improve on the current industry standard: the overlapping feature available in the slicer Cura. This overlapping feature will be explained in more depth in chapter 5 as it will be used as a benchmark. Chapter 5 will also show that our proposed concept creates a stronger bond than this benchmark. As we have learned from the literature review (chapter 2), the shape of the interlocking structure is important for the strength of the bond. Considerations about the shape can be found in paragraph 4.2. Also, we consider the size of the shape since this is relevant for the strength of the bond, see paragraph 4.3.

Applicability

We want to apply the mechanical interlocking structure to parts of any size. The structure can only be applied to parts larger than the size of the interlocking shape. Therefore, we prefer to keep the interlocking shape small to be able to apply the method to small parts. Paragraph 4.3 show the considerations regarding the size of our interlocking shape.

Process continuity

In general, a discontinue production process is more difficult to regulate since input variables have to change much more to control the process. Inherently, this creates greater output uncertainty. This holds for FDM printing as well; it is useful to keep the material flow continuous to prevent local under- or over extrusion. Therefore, we want to optimize the bonding method to be a continuous process as much as possible.

4.2 - Form interlocking shape

The shape of the interface greatly affects the strength of the bond. When joining two materials face-to-face, the strength will be determined purely by its adhesive forces, see Figure 4.1. Since the adhesive forces of chemically incompatible materials are small, this will be a weak bond.

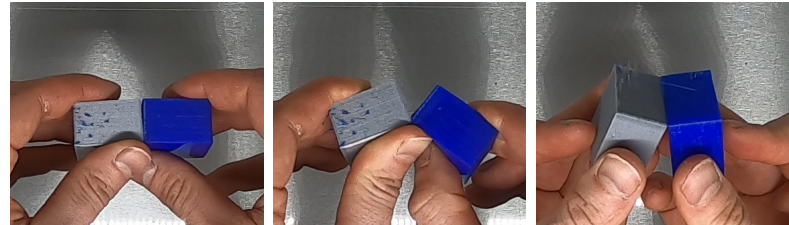


Figure 4.1 face-to-face bonding of PLA and TPU

One could also create an interface of overlapping material, see Figure 4.2. Here, friction forces will play a role.

$$F = \mu F_N$$

Here, the friction coefficient is dependent on the chemical composition of the two materials and the surface roughness. The two materials can still be disconnected without breaking them, i.e. they slip.

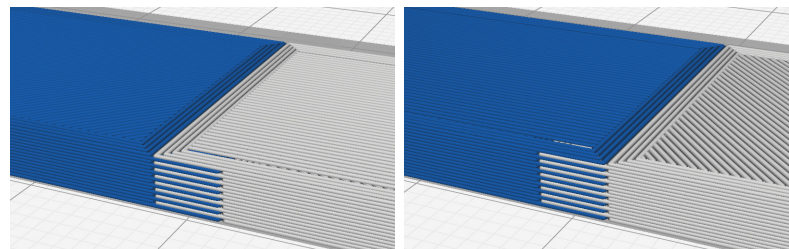


Figure 4.2 overlapping material to create friction

Alternatively, we can create shapes that are form interlocking (three different shapes are shown in Figure 4.3). This means that either of the two materials will have to break to disconnect the two parts. The force to break a material is larger than its friction force. Therefore, form interlocking is the strongest type of interface so this interface type is used in our joining method. Appendix B shows alternative ideas having either a friction based shape, semi-form interlocking shape or form interlocking shape.

Our proposed concept explained in chapter 3 is such an interlocking shape. In order to disconnect the parts, either the PLA bridge pattern must break or the TPU which is extruded under and around the bridges.

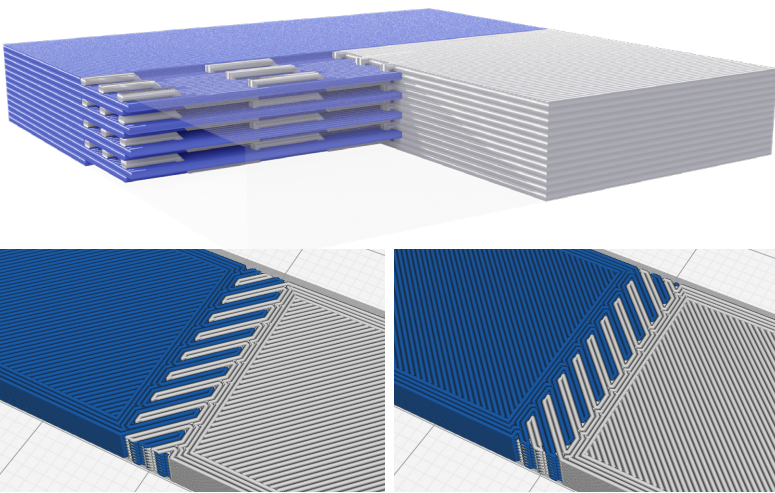


Figure 4.3 variety of form interlocking shapes

4.3 - PLA bridge pattern

Chapter 3 showed the bridge pattern which is part of the interlocking shape. The bridge pattern is produced in a non-planar fashion. Two aspects have influenced this design choice: a non-planar printing process has the potential of producing stronger parts compared to a planar printing process and it allows to print the PLA bridge as one continuous bead (process continuity).

Strength

We take a look at the bridge pattern (see Figure 4.4). A planar printing procedure causes interlayer interfaces. When applying a force orthogonal to the interface, we could break the connection by shearing the pillars of the PLA bridge pattern (see Figure 15). We apply the following equation:

$$F_A = \sum F_R = \sum A \times \sigma_{shear}$$

As explained in the Introduction, interlayer adhesion is a weaker bond than intralayer adhesion: the shear stress of interlayer bonding (interlayer shear stress - ILSS - created by planar printing process) of PLA is 11.4 MPa (Reverte et al.,

2020). The shear stress for intralayer bonding (enabled by non-planar printing process) of PLA is 24.75 MPa. So:

$$\sigma_{intralayer\ shear} > \sigma_{interlayer\ shear}$$

$$F_{A\ intralayer} > F_{A\ interlayer}$$

Therefore, we aimed to keep the PLA bridge pattern continuous and created a non-planar printing procedure.

Process control

Another benefit regarding the continuity of this non-planar printing procedure is the control of the process. As explained in paragraph 4.1, a continuous process decreases output uncertainty. The next paragraph will elaborate on the printing sequence of the interlocking shape.

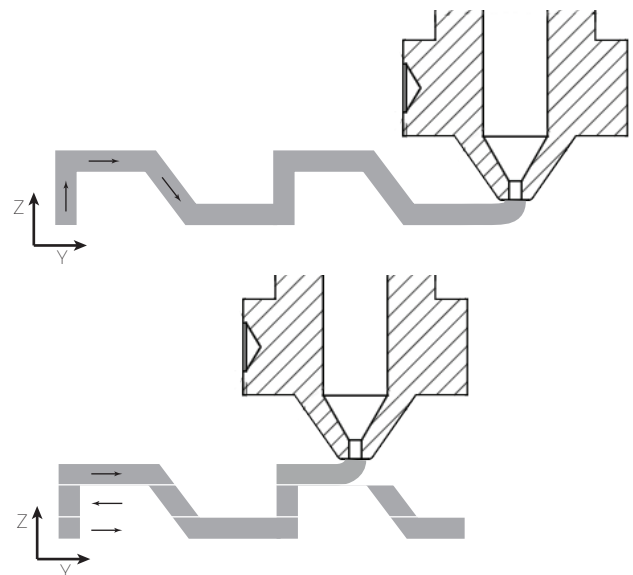


Figure 4.4 sideview of bridge pattern. From top to bottom: non-planar approach and planar approach

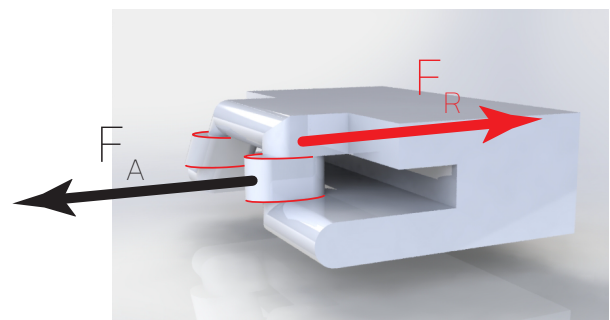


Figure 4.5 PLA bridge section. F_a = applied force. F_r = reactant force.

Toolpath

As described in the previous paragraph, a non-planar approach is chosen for creating the PLA bridges. Creating this continuous bead across multiple layers requires the nozzle to move up and downwards with respect to the building plate whilst moving in-plane. The nozzle is shaped like a flat cone with an angle of 90° . The underside of the nozzle (smallest diameter of the cone) has a diameter of 1 mm with an extrusion hole of 0.4 mm. Therefore, the downwards path of the nozzle (second pillar of each bridge) is at a 45° angle. Due to the horizontal area around the hole of the nozzle, the extruded material curves around the nozzle (see Figure 4.7).

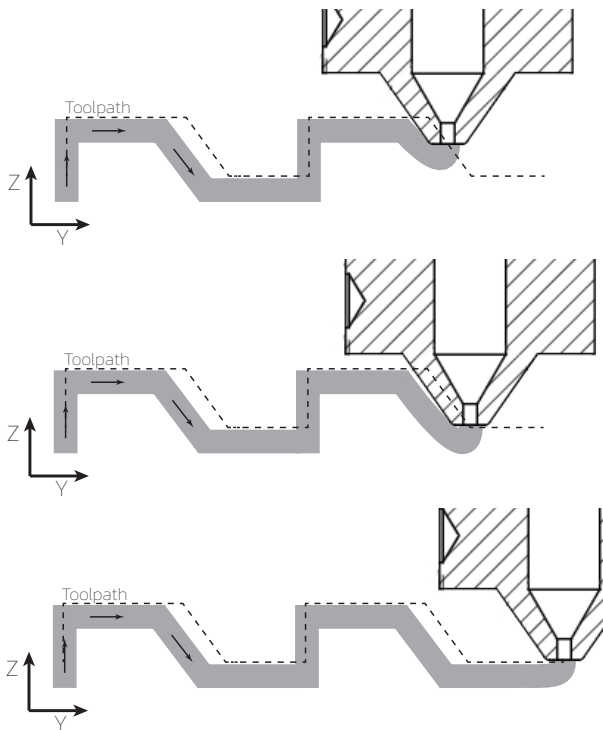


Figure 4.7 PLA bridge printing

Bridge size

The period with which the PLA pattern repeats and the toolpath of the TPU grid are accommodated to avoid collision of the nozzle with already printed material (PLA bridges). A critical moment occurs when extruding the second TPU grid (see Figure 16). Due to the geometry of the nozzle explained in the previous paragraph, a certain offset is required to avoid collision. We define this offset as: distance from the center of the nozzle until the already printed material (PLA) and call it D . This offset (D) is dependent on layer height. Table 4.1 shows the offset for the most commonly used layer heights.

Also, it shows the period (P) with which the pattern repeats.

A layer height of 0.20 mm will be used for any further calculations, prints, models or explanations.

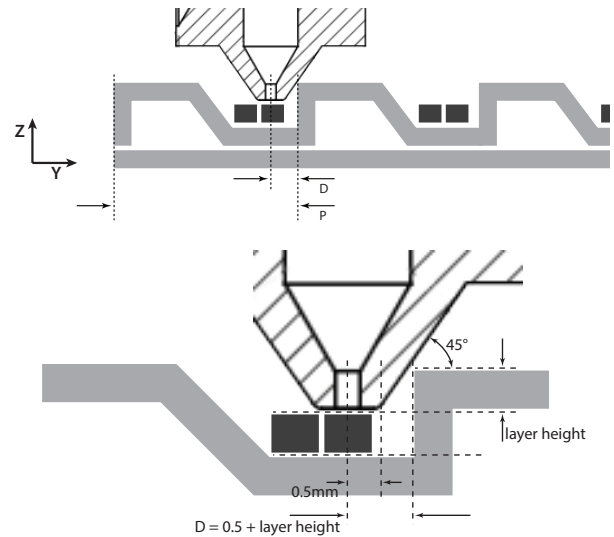


Figure 4.6 distance to PLA bridges to avoid collision of already printed material. PLA is denoted with light grey. TPU is denoted with dark grey.

Table 4.1 pattern geometry depending on layer height.

Layer height [mm]	D [mm]	P [mm]
0.06	0.56	3.56
0.08	0.58	3.68
0.10	0.60	3.80
0.15	0.65	4.10
0.20	0.70	4.46
0.25	0.75	4.70
0.30	0.80	5.00

Since the pattern height is three layers, it's maximum height is 0.9 mm when printing with a 0.4 mm diameter nozzle. The Ultimaker S5 has a silicone protective cover around the nozzles (see Figure 4.11). The distance between the underside of the nozzle and the underside of this silicon cover is 1.2 mm so this still allows clearance. The silicon cover will not collide with the PLA bridges.



Figure 4.11 Ultimaker S5 printing head

4.4 - Printing sequence

Chapter 3 showed the chosen printing sequence of the interlocking shape: 1) TPU grid, 2) PLA bridges and 3) TPU grid 4) PLA top layer. This paragraph explains why this particular sequence was chosen.

The desired result of the initial printing sequence was that the TPU would flow under and around the PLA bridges when printed in a single continuous extrusion. This would create a form interlocking shape, continuously extruded so without TPU interlayer interfaces (see Figure 4.9).

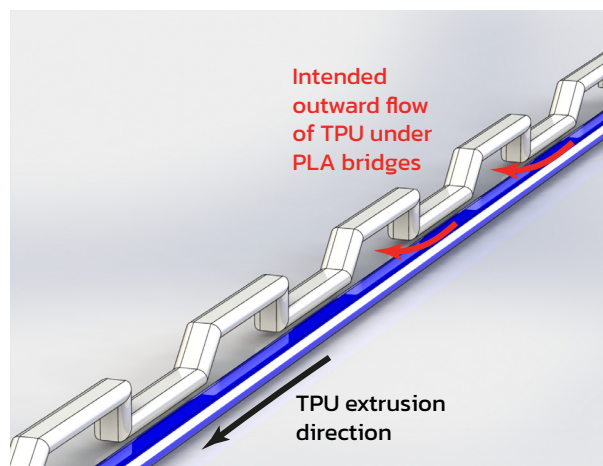


Figure 4.9 TPU extrusion and intended flow

Hence the initial sequence was: 1) printing PLA bridge pattern (see Figure 4.8). Appendix A shows all information for creating these overhanging structures. 2) TPU is printed alongside and around the PLA bridges.

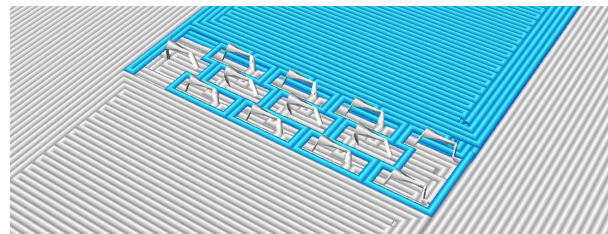
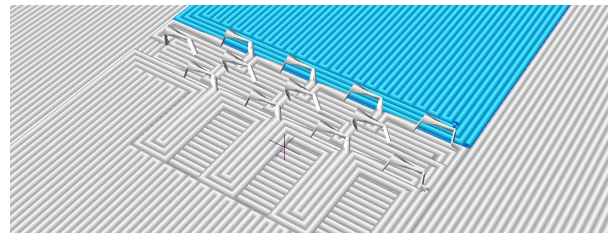


Figure 4.8 initial printing sequence: 1) create PLA bridges 2) TPU extrusion alongside and around PLA bridges

The actual printing result of this initial sequence is shown in Figure 4.10. Here we can distinguish the empty areas under the PLA bridges. The intended outward flow (Figure 4.9) could not be realized.

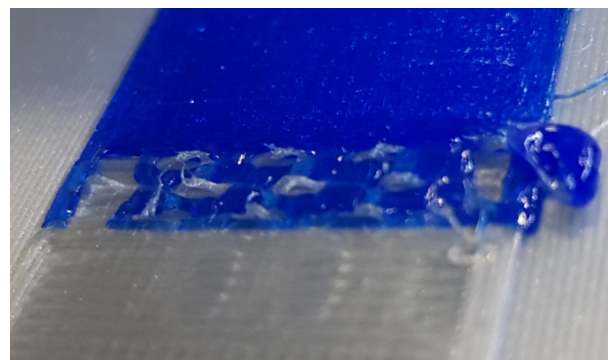


Figure 4.10 actual TPU flow

Therefore, we changed the printing sequence into a two-step approach which is shown in Figure 4.12. 1) A TPU grid is printed. 2) The PLA bridge pattern is printed across this grid. 3) A second TPU grid is extruded around the PLA bridges. This sequence greatly improved the TPU fill under the PLA bridges. Subsequently, this improved TPU fill under the PLA bridges and the changed layout of the grids resulted in an increase in peak force. These peak force results can be found in chapter 5. The TPU grid layout is explained in the next paragraph.

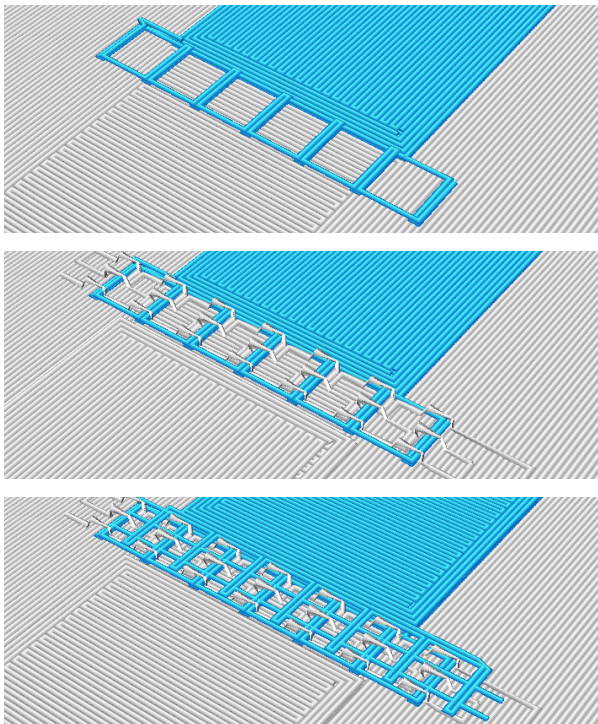


Figure 4.12 final printing sequence: 1) create TPU grid 2) create PLA bridges 3) create second TPU grid around PLA bridges

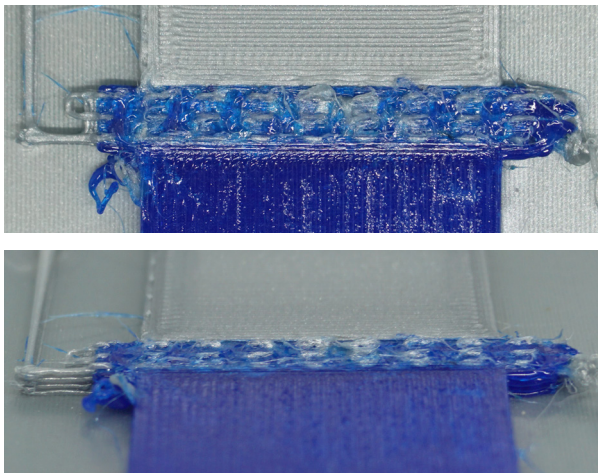


Figure 4.15 improved TPU fill

4.4 - TPU grids

Besides the printing sequence of the TPU grids, the toolpath is important as well because the orientation of the fibers affects the strength. A fiber is strongest when oriented in-line with the applied force. Also, stresses can only be distributed between multiple fibers if they connect. Therefore, the continuous fibers of the first TPU grid are oriented in-line with the applied force (Figure 4.13). The second TPU grid extrudes material between the PLA rows as well to fuse the multiple fibers together (Figure 4.14). The peak force results of these layout changes can be found in chapter 5.

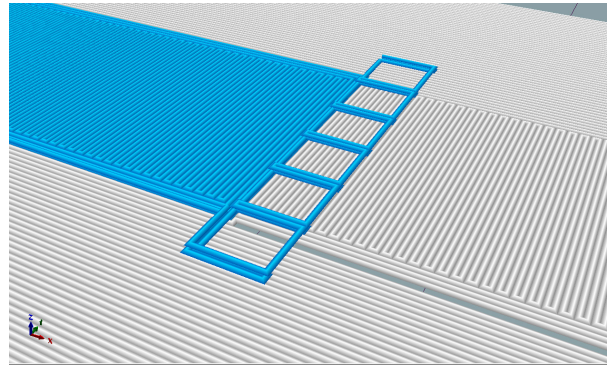


Figure 4.13 1st TPU grid

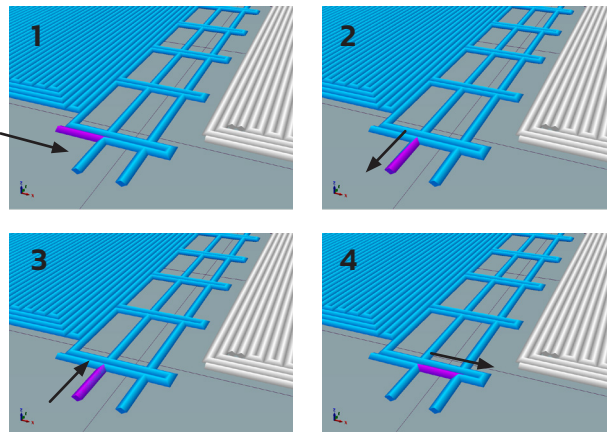
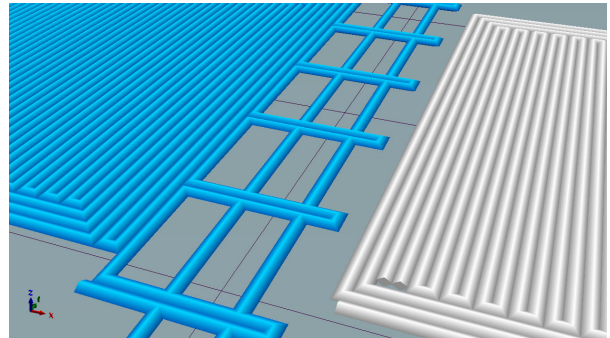


Figure 4.14 2nd TPU grid

4.5 – Bonding strength

The previous paragraphs showed the size limitations of the pattern due to hardware constraints (height and period of PLA bridges), material flow (printing sequence of TPU) and applicability to small parts (pattern height of only three layers). With these limitations in mind we must maximize the bonding strength.

We prepared a model to calculate the peak force of a part. This model allowed us to iterate the shape and maximize the peak force of the part. This theoretical peak force is evaluated with practical tensile tests which are shown in chapter 5.

Model for calculating peak force

A tensional force is applied orthogonal to the interface. The interface is basically a repetition of the same section. A single section is used for calculations. That section is then extrapolated to a larger cross-sectional area for calculating the peak force of the test specimen. Also, the model does not take into account imperfections in printing. These simplifications caused a higher predicted value of the peak force than the evaluation (see chapter 5).

As explained in chapter 3, the shape is form interlocking so either the PLA or TPU part will break. Three failure scenarios are described and calculated in the next paragraphs. We saw all of these three during testing throughout the iterations (see chapter 5).

Such a scenario will be called a failure mode from now on. For each failure mode, the peak force is calculated.

Failure mode C1

Failure mode C1 can be described as the tearing apart of the TPU, which is extruded under, over and around the PLA bridges (see Figure 4.16). The PLA bridges to remain intact.

This cross-sectional area of TPU at its failure location (marked red) is determined for one section. Extrapolating this gives a theoretical maximum force that can be applied to the test specimen. The geometry of the test specimen is shown in chapter 5.

$$A_{TPU,C1} = 1.23 \text{ mm}^2 \text{ see Figure 4.17}$$

$$F_{section} = A_{TPU,C1} \times \sigma_{TPU,tensile,break} = 1.23 \times 39.0 = 48.0 \text{ N}$$

$$A_{section} = H_{section} \times W_{section} = 0.6 \times 4.46 = 2.676 \text{ mm}^2$$

$$A_{specimen} = H_{specimen} \times W_{specimen} = 4 \times 20 = 80 \text{ mm}^2$$

$$F_{specimen} = F_{section} \times \frac{A_{specimen}}{A_{section}} = 48.0 \times \frac{80}{2.676} = 1434.1 \text{ N}$$

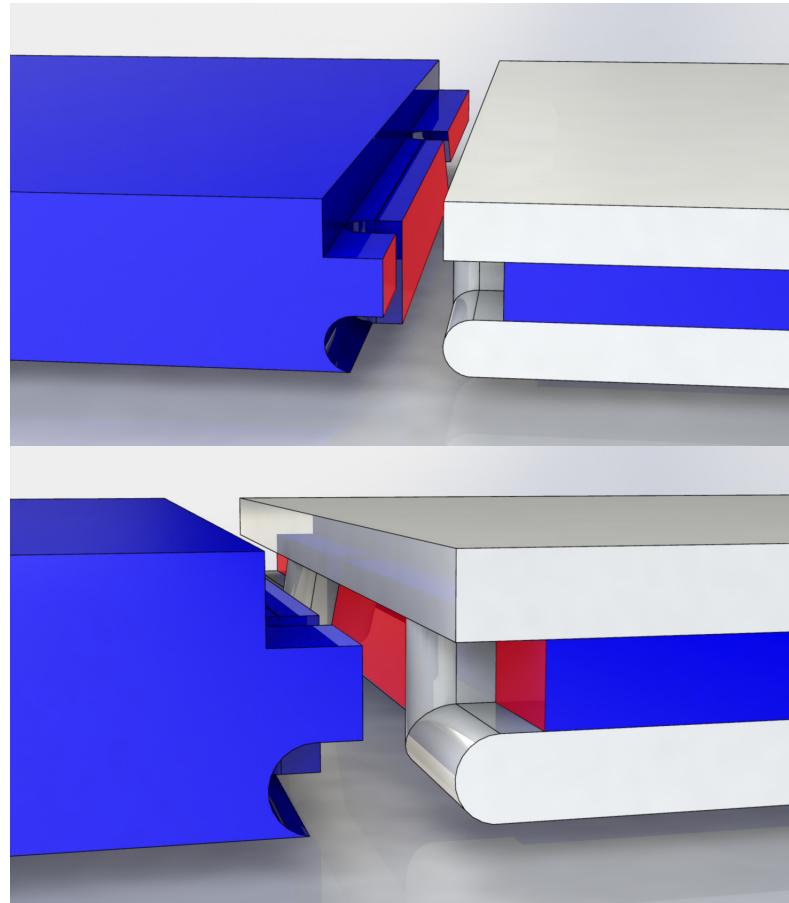


Figure 4.16 failure mode C1

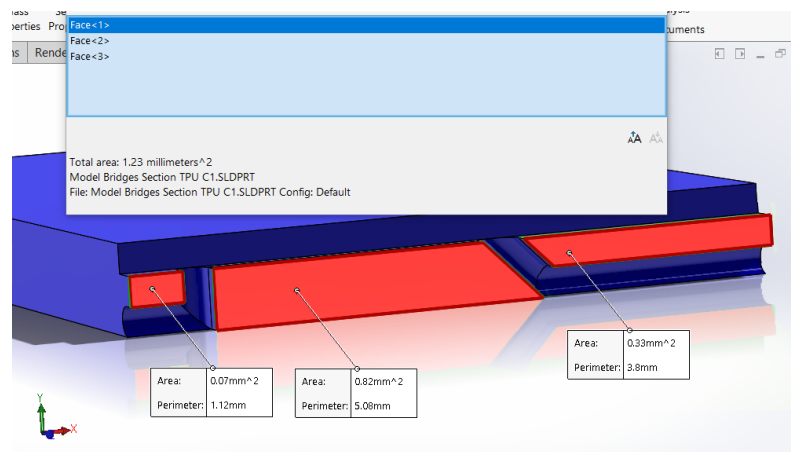


Figure 4.17 cross-sectional area TPU for failure mode C1

Failure mode C2

Failure mode C2 can be described as the breaking of the pillars of the PLA bridge pattern (see Figure 4.18). Three rows of PLA bridges are placed in parallel. All PLA pillars must fail to disconnect the two parts. The maximum force that can be applied is thus limited by the shear strength of PLA and the cross-sectional area of the pillars. Note that this is not the interlaminar shear strength which would be relevant for stacked layers. Here, the PLA bridge is printed continuously so we use the value of PLA shear strength.

$$A_{PLA,C2} = 1.03 \text{ mm}^2 \text{ see Figure 4.19}$$

$$F_{section} = A_{PLA,C2} \times \sigma_{PLA, shear} = 1.03 \times \frac{49.5}{2} = 25.5 \text{ N}$$

$$F_{specimen} = F_{section} \times \frac{A_{specimen}}{A_{section}} = 25.5 \times \frac{80}{2.676} = 762.1 \text{ N}$$

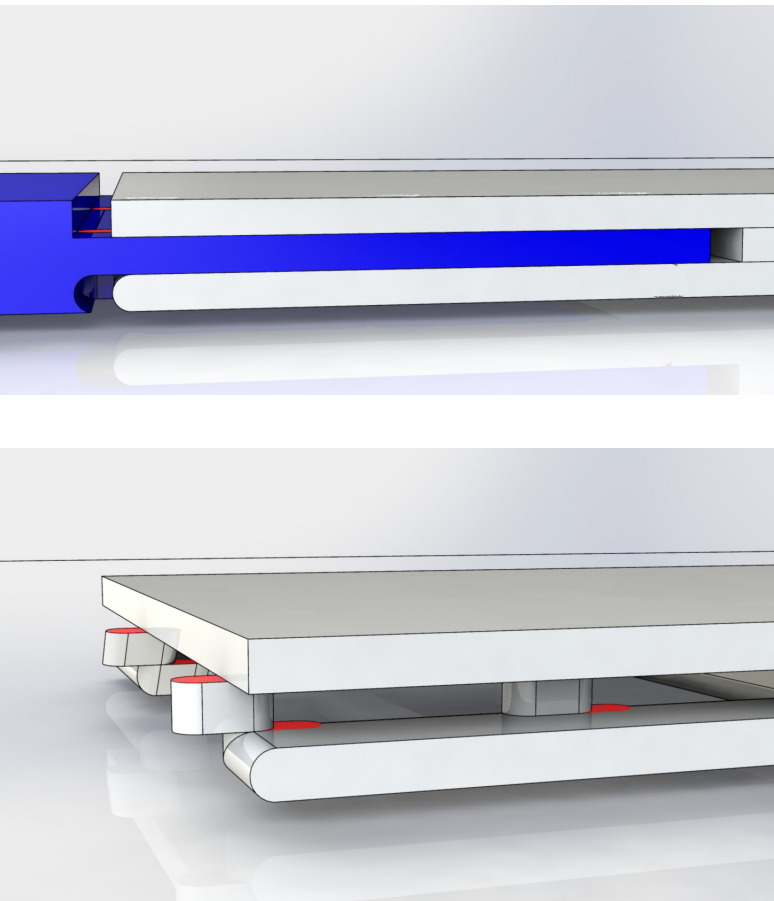


Figure 4.18 failure mode C2

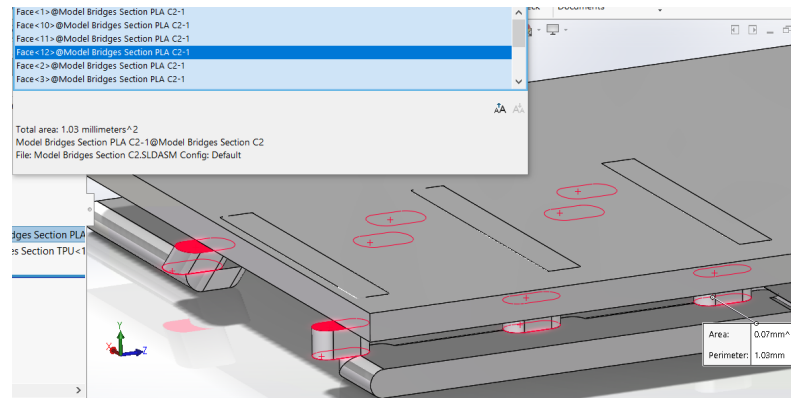


Figure 4.19 cross-sectional area TPU for failure mode C2

Failure mode C3

Last possible failure scenario considered is visualized in Figure 4.20 and can be described as the tearing off of the PLA pattern from the PLA solid. This happens at the third row of the PLA bridge patterns. The TPU part remains intact. Table 4.2 shows an overview of the peak forces of the failures modes

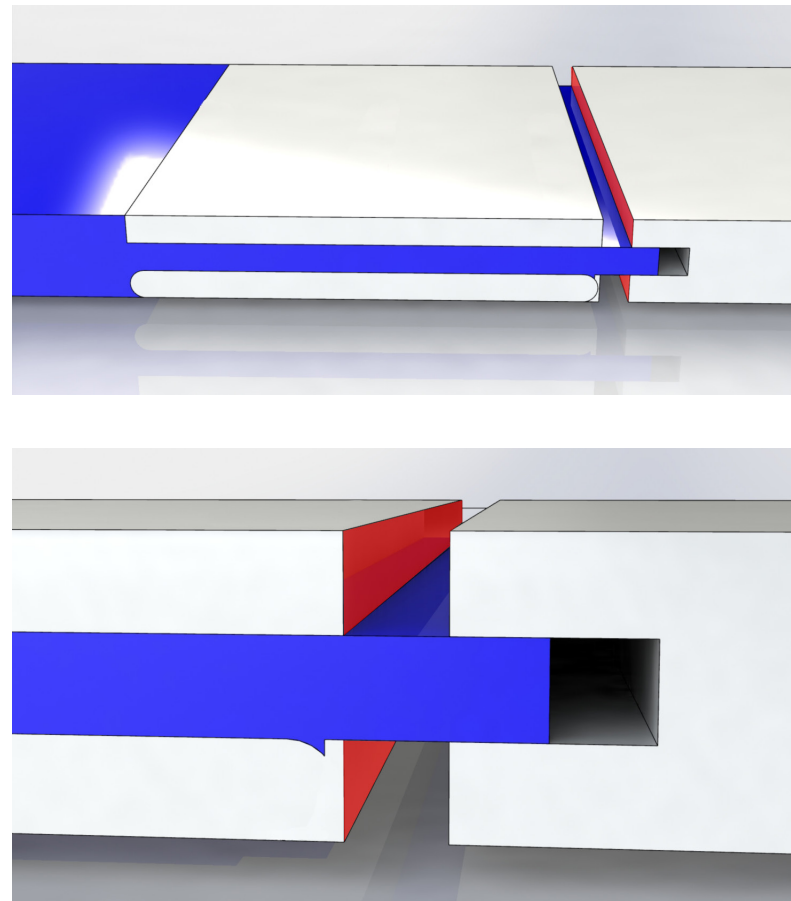


Figure 4.20 failure mode C3

$$A_{PLA,C3} = 1.77 \text{ mm}^2 \text{ see Figure 4.21}$$

$$F_{section} = A_{PLA,C3} \times \sigma_{PLA,tensile} = 1.77 \times 49.5 = 46.2 \text{ N}$$

$$F_{specimen} = F_{section} \times \frac{A_{specimen}}{A_{section}} = 46.2 \times \frac{80}{2.676} = 1381.1 \text{ N}$$

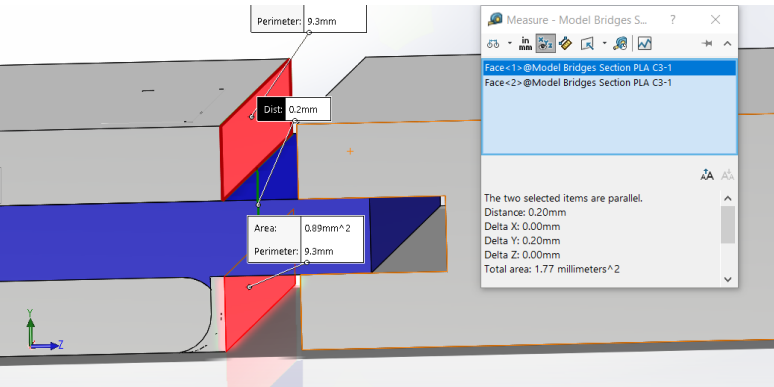


Figure 4.21 cross-sectional area TPU for failure mode C3

4.6 - Slicing software

As explained in the Introduction, the FDM production flow includes slicing a CAD model. The current way of printing is a planar approach. Since the proposed method is a non-planar approach, current slicing software does not suffice. Hence we developed a custom script to generate the toolpath required to create the pattern. The general workflow of the script is depicted in Figure 4.22 and is created using Matlab.

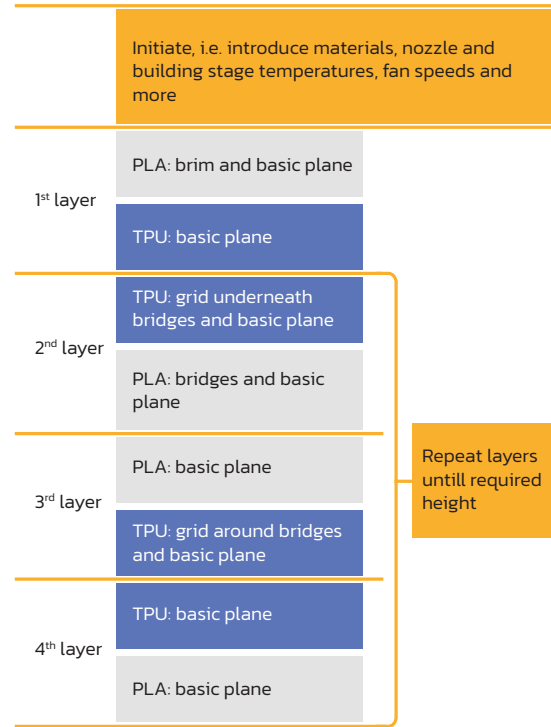
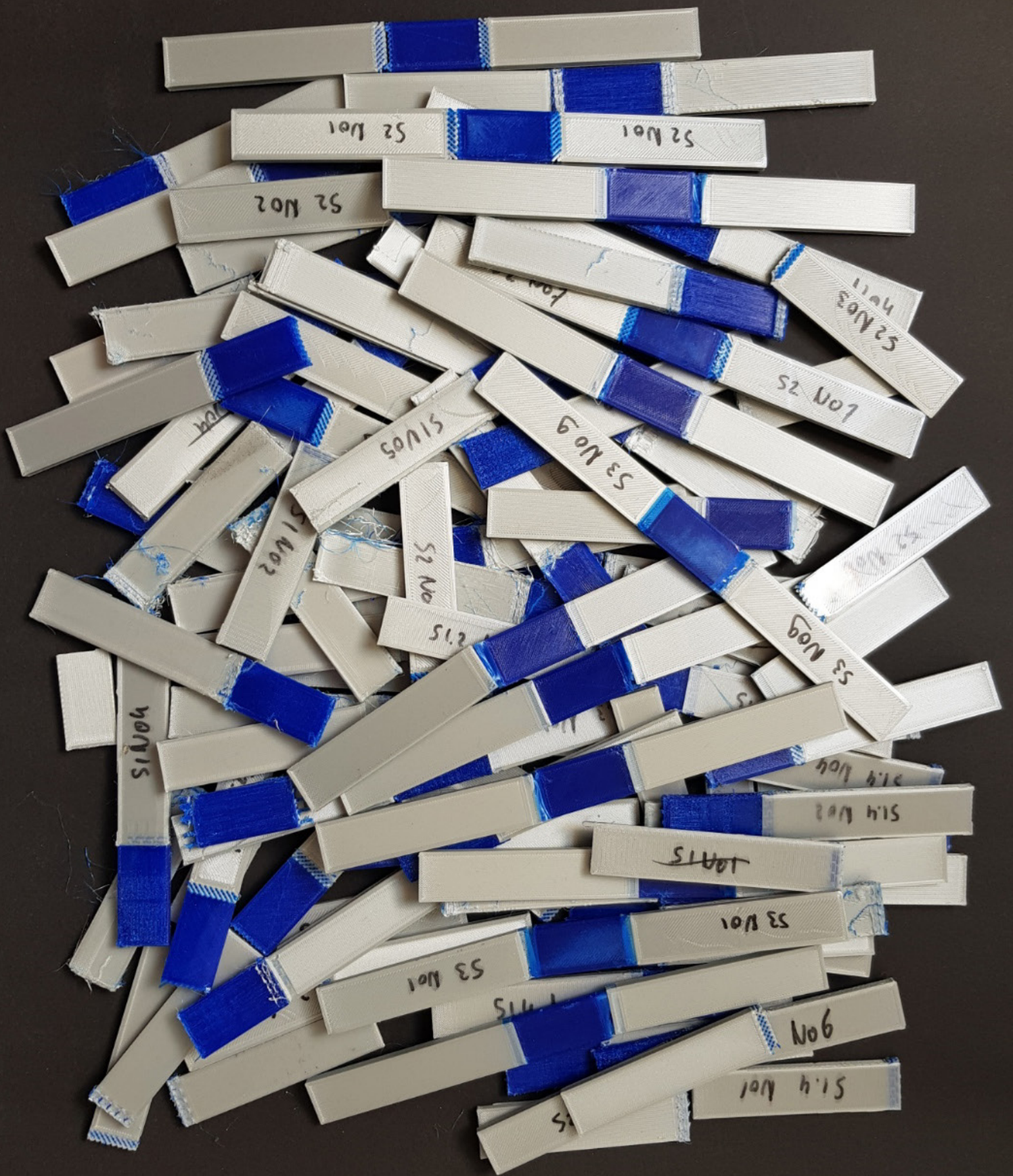


Figure 4.22 Matlab workflow for creating the non-planar pattern

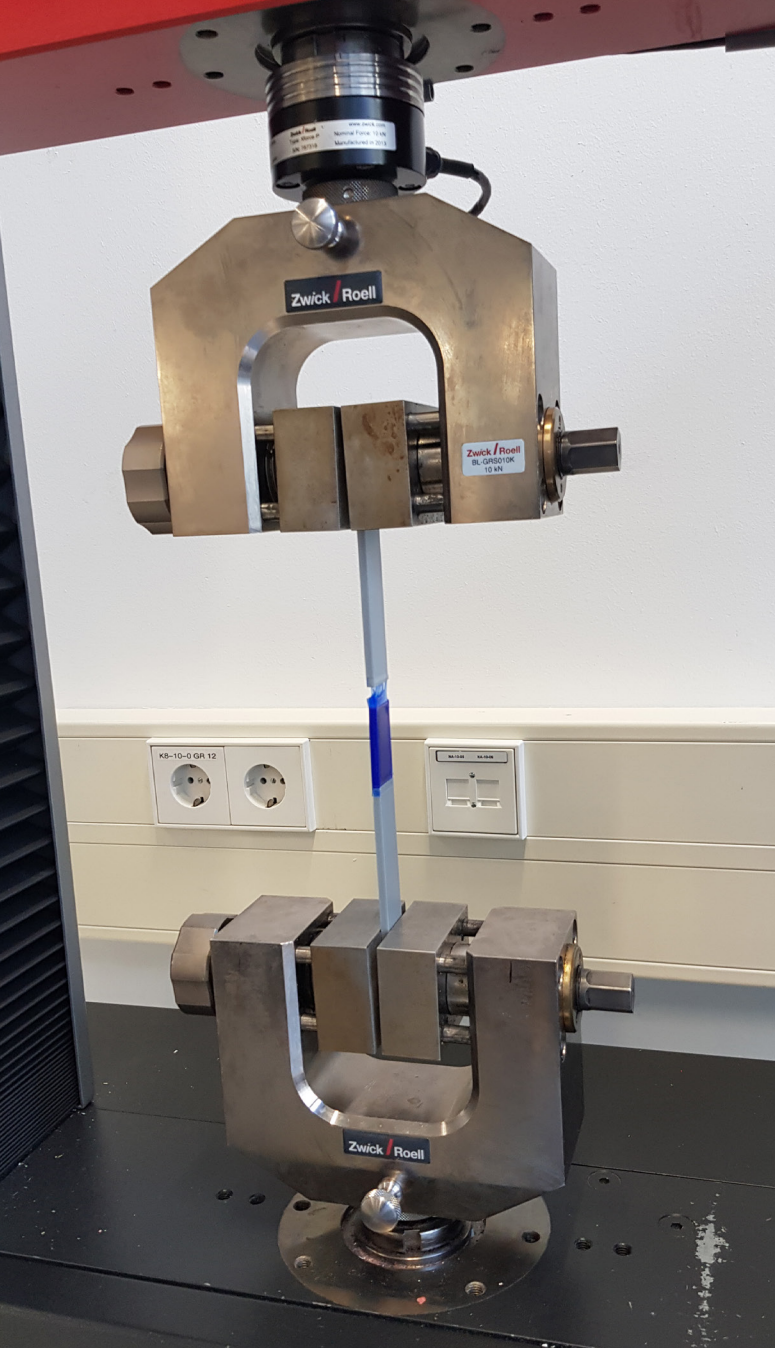
Table 4.2 Overview failure modes

	Failure mode	Failing material	Theoretical peak force of test specimen [N]
	C1	TPU	1434.1
	C2	PLA	762.1
	C3	PLA	1381.1



5: EVALUATION

We created test specimens of TPU and PLA to determine the force–displacement relationship. We used the peak force as a measure of performance of the interface. The performance of the interface created using our proposed method (bridge pattern) is compared with two benchmarks: the overlapping function of Cura (current industry standard) and a planar interlocking pattern (as opposed to the non–planar nature of our solution). This chapter shows the test method including the testing procedure, specimen geometry and it explains what the benchmarks look like. This chapter then reports the results of the iterations of the bridge concept. Here, we explain what and why changes have been made to the bridge concept.



5.1 - Test method

Testing procedure

A Zwick/Roell Z10 testing machine is used for the tensile strength tests. The force is applied orthogonal to the interface. The evaluation of the test specimens is in accordance with the Ultimaker testing procedure. All specimens are pulled at 1 mm/s. The machine stops pulling when the resultant force drops below 70% of its peak force.

Specimen geometry

The standard outer dimensions of an Ultimaker tensile specimen are 215 x 20 x 4 mm (LxWxH). The standard Ultimaker tensile specimen geometry does not account for multi-materiality so an alteration is made (see Figure 5.1). The outer parts of the test samples are made of PLA which are gripped into the tensile machine. The middle part is made of TPU. Having TPU at one end and PLA at the other may otherwise cause a mismeasurement because of different required clamping forces. This means that the specimen has two boundary interfaces. The middle part (TPU) has a length of 40mm.

In total, 10 specimens are printed at room temperature for each test. Specimens with signs of defects or any abnormalities before, during or after testing were discarded, hence the slightly differing sample sizes.

The interfaces containing the bridge pattern were printed 10mm wider than the width of the test specimen (see Figure 5.2). This way, the pattern,

which is discrete, is not discontinued within a section during printing. After printing, the interfaces are manually cut to its appropriate width. The following print parameters are applied to all specimens (see Table 5.1).

Table 5.1 printing parameters

	PLA	TPU	
Layer height [mm]	0.2		
Layer width [mm]	0.4		
Nozzle temperature [°C]	200	230	
Bed temperature [°C]	60		
Printing speed [mm/s]	70	25	*printing speeds of inner walls, first layer, brim and bridge pattern may differ
Fan speed [%]	100	20	
Density [%]	100		
Shell [mm]	1.2		

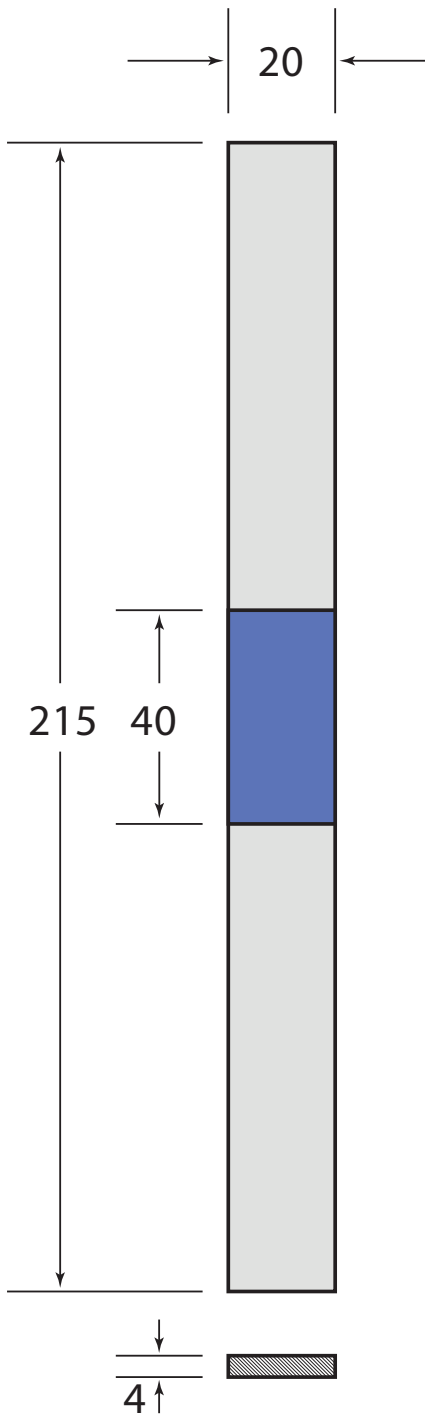


Figure 5.1 specimen geometry

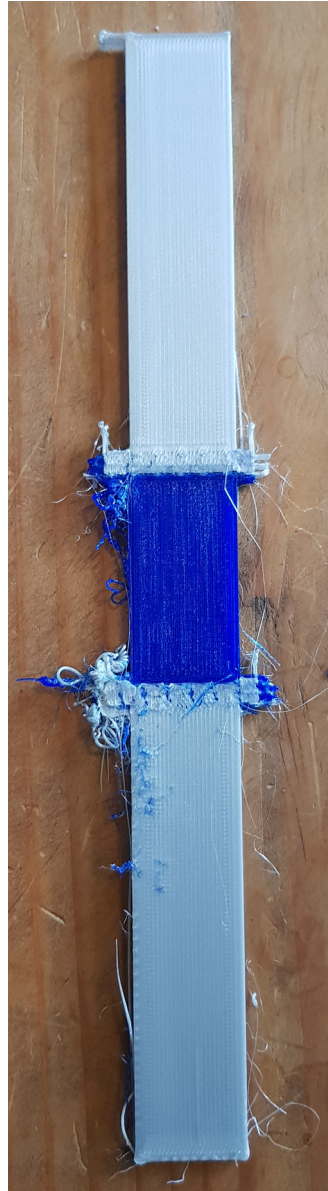


Figure 5.2 extended interface

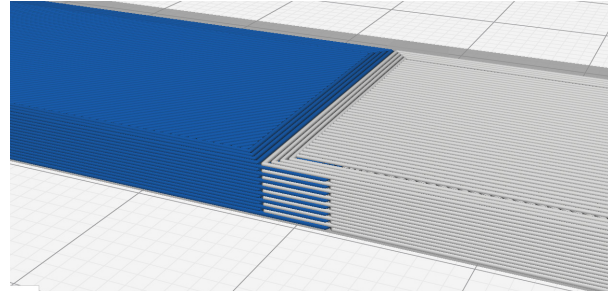


Figure 5.3 Cura overlapping feature layer 16

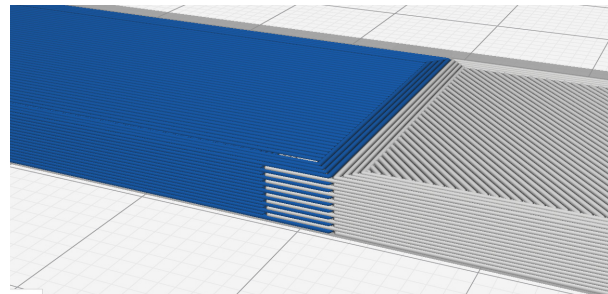


Figure 5.4 Cura overlapping feature layer 17

Benchmark 2 - Hacksaw pattern

One of the features of the bridge pattern is the non-planar printing approach. As a second benchmark, we tested an interface using a form interlocking shape created with a planar printing approach. This interlocking shape is based on the Technical disclosure common of Kuipers (2020) and looks the following (see Figure 5.5 and Figure 5.6): fingers are attached to the circumference of both volumes. Under 45°, these fingers protrude the other material. Each layer, this 45° orientation is reversed, creating a form interlocking shape in three directions (X, Y, Z).

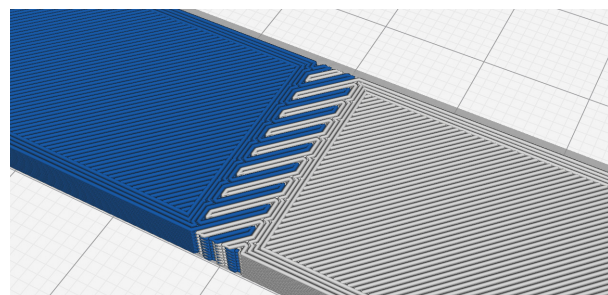


Figure 5.5 Hacksaw pattern layer 16

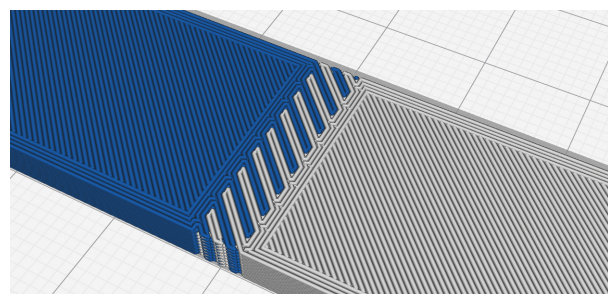


Figure 5.6 Hacksaw pattern layer 17

5.2 - Benchmarks

Benchmark 1 - overlapping function Cura

The bridge pattern is tested against the current industry standard: the overlapping function of Cura. Cura allows two models to partly overlap. At this overlapping section, it alternates between the two models creating an alternating pattern of overlapping layers. As explained in chapter 4, such overlapping layers create friction. See Figure 5.3 and Figure 5.4.

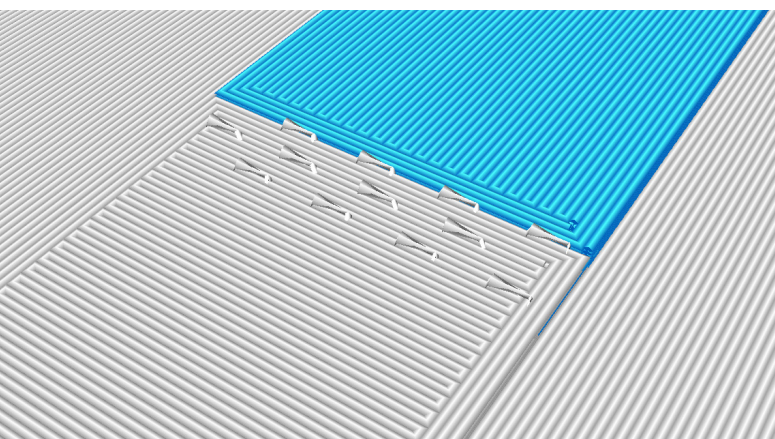
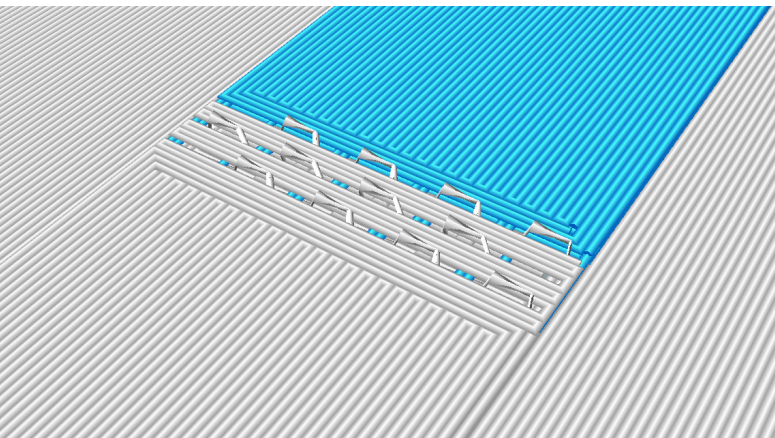
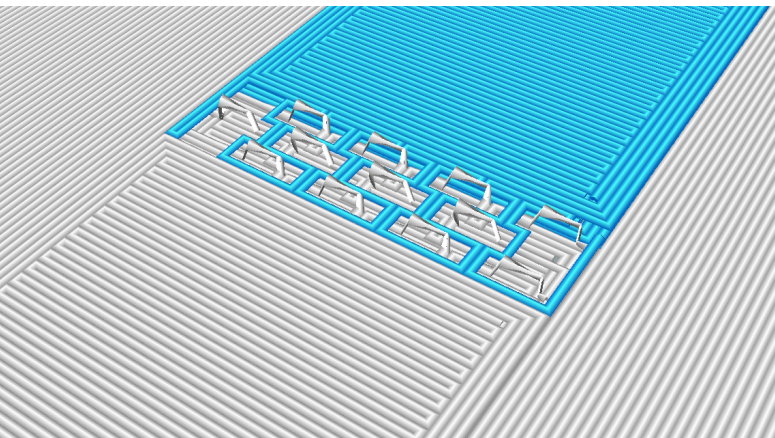
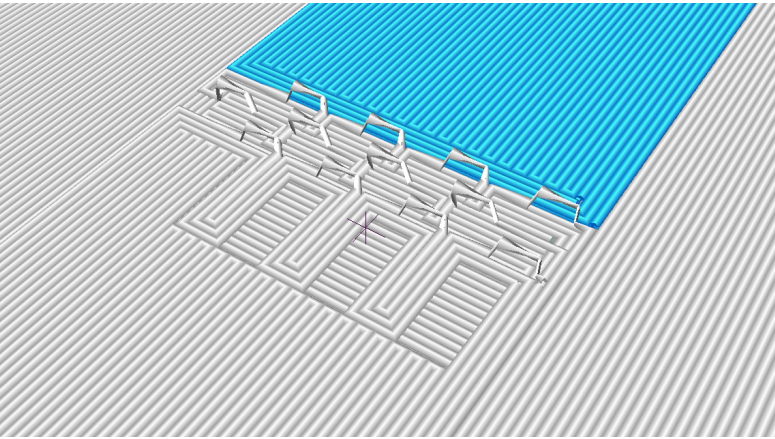


Figure 5.8 S1.1 printing toolpath

5.3 – Testing

This iterative process has been divided into four sections which all contain an explanation of the tested specimen, the result and a conclusion. It is the last iteration (specimen 1.4) that is shown in chapter 3 and further explained in chapter 4.

Specimen 1.1

The first specimen was created in the following sequence (see Figure 5.8): PLA bridges are printed on top of a PLA plane. TPU is extruded around the bridges and between the rows of bridges. This TPU extrusion was done in a zigzag pattern to prevent path crossing, i.e. printing material at places where the nozzle had already extruded material. Then, a PLA plane was printed to connect the tops of the PLA bridges. When extruding material between the rows of PLA bridges, the printing head runs parallel with the bridge pattern. Another PLA plane is printed as top plane.

Result S1.1

We have already seen in chapter 4 that this printing sequence led to a lack of TPU fill under the PLA bridges. This effect could be distinguished during production (see Figure 5.9) and after testing when analyzing the intersection after tearing (see Figure 5.7).

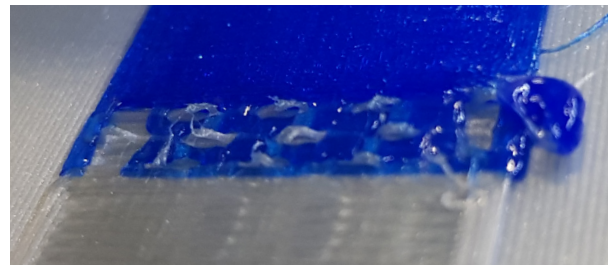


Figure 5.9 S1.1 lack of TPU fill under PLA bridges

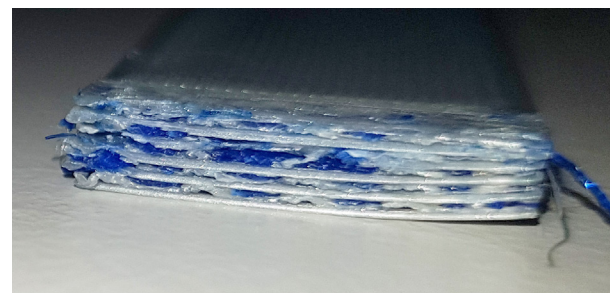
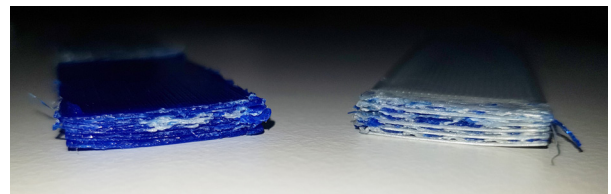


Figure 5.7 failed interface S1.1

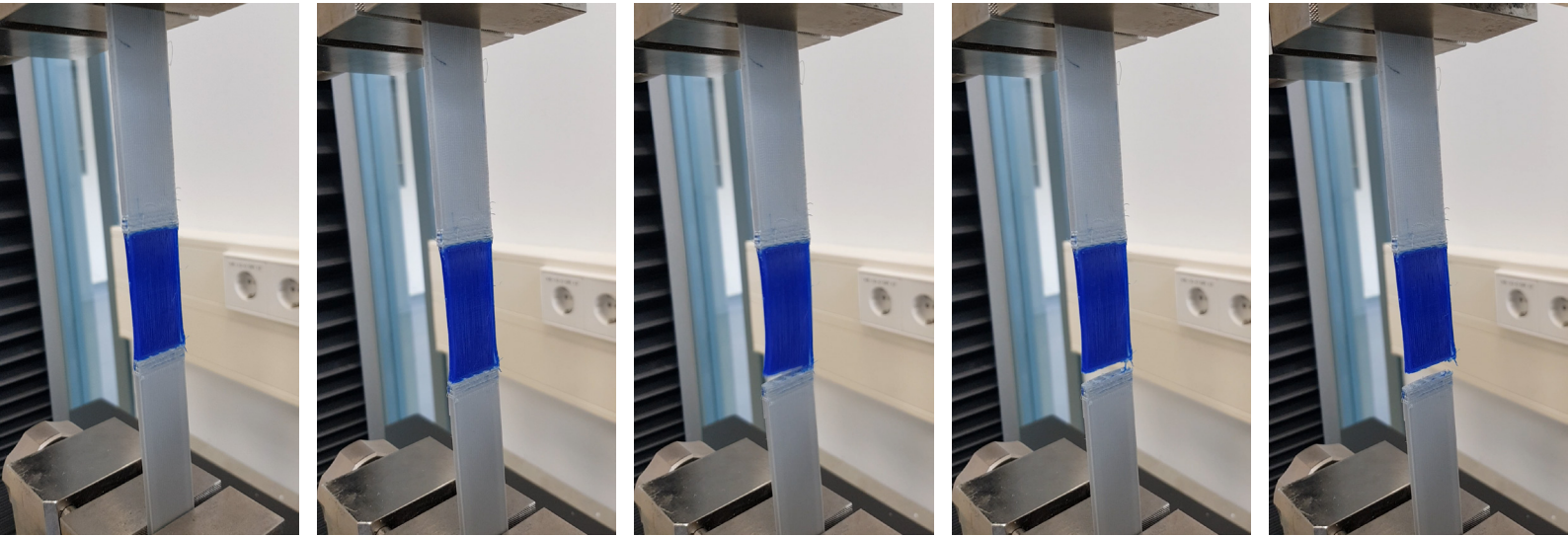


Figure 5.10 tensile test S1.1

Conclusion S1.1

These results show that the TPU does not flow enough to fill the areas under the PLA bridges. The TPU grid does not bond everywhere with the TPU solid causing extra stress in the other TPU fibers of the grid. Therefore, the TPU tears which was described as failure mode C1. The solution is presented in the next paragraph.

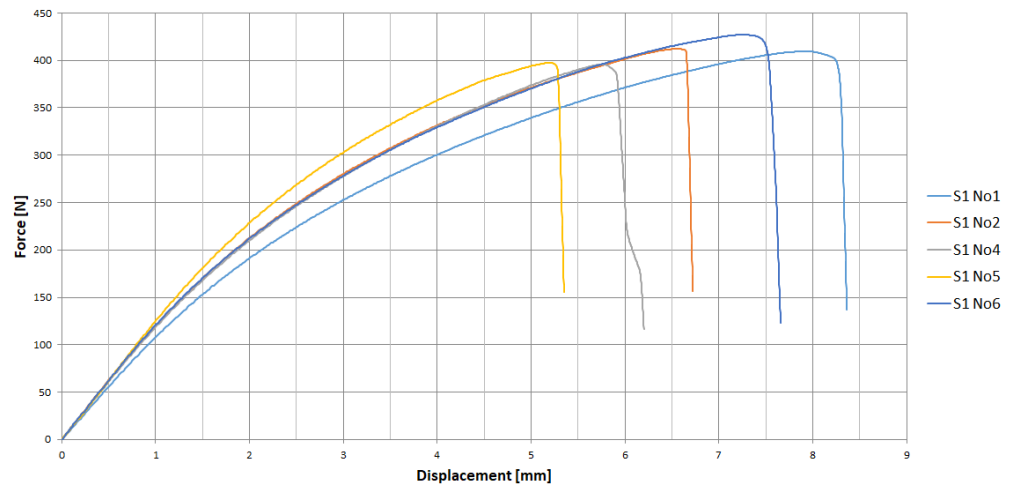
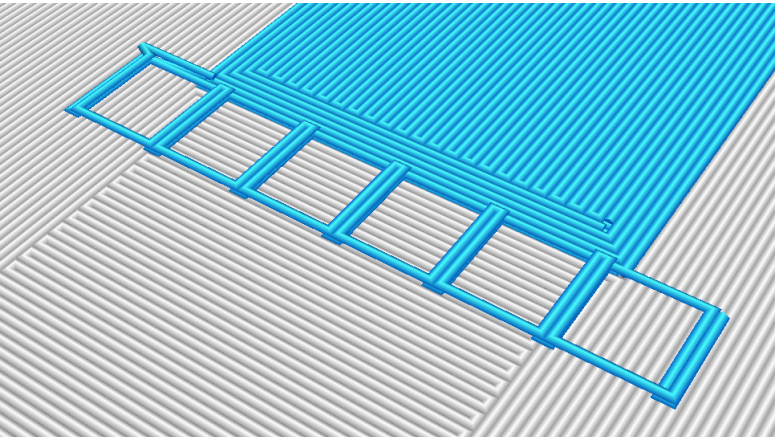
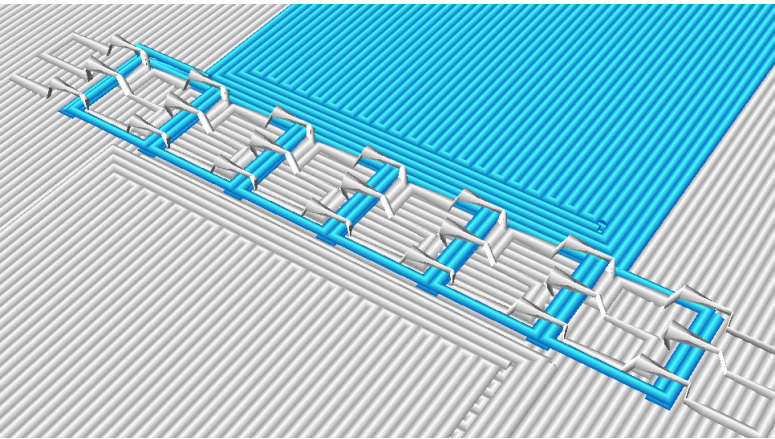


Figure 5.11 force-displacement graph S1.1



Specimen 1.2

In order to fill the areas under the PLA bridges, the printing sequence was changed. A TPU grid is now printed first. The fibers of the grid are now oriented in-line with the applied force instead of a zigzag. Across this grid, the PLA bridge pattern is printed. Then after printing the PLA bridges, another TPU grid is printed to interlock the pattern. Thirdly, we decreased the structures height. We expected that creating more of these bridge sections within a specific height would improve the strength. The structure height is now three layers instead of four. Also, a lower pattern increases the applicability to small parts.



Result S1.2

This iteration shows an improvement in TPU material fill under the PLA bridges. The peak force is however only 73% of specimen 1.1. Specimen 1.2 fails according to failure mode C3: failure at the innermost PLA bridge. The PLA bridge structure breaks away from the PLA solid. The TPU part remains intact.

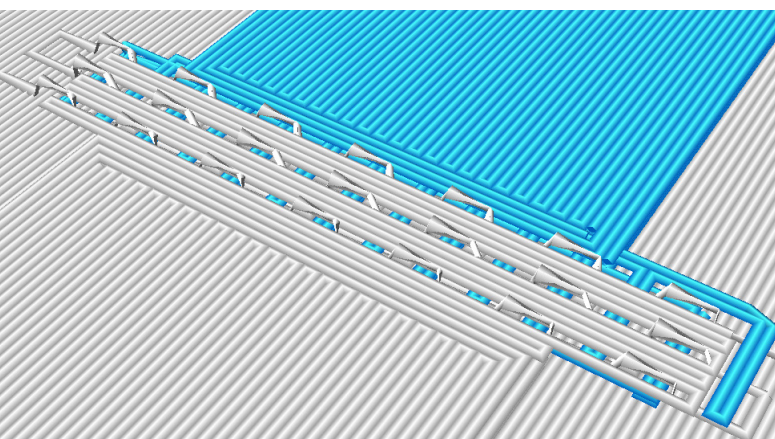
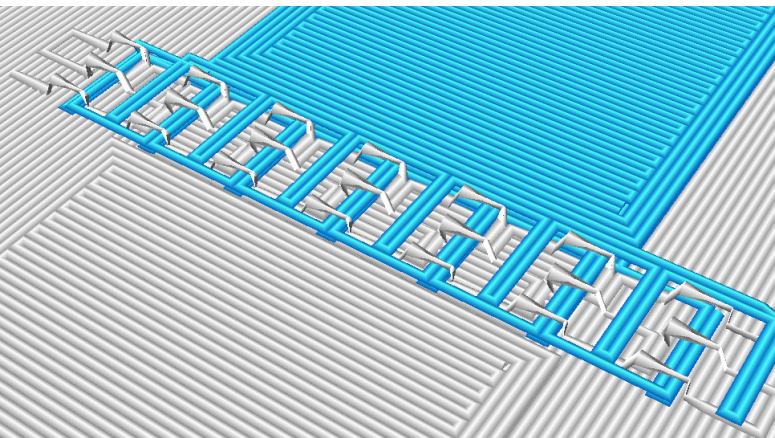


Figure 5.12 S1.2 printing toolpath

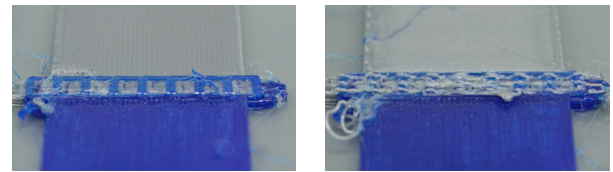


Figure 5.14 S1.2 printing step (1) and step (2)

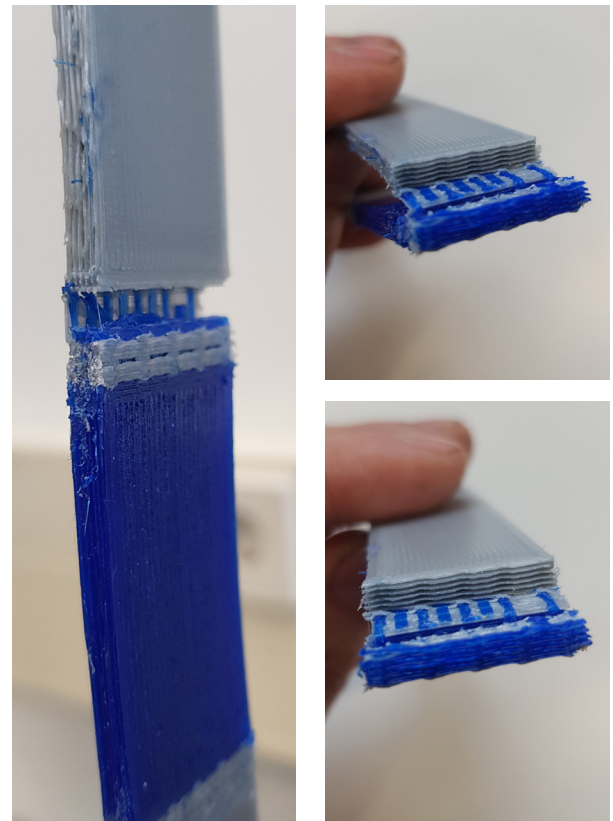


Figure 5.13 S1.2 interface failure

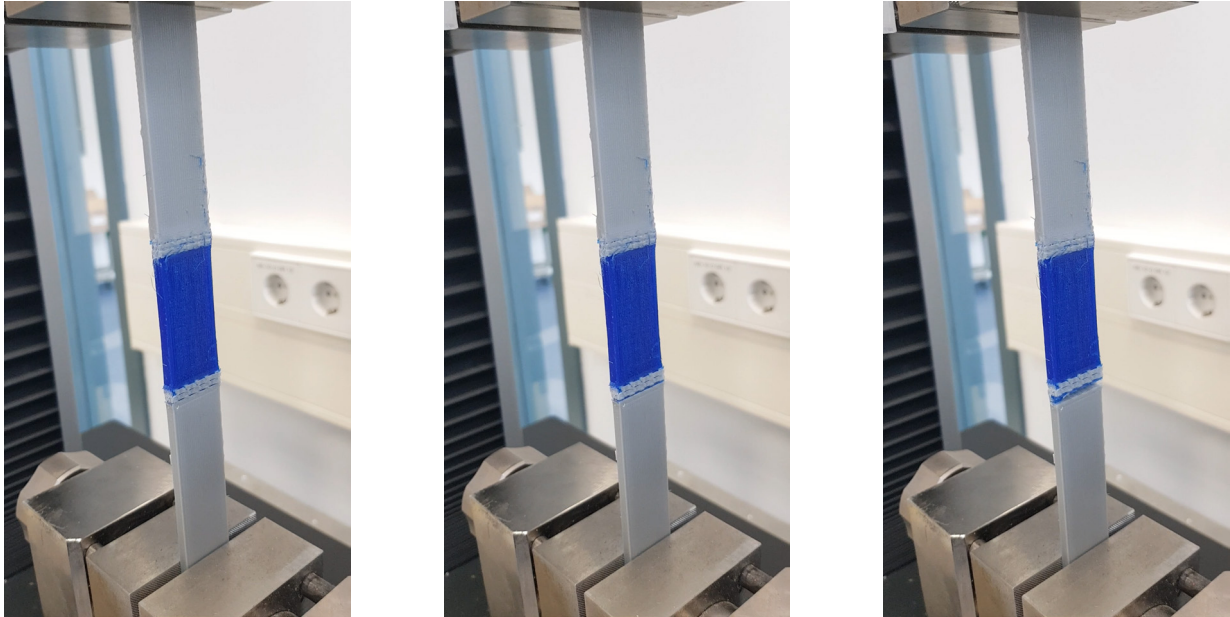


Figure 5.15 tensile test S1.2

Conclusion S1.2

These results show that changing the printing sequence improved the TPU fill under the PLA bridges.

Decreasing the structure height did not yield the intended results. Since we removed the last PLA layer of every section of S1.1 (see Figure 5.8), the current top PLA layer (see Figure 5.12) is aligned orthogonal to the applied load. The fibers of the PLA top layer run parallel with the PLA bridges. The applied force is orthogonal to the interface (see Figure 46). As we have seen in chapter 1, the strength orthogonal to a fiber is lower than in-line with the fiber. Next paragraph shows what changes were made to solve this.

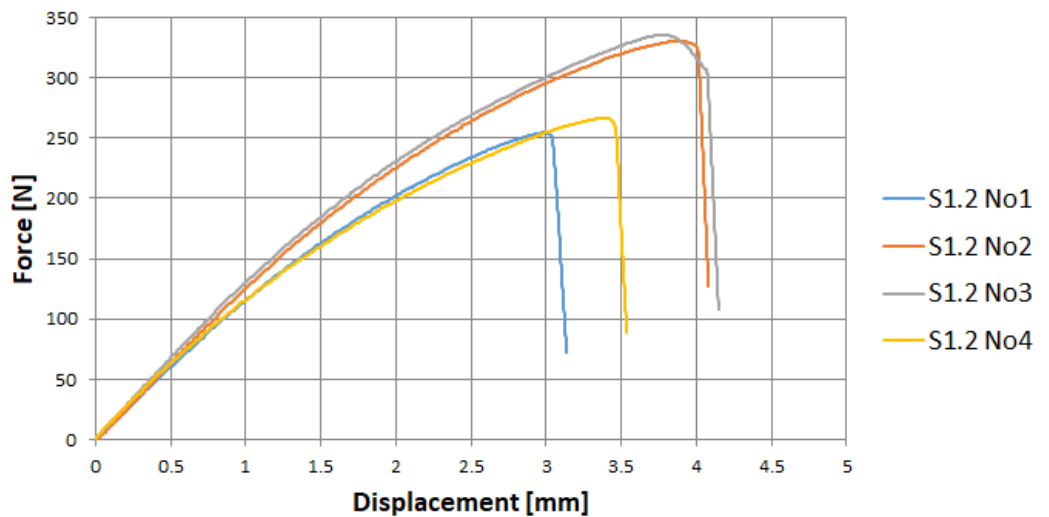


Figure 5.16 force-displacement graph S1.2

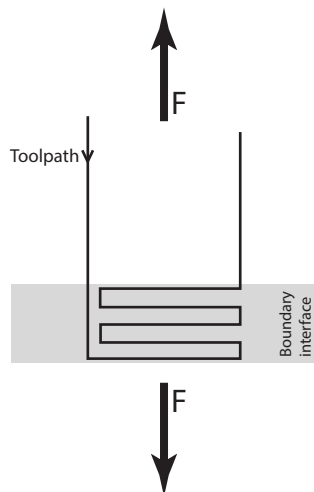


Figure 5.17 S1.2 toolpath alignment

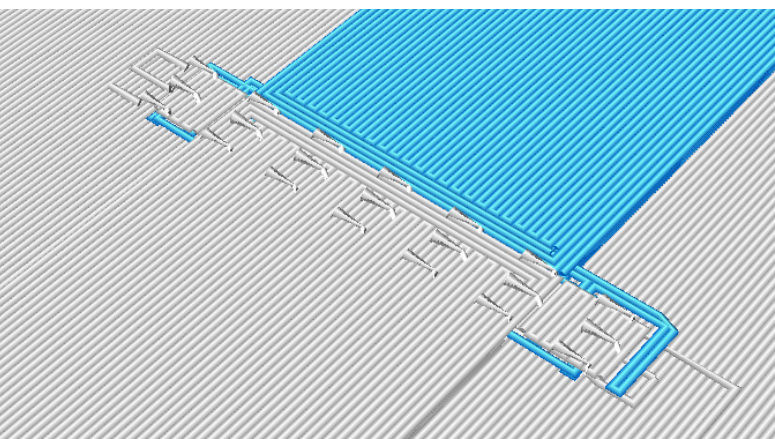
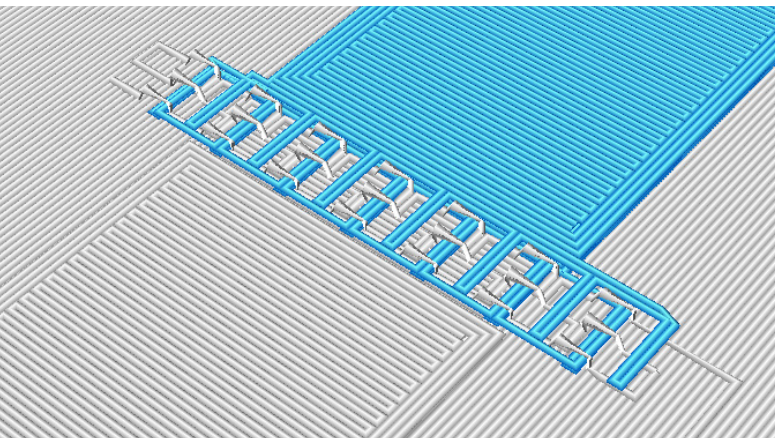
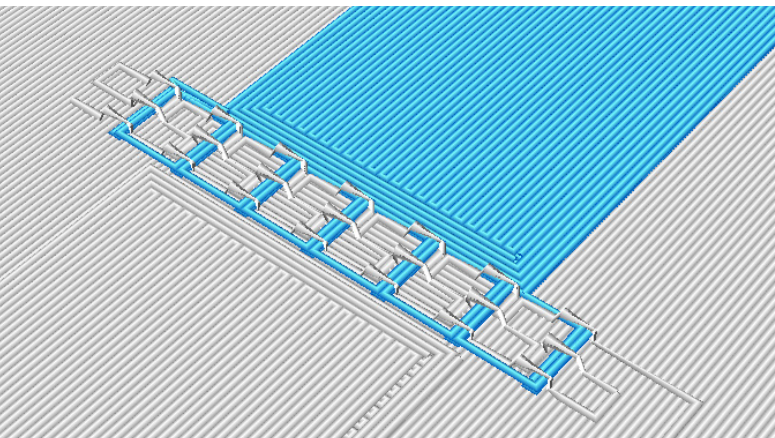
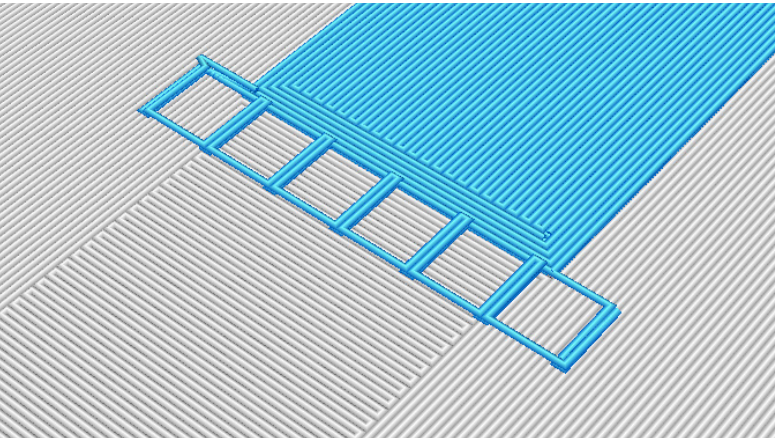


Figure 5.18 S1.3 printing toolpath

Specimen 1.3

Since the orientation of the PLA top layer was incorrect, we changed this to a plane with fibers in-line with the applied load. Also, where we extruded the material of the top layer of specimen 1.2 between the tops of the PLA bridges, we are now printing right over the top of the PLA bridges (see sideview of the structure in Figure 5.19). This will improve the bonding of the tops of the bridges with the top plane.

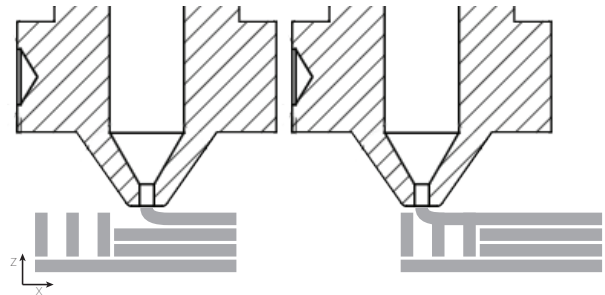


Figure 5.19 S1.3 printing PLA toplayer, sideview

Result 1.3

The PLA bridges remain intact. The TPU fails at the start of the interface (failure mode C1). The peak force has now increased to 468N.

By peeling off some layers of the specimen, we distinguished a lack of interconnection of the TPU grids. The two TPU grids (one extruded before printing PLA bridges, and one afterwards) are currently not connected with each other.

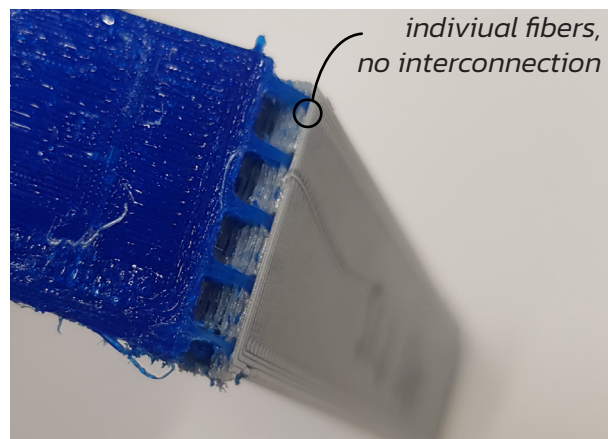
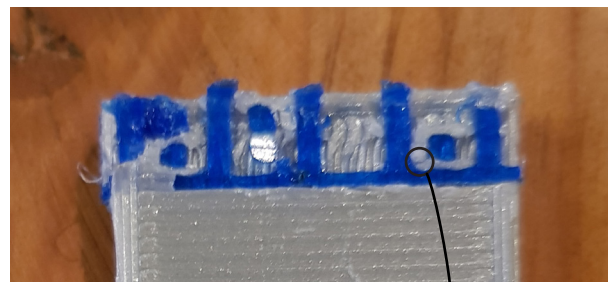


Figure 5.20 S1.3 interface failure

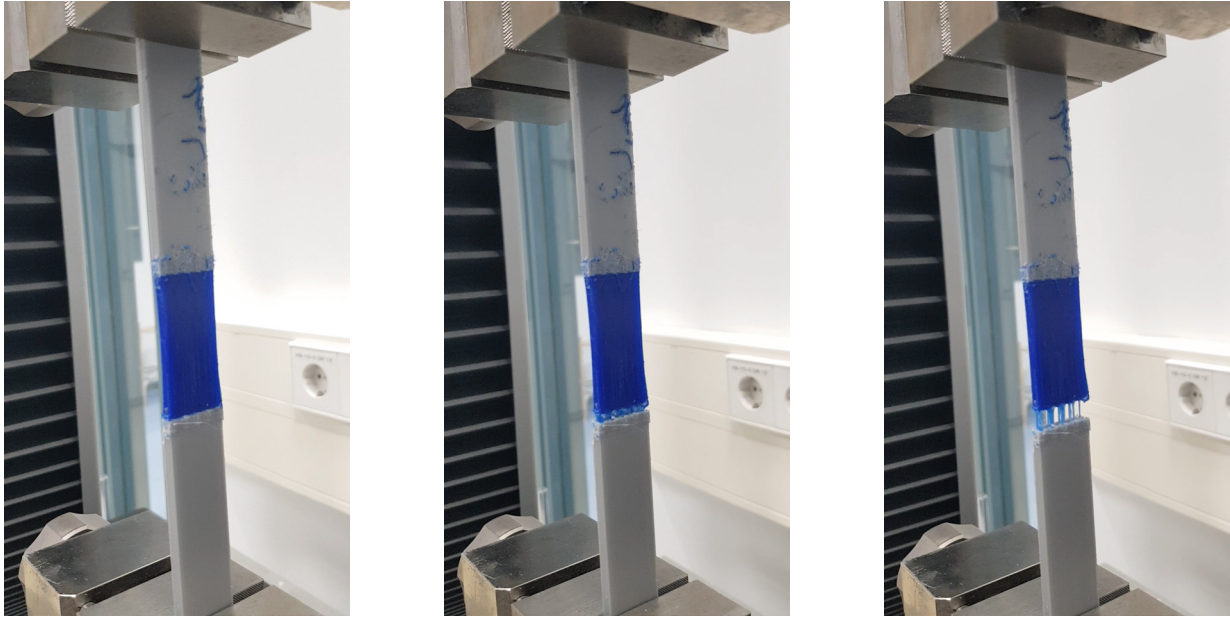


Figure 5.21 tensile test S1.3

Conclusion 1.3

Changing the orientation and extrusion of the PLA top layer improved the bond between the PLA bridge structure and PLA solid. The two TPU grids are currently unconnected. This way, the stresses cannot be distributed between the TPU fibers. Creating these interconnections will improve the tensional strength. The next paragraph shows how we solved this.

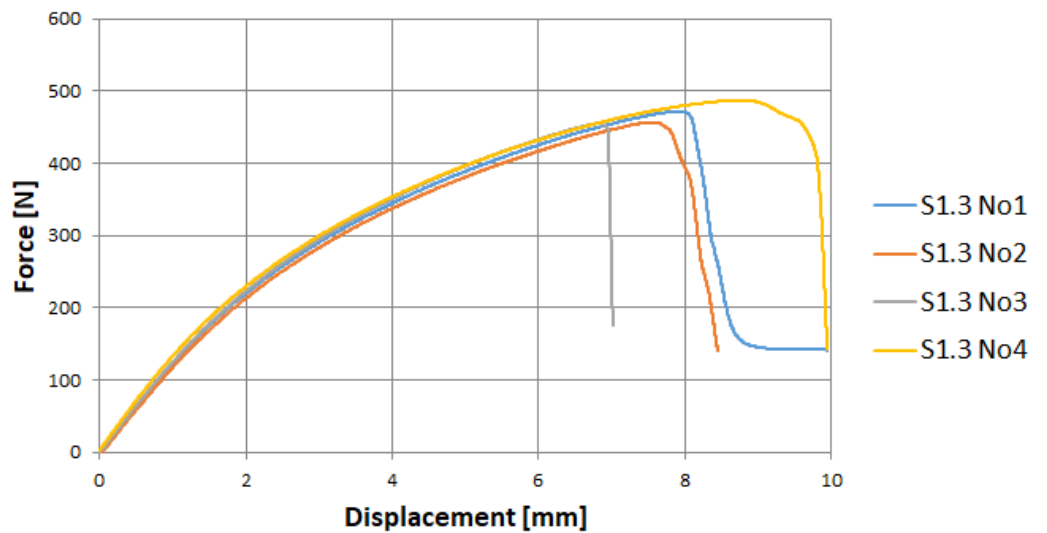


Figure 5.22 force-displacement graph S1.3

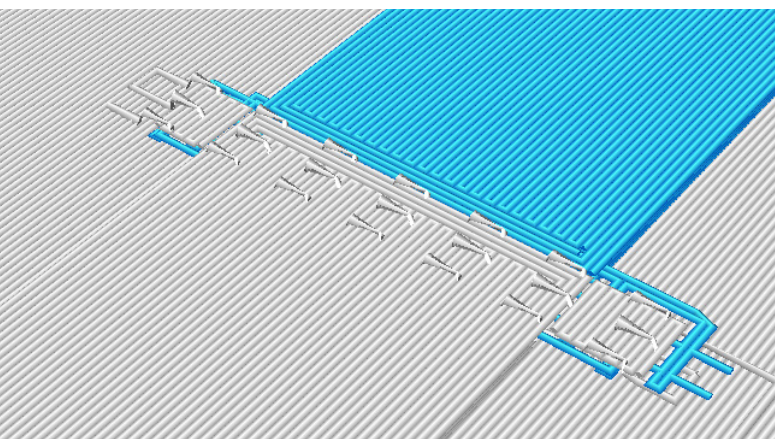
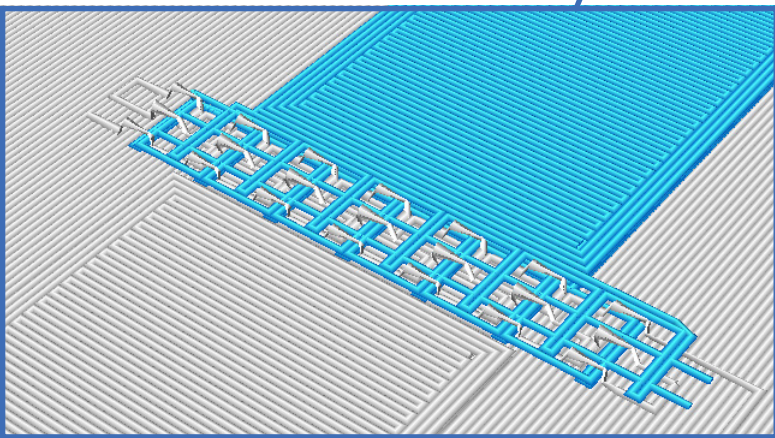
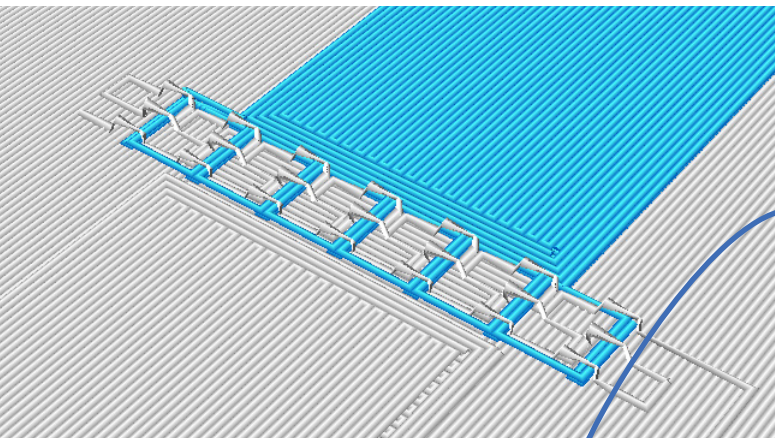
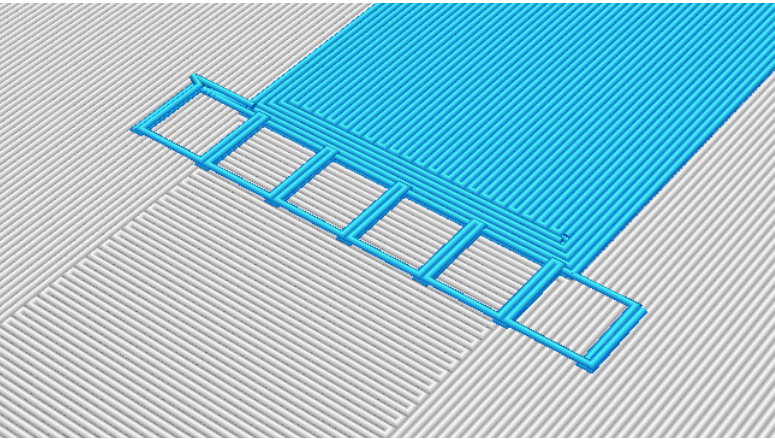


Figure 5.23 S1.4 printing toolpath

Specimen 1.4

In order to create the interconnections between the two TPU grids, we changed the extrusion path of the second grid. Between each PLA row, the printing head makes a sidestep. Here, the printing head moves back-and-forth along the same path (see Figure 5.24). This should improve the TPU material fill around the PLA bridges and so the connection towards the first TPU grid.

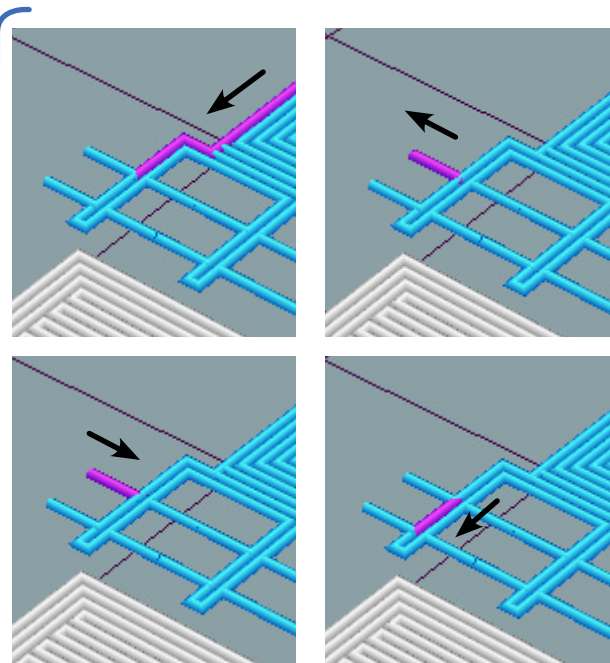


Figure 5.24 S1.4 TPU grid printing toolpath

Result 1.4

This iteration results in a peak force of 491N, an increase of 5% compared to specimen 1.3. We observed two failure modes. The TPU fails at the start of the interface which is failure mode C1. Failure mode C1 describes failure of the TPU as a straight line just between the TPU solid and PLA bridges. We observed that it actually fails with an offset. The TPU under every PLA bridge fails at an offset relative to the material around the PLA bridge (see Figure 5.29).

Also, we observe a partial failure of PLA bridge pillars. Failure mode C2 describes failure of all PLA bridge pillars. This is however not the case, not all pillars fail. Only every second pillar of the first row of bridges fail (see Figure 5.27).

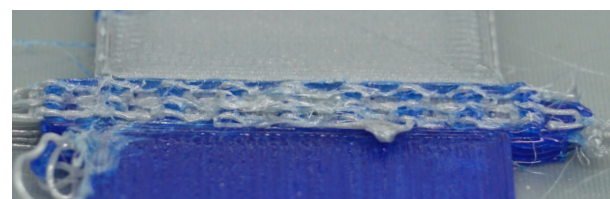


Figure 5.25 printing PLA bridges

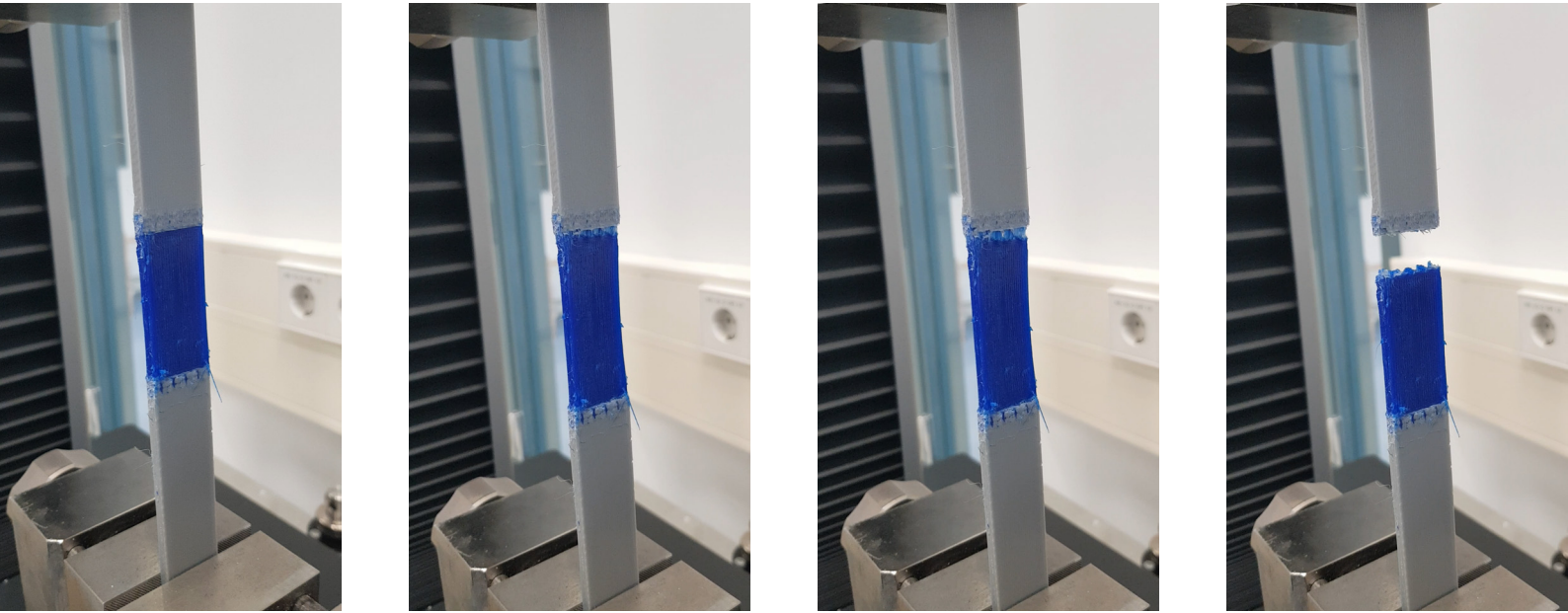


Figure 5.26 tensile test S1.4

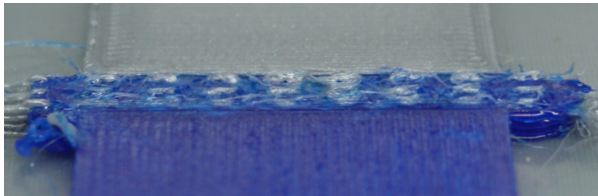


Figure 5.30 printing 2nd TPU grid

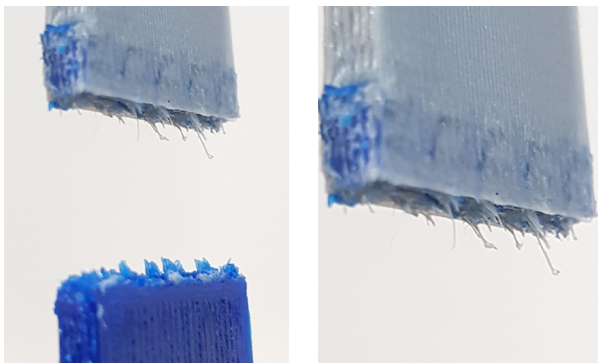


Figure 5.27 S1.4 interface failure

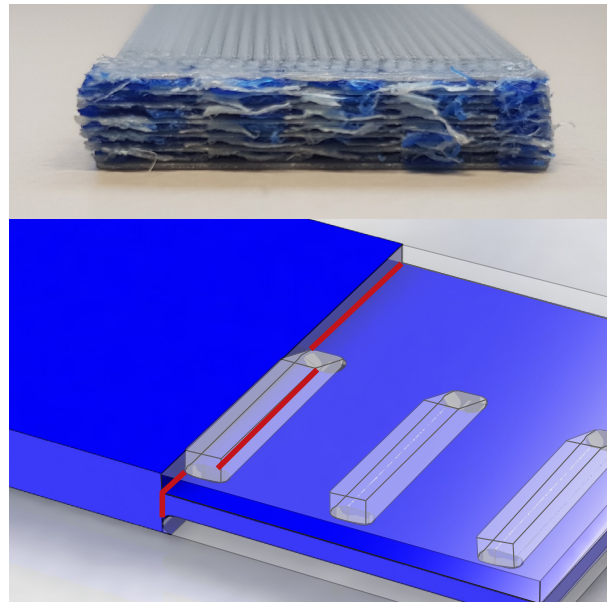


Figure 5.29 TPU failure of S1.4

Conclusion 1.4

We have shown that changing the toolpath of the second TPU grid improves the connections of the TPU part of the interface. This last iteration resulted in a peak force of 491N.

We noticed failure of the second pillars of the PLA bridges which could be explained by the following: the second pillar is created

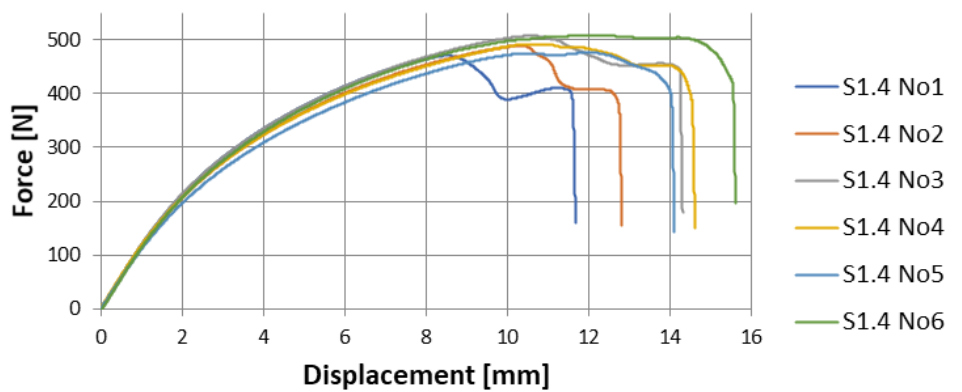


Figure 5.28 force-displacement graph S1.4

by extruding whilst moving downwards at a 45° angle. As shown in chapter 4, the extruded material curves around the nozzle. This effect decreases the integrity of the second PLA bridge pillar.

In addition to this, a simulation shows the stresses throughout the TPU (see Figure 5.31). The flexibility of TPU causes an unequal distribution of stresses along the rows. The TPU around the first PLA bridges row will encounter higher stresses than the second and third row. Even when all second pillars in the first row fail, the stresses are not passed down through the third row (see Figure 5.32). This suggests that adding more than two rows would not increase the peak force.

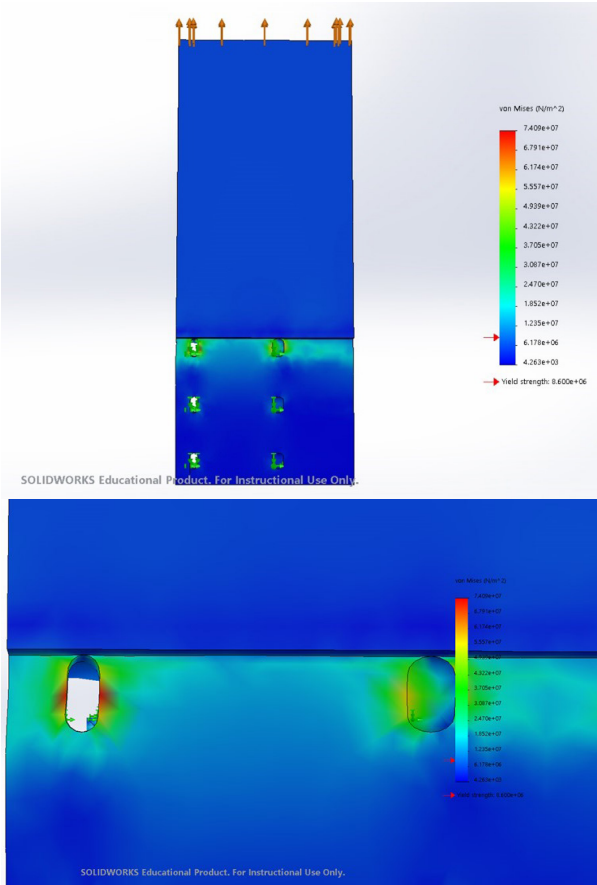


Figure 5.31 TPU simulation

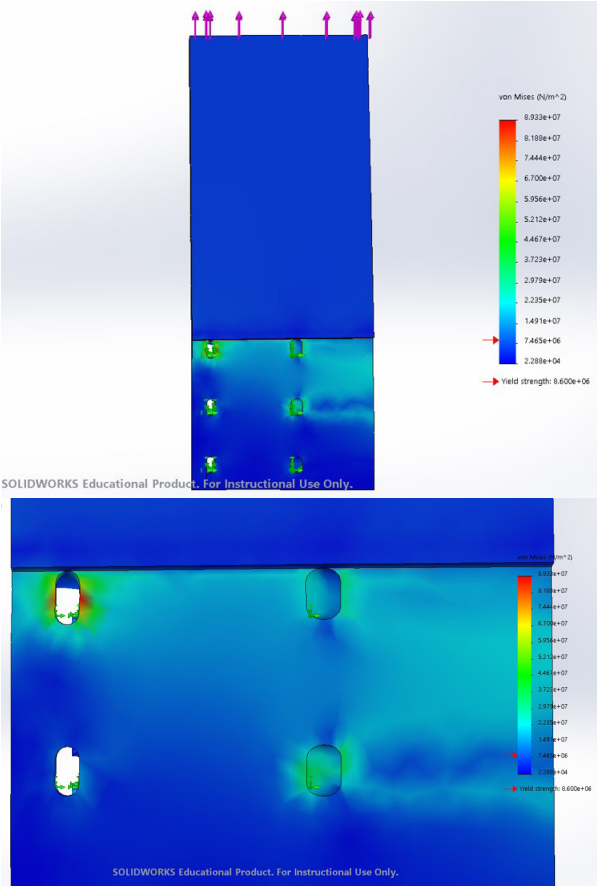


Figure 5.32 TPU simulation given a failed second PLA pillar

Benchmark 1

We created an overlap of 4 mm for the PLA and TPU sections of the test specimen. This interface width is slightly wider than the bridge pattern (width 3.6 mm).

Result B1

The friction force is enough to create some TPU yielding and transverse contraction but not enough to break one of the materials. Both materials remain intact. The TPU slips out of the PLA overlapping layers.

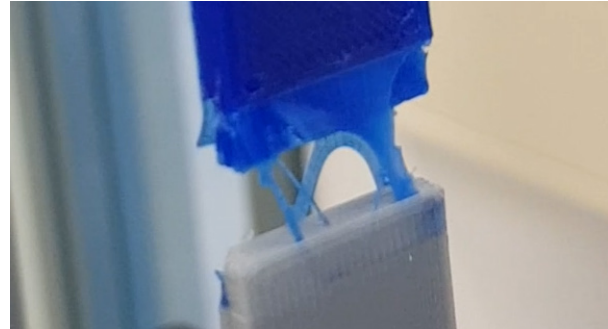


Figure 5.34 B1 interface failure

Conclusion B1

The maximum friction force that this overlapping method can generate is 415N. After the peak force, the parts start to slip away from each other. Besides observing this slipping effect, it can be seen from the slowly falling line after the peak force in the force-displacement graph (see Figure 5.35).

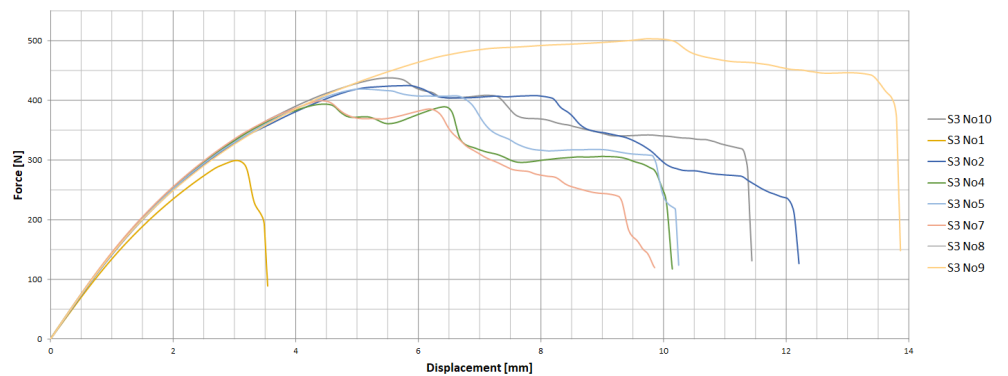


Figure 5.35 force-displacement graph B1

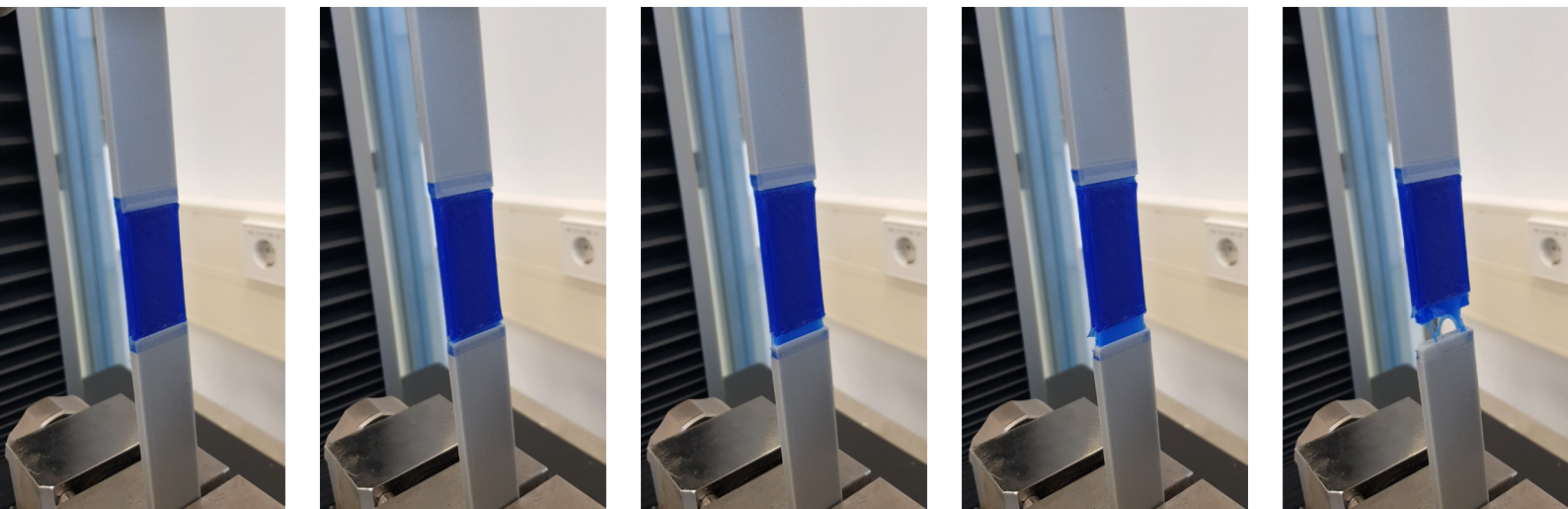


Figure 5.33 tensile test B1

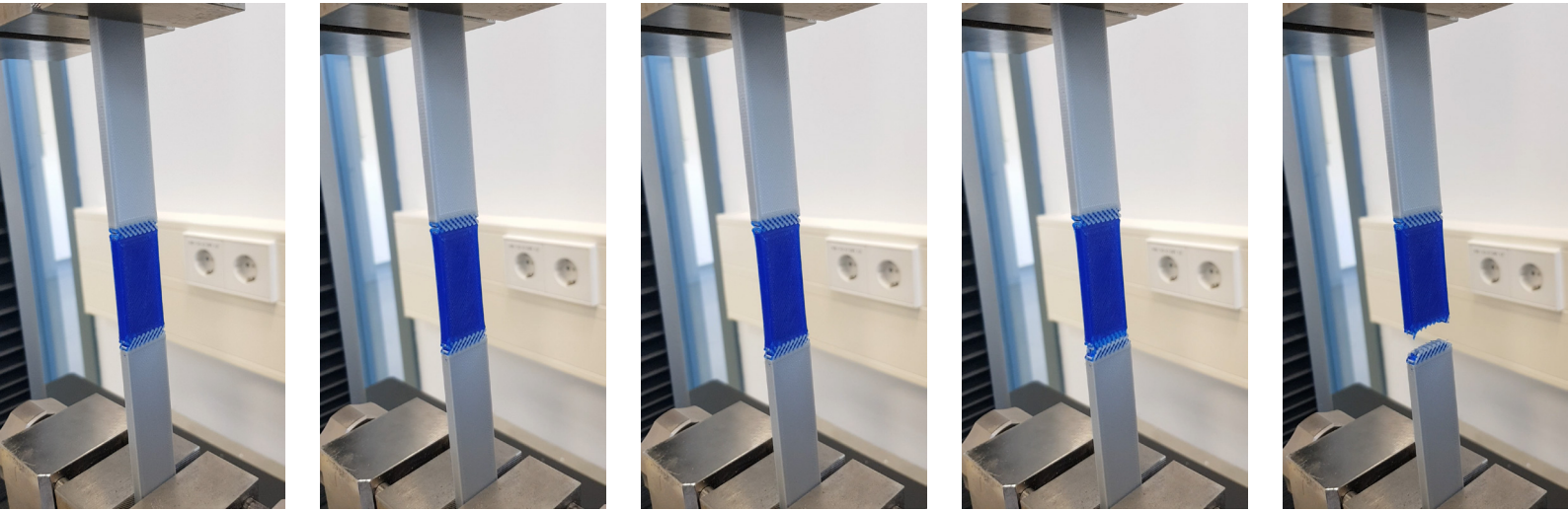


Figure 5.36 tensile test B2

Benchmark 2

We created an interface width of 4mm, equal to benchmark 1.

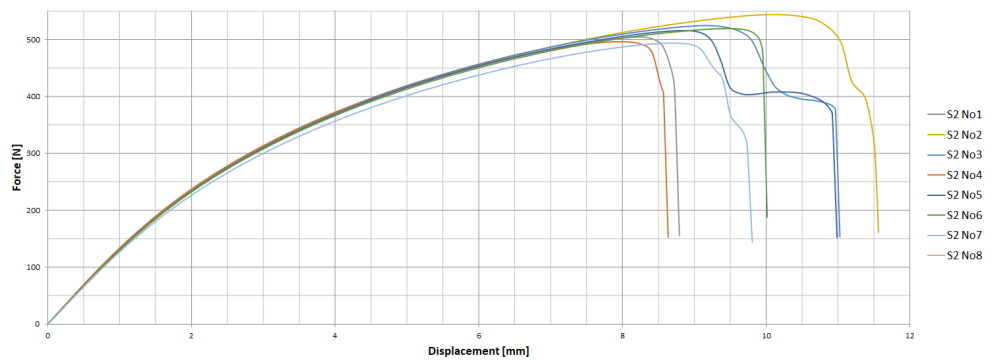


Figure 5.37 force-displacement graph B2

Result B2

We found a peak force of 504N. The interface fails at the base of the TPU fingers, orthogonal to the fiber direction.

Conclusion B2

The TPU fingers fail because TPU is the weaker material and the volumetric material composition is 1:1 at the interface. They break orthogonal to the fiber direction because the shear strength is lower than the tensile strength. See Appendix D for a more elaborate strength calculation of this model.

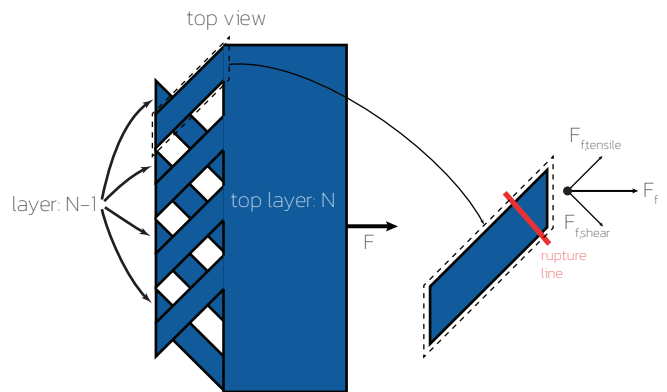


Figure 5.39 B2 rupture line

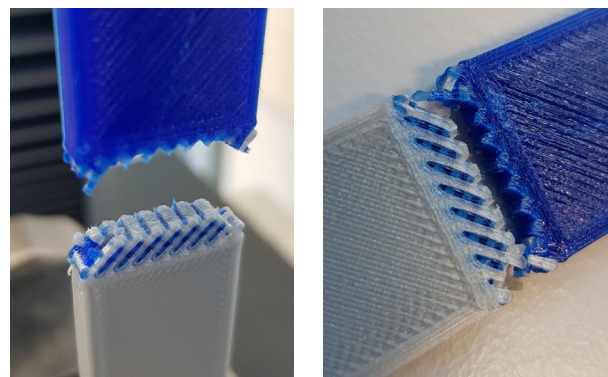


Figure 5.38 B2 interface failure

Interim conclusion

We have shown a gradual improvement along the iterations of the bridge pattern. The final peak force of the bridge pattern is 491N. This is an increase of 18% compared to the industry standard (415N). The Hacksaw pattern shows an even larger peak force of 504N. Figure 5.40 shows the peak forces of all specimens together. In chapter 7 we will discuss further improvements of the concept.

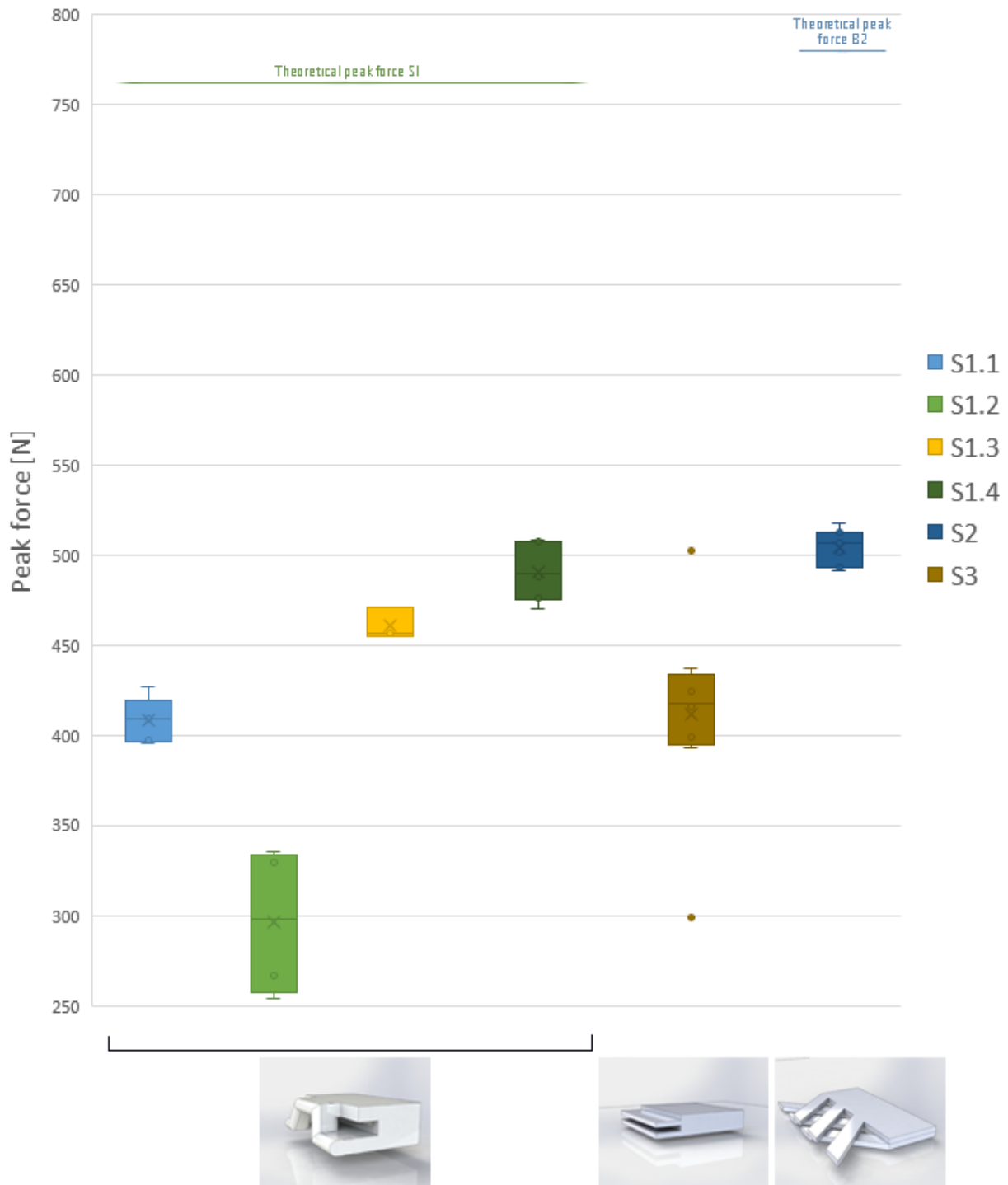
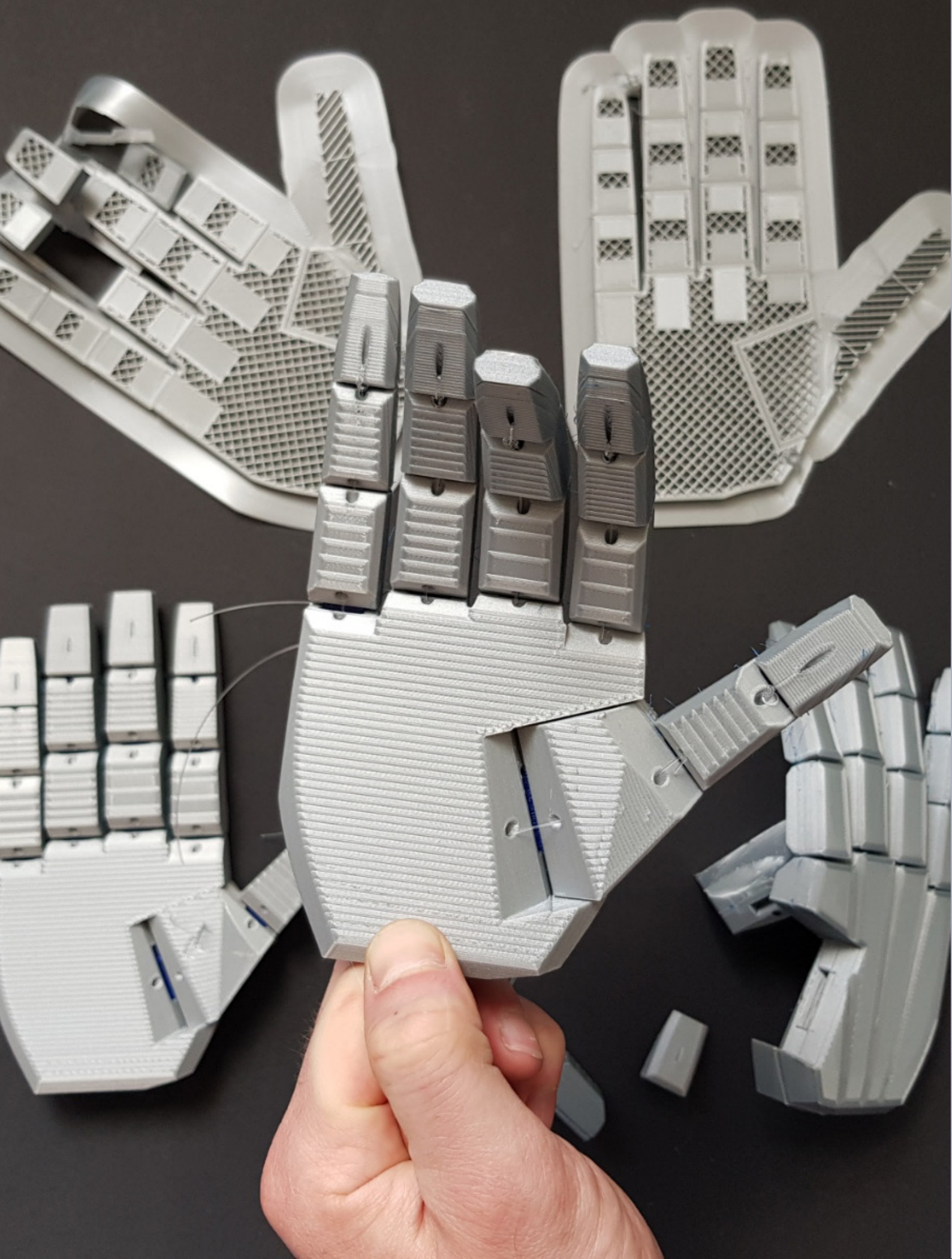


Figure 5.40 peak force of PLA-TPU specimens



6: APPLICATIONS

The proposed joining method opens up new possibilities for manufacturing. We have created an overview of possible applications. A brainstorm of this can be found in Appendix J. From this overview, we have chosen one application as a demonstrator: a prosthetic hand which has already been shown in chapter 3. This chapter shows some design challenges and finishes with an evaluation of the prosthetic hand.

6.1 - Applications

Robotics and prosthetics

Current robotics components and prosthetics are assembled after production. Rotating components usually rely on joints such as pin-hole connections. Creating closed structures using flexible and rigid materials could decrease wear of rotating components (pin-hole assemblies). In addition, assembly would not be required. Also, adding a grippy material to fingertips of a prosthetic or wheels of a robotic transport device could improve performance of these devices. The combination of rigid and flexible materials could also be used for shock absorption of certain devices, e.g. drones or other fast-moving devices.

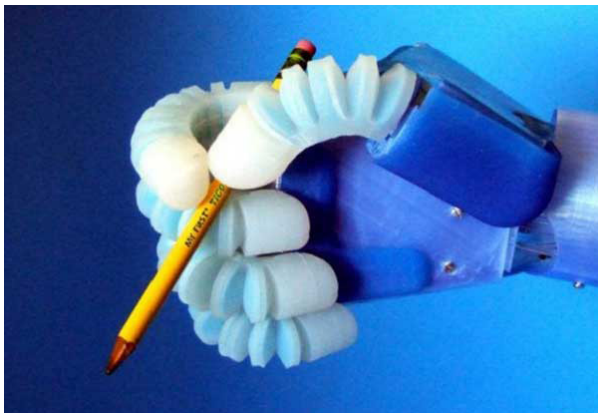


Figure 6.1 soft robotics - pneumatic hand (Rastogi, 2021)

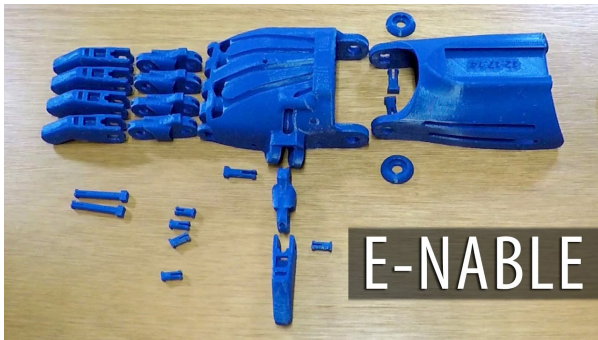


Figure 6.4 FDM printed prosthetic hand (3D printing nerd, 2019)

Compliant mechanisms

Other than replacing joints with a flexible material, we could also create mechanisms that employ the flexibility of a material to create a movement. Instead of using an actuator (such as a cable running through the part), the part is the actuator itself. The desired movement could be a rotation or translation. We can now create compliant mechanisms with rigid and flexible materials, printed at once.

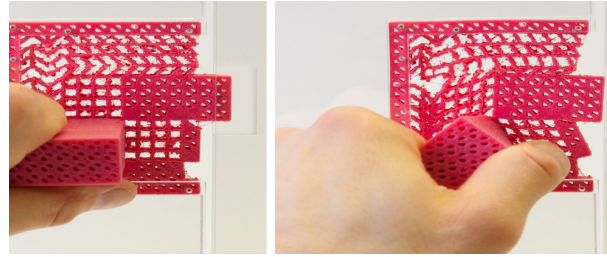


Figure 6.2 single material compliant mechanism - door latch (Papp, 2016)

Wearables

Personalization of wearables is a popular topic. Product fit and comfort could be improved by locally applying rigid or soft parts in products like bicycle seats or shoes without the need for assembling or bonding different materials post-production. For products like helmets or protective clothing, a proper fit is also essential for safety.



Figure 6.3 road cycling helmet. Retrieved from: <https://zortrax.com/3d-printers/m300-/>

6.2 - Demonstrator

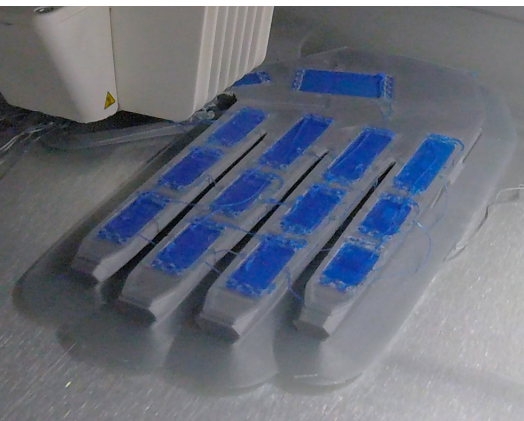
As already shown in chapter 3, we chose to work on a prosthetic hand to demonstrate the new joining method. This paragraph shows how we applied the new bonding method (see Figure 6.6) and a qualitative evaluation of the strength of the bond. A full report about the design choices of the prosthetic hand can be found in Appendix I.

Evaluation prosthetic hand

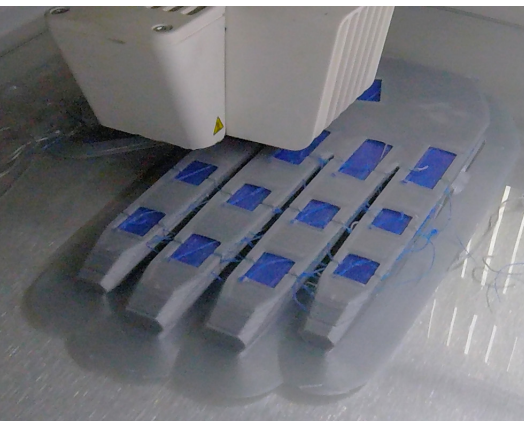
Two prosthetic hands were manufactured. One using the overlap feature (benchmark 1) and one using the bridges concept. The ring finger of both hands was pulled until failure. We did not perform any quantitative tests to the prosthetic hand.



The main body and phalanges are printed using PLA.



Halfway of the phalanges' height, the TPU links are printed. The PLA phalanges are connected with this TPU link at two faces only. The left and right (in sideview) faces of the TPU link are connected, i.e. a vertical interface. This allows the entire link to curve so to distribute the compression and tension forces along the length of the link. The links are 20 x 10 x 2mm (LxWxH).



In the PLA phalanges, relief cuts of 90° are created.

Figure 6.6 printing process prosthetic hand

Benchmark 1

The ring finger was pulled until failure. About half of the TPU layers remained intact so those slipped away from the PLA phalange. This means that the friction force of the bond is lower than the required force to break the material.

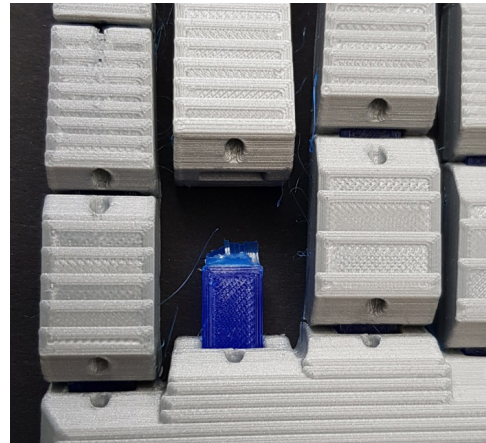


Figure 6.7 B1 ring finger failure

Bridges concept

Using manual force only (applied in-line with the finger), we were unable to break either the link itself or the interface bond (see Figure 6.5). The TPU link yielded so it did not return to its original position.

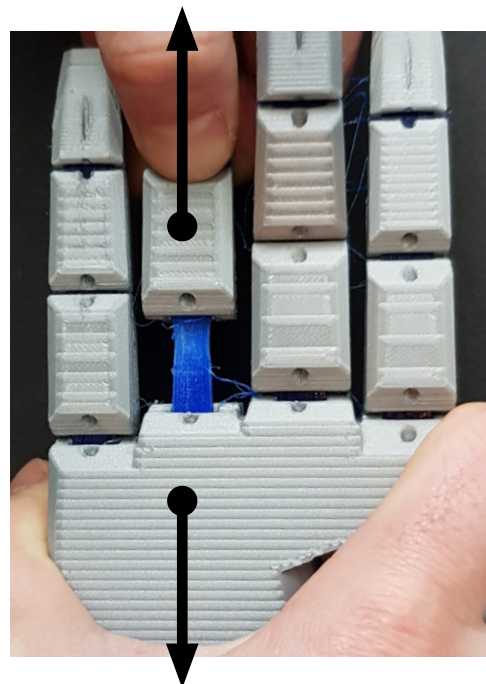


Figure 6.5 bridges concept ring finger under tensional load

Conclusion prosthetic hand

The bonding force that was generated by using the bridge concept suffices for this application. Possible improvements and further work will be discussed in chapter 7.

7: CONCLUSION & DISCUSSION

In this chapter, we will reflect on the initial problem, the goal and proposed solution. We will propose improvements, point out the limitations of this study and suggest future work.

The material selection of multi-material FDM printing was limited because most different polymers do not chemically bond. Chemical incompatibility resulted in dual material parts that were easily separable. Therefore our goal was:

Generate a method to create a dual material object, made of two chemically incompatible materials during the FDM production process.

We proposed a method that joined PLA and TPU (chemically incompatible) by creating a form interlocking shape at the interface. A pattern was created of rows of PLA bridges which were attached to the PLA part. A non-planar printing approach was chosen to create the PLA bridges: the PLA bridges were printed in one continuous bead across multiple layers. Under and around these bridges, TPU material was extruded to create this form interlocking shape.

We have shown that our proposed concept (bridge pattern) outperforms the industry standard for joining two chemically incompatible materials during FDM printing. We created specimens made of PLA and TPU and a demonstrator: a prosthetic hand.

Specimens created using the industry standard method (overlapping feature in Cura) yielded a peak force of 415N. Specimens created using our proposed method yielded a peak force of 491N which is an increase of 18%.

Our proposed method does not create a stronger bond than the planar benchmark (peak force of 504N). For this interface orientation (vertical interface) the planar interlocking shape (Hacksaw) creates a stronger bond. So we have created a solution that achieves the set goal but there is an even better solution.

Joining method improvements

Bridges concept

The results show that TPU is the failing material. Therefore, we should increase the volumetric material composition TPU-PLA at the interface to increase the interface strength.

Also, one of the simulations showed that the stresses within the TPU are centered around the first and second row of PLA bridges. We could therefore decrease the amount of rows of PLA bridges since the third row is barely subjected to any stresses. This will decrease the width of the interface and therefore improve the applicability to small parts. Testing is required to confirm these hypotheses.

Hacksaw concept

The Hacksaw concept could be improved by optimizing the volumetric material composition at the interface, which currently is 1:1. Increasing the amount of TPU to 55% will increase the peak force.

To improve the applicability to small sized parts, we could reduce the interface width by decreasing the length of the fingers. Testing is required to confirm these hypotheses.

Limitations

We limited the surface orientation to the vertical interface. We suggest to investigate horizontal and freeform interfaces as well. Investigating the horizontal interface would be especially relevant since there currently is no alternative option available to create a horizontal interface. Both patterns could be used for creating a horizontal interface. Using this Hacksaw pattern for horizontal interfaces would create the typical anisotropic behavior of regular FDM printing: parts are weaker in Z-direction than XY-direction due to interlayer bonding. The bridge pattern on the other hand is created in one continuous bead so the bridge pattern could be relevant for this application.

During this project, we focused on joining materials. The proposed interlocking structure imposes new challenges regarding repairing or recycling. So we suggest to investigate how we could repair products (or recycle the materials) that use this interlocking pattern.

Future work

We have investigated mechanical interlocking to join chemically incompatible materials. Other methods for joining incompatible materials could be investigated as well. This could be a transitional material that adheres well to the two materials or a reactive agent sprayed between the interface to improve bonding.

We used the bridge pattern, printed using a non-planar approach, for multi-material printing. One could investigate whether this continuous bridge pattern could also be used for other purposes. Potentially, one could improve the interlayer strength (force applied in Z-direction) for single materials. Also, one could change the hardware into a system with more degrees of freedom to create long continuous patterns throughout the entire part, in many different directions to create a more homogeneous part.

References

- Bijadi, S., De Bruijn, E., Tempelman, E. Y., & Oberdorf, J.** (2017). Application of multi-material 3D printing for improved functionality and modularity of open source lowcost prosthetics – A case study. *Frontiers in Biomedical Devices, BIOMED – 2017 Design of Medical Devices Conference, DMD 2017*, 2017–2018. <https://doi.org/10.1115/DMD2017-3540>
- Busch, P., & Weidisch, R.** (2008). Interfaces between incompatible polymers. *Polymer Surfaces and Interfaces: Characterization, Modification and Applications*, 161–182. https://doi.org/10.1007/978-3-540-73865-7_8
- Da Silva, L. F. M., Öchsner, A., Adams, R. D.** (2011). *Handbook of adhesion technology*. Springer
- de Backer, W., van Tooren, M. J. L., & Bergs, A. P.** (2018). Multi-axis multi-material fused filament fabrication with continuous fiber reinforcement. *AIAA/ASCE/AHS/ASC Structures, Structural Dynamics, and Materials Conference, 2018*, 210049. <https://doi.org/10.2514/6.2018-0091>
- Duty, C., Failla, J., Kim, S., Smith, T., Lindahl, J., & Kunc, V.** (2019). Z-Pinning approach for 3D printing mechanically isotropic materials. *Additive Manufacturing*, 27(December 2018), 175–184. <https://doi.org/10.1016/j.addma.2019.03.007>
- Espalin, D., Ramirez, J., Medina, F., & Wicker, R.** (2012). Multi-material, multi-technology FDM system. *23rd Annual International Solid Freeform Fabrication Symposium – An Additive Manufacturing Conference, SFF 2012*, 828–835.
- Fernández, P., Pelayo, F., Ávila, D., Beltrán, N., & Blanco, D.** (2019). Failure analysis of Bi-material FFF parts. *Procedia Manufacturing*, 41, 571–578. <https://doi.org/10.1016/j.promfg.2019.09.044>
- Freund, R., Watschke, H., Heubach, J., & Vietor, T.** (2019). Determination of influencing factors on interface strength of additively manufactured multi-material parts by material extrusion. *Applied Sciences (Switzerland)*, 9(9). <https://doi.org/10.3390/app9091782>
- Gent, A. N., & Lin, C. W.** (1990). Model Studies of the Effect of Surface Roughness and Mechanical Interlocking on Adhesion. *The Journal of Adhesion*, 32(2–3), 113–125. <https://doi.org/10.1080/00218469008030185>
- Gibson, I., Rosen, D. W., & Stucker, B.** (2010). Additive manufacturing technologies: Rapid prototyping to direct digital manufacturing. *Additive Manufacturing Technologies: Rapid Prototyping to Direct Digital Manufacturing*, 1–459. <https://doi.org/10.1007/978-1-4419-1120-9>
- Goodship, V., & Kirwan, K.** (2001). Interfacial instabilities in multimaterial co-injection mouldings: Part 1 – Background and initial experiments. *Plastics, Rubber and Composites Processing and Applications*, 30(1), 11–15. <https://doi.org/10.1179/146580101101541372>
- Gouker, R. M., Gupta, S. K., Bruck, H. A., & Holzschuh, T.** (2006). Manufacturing of multi-material compliant mechanisms using multi-material molding. *International Journal of Advanced Manufacturing Technology*, 30(11–12), 1049–1075. <https://doi.org/10.1007/s00170-005-0152-4>
- Hüttenbach, S., Stamm, M., Reiter, G., & Foster, M.** (1991). The Interface between Two Strongly Incompatible Polymers: Interfacial Broadening and Roughening near T_g. *Langmuir*, 7(11), 2438–2442. <https://doi.org/10.1021/la00059a007>
- Khan, A. S., Ali, A., Hussain, G., & Ilyas, M.** (2019). An experimental study on interfacial fracture toughness of 3-D printed ABS/CF–PLA composite under mode I, II, and mixed-mode loading. *Journal of Thermoplastic Composite Materials*. <https://doi.org/10.1177/0892705719874860>
- Khondoker, M. A. H., Baheri, N., & Sameoto, D.** (2019). Tendon-Driven Functionally Gradient Soft Robotic Gripper 3D Printed with Intermixed Extrudate of Hard and Soft Thermoplastics. *3D Printing and Additive Manufacturing*, 6(4), 191–203. <https://doi.org/10.1089/3dp.2018.0102>

- Khudiakova, A., Arbeiter, F., Spoerk, M., Wolfahrt, M., Godec, D., & Pinter, G.** (2019). Inter-layer bonding characterisation between materials with different degrees of stiffness processed by fused filament fabrication. *Additive Manufacturing*, 28(January), 184–193. <https://doi.org/10.1016/j.addma.2019.05.006>
- Kim, H., Park, E., Kim, S., Park, B., Kim, N., & Lee, S.** (2017). Experimental Study on Mechanical Properties of Single- and Dual-material 3D Printed Products. *Procedia Manufacturing*, 10, 887–897. <https://doi.org/10.1016/j.promfg.2017.07.076>
- Liu, F., Li, T., Jiang, X., Jia, Z., Xu, Z., & Wang, L.** (2020). The effect of material mixing on interfacial stiffness and strength of multi-material additive manufacturing. *Additive Manufacturing*, 36(January). <https://doi.org/10.1016/j.addma.2020.101502>
- Lopes, L. R., Silva, A. F., & Carneiro, O. S.** (2018). Multi-material 3D printing: The relevance of materials affinity on the boundary interface performance. *Additive Manufacturing*, 23, 45–52. <https://doi.org/10.1016/j.addma.2018.06.027>
- Lumpe, T. S., Mueller, J., & Shea, K.** (2019). Tensile properties of multi-material interfaces in 3D printed parts. *Materials and Design*, 162, 1–9. <https://doi.org/10.1016/j.matdes.2018.11.024>
- Matsuzaki, R., Kanatani, T., & Todoroki, A.** (2019). Multi-material additive manufacturing of polymers and metals using fused filament fabrication and electroforming. *Additive Manufacturing*, 29(July), 100812. <https://doi.org/10.1016/j.addma.2019.100812>
- Mirzaali, M. J., Cruz Saldívar, M., Herranz de la Nava, A., Gunashekar, D., Nouri-Goushki, M., Doubrovski, E. L., & Zadpoor, A. A.** (2020). Multi-Material 3D Printing of Functionally Graded Hierarchical Soft-Hard Composites. *Advanced Engineering Materials*, 22(7). <https://doi.org/10.1002/adem.201901142>
- Mohammadi, A., Lavranos, J., Zhou, H., Mutlu, R., Alici, G., Tan, Y., Choong, P., & Oetomo, D.** (2020). A practical 3D-printed soft robotic prosthetic hand with multi-articulating capabilities. *PLoS ONE*, 15(5), 1–23. <https://doi.org/10.1371/journal.pone.0232766>
- Mueller, S., Im, S., Gurevich, S., Teibrich, A., Guimbretière, F., & Baudisch, P.** (2014). WirePrint: Fast 3D Printed Previews. *Procedure of UIST 2014*, Figure 2, 273–280.
- Papp, D.** (2016). [Photograph]. 3D printed door latch has one moving part – itself! <https://hackaday.com/2016/09/14/3d-printed-door-latch-has-one-moving-part-itself/>
- Parupelli, S. K., & Desai, S.** (2020). Hybrid additive manufacturing (3D printing) and characterization of functionally gradient materials via in situ laser curing. *International Journal of Advanced Manufacturing Technology*, 110(1–2), 543–556. <https://doi.org/10.1007/s00170-020-05884-9>
- Pizzi, A., and Mittal, K.** (1999). Adhesion promotion techniques.
- Raphelson, S.** (2014). [Photograph]. The prosthetics industry gets a human touch. <https://www.npr.org/2014/11/11/358048818/the-prosthetics-industry-gets-a-human-touch?t=1615887247513>
- Rastogi, N.** (2021). [Photograph]. Soft robotics: robots featuring biological movements. <https://www.engineersgarage.com/tech-articles/soft-robotics-robots-featuring-biological-movements/>
- Reverte, J. M., Caminero, M. ángel, Chacón, J. M., García-Plaza, E., Núñez, P. J., & Becar, J. P.** (2020). Mechanical and geometric performance of PLA-based polymer composites processed by the fused filament fabrication additive manufacturing technique. *Materials*, 13(8). <https://doi.org/10.3390/MA13081924>
- Ribeiro, M., Sousa Carneiro, O., & Ferreira da Silva, A.** (2019). Interface geometries in 3D multi-material prints by fused filament fabrication. *Rapid Prototyping Journal*, 25(1), 38–46. <https://doi.org/10.1108/RPJ-05-2017-0107>
- Rossing, L., Scharff, R. B. N., Chömpff, B., Wang, C. C. L., & Doubrovski, E. L.** (2020). Bonding between silicones and thermoplastics using 3D printed mechanical interlocking. *Materials and Design*, 186, 108254. <https://doi.org/10.1016/j.matdes.2019.108254>

- Song, P., Fu, Z., Liu, L., & Fu, C. W.** (2015). Printing 3D objects with interlocking parts. *Computer Aided Geometric Design*, 35–36, 137–148. <https://doi.org/10.1016/j.cagd.2015.03.020>
- Spaggiari, A., & Denti, F.** (2019). Mechanical strength of adhesively bonded joints using polymeric additive manufacturing. *Proceedings of the Institution of Mechanical Engineers, Part C: Journal of Mechanical Engineering Science*, 0(0), 1–9. <https://doi.org/10.1177/0954406219850221>
- Tamburrino, F., Graziosi, S., & Bordegoni, M.** (2019). The influence of slicing parameters on the multi-material adhesion mechanisms of FDM printed parts: an exploratory study. *Virtual and Physical Prototyping*, 14(4), 316–332. <https://doi.org/10.1080/17452759.2019.1607758>
- Wolszczak, P., Lygas, K., Paszko, M., & Wach, R. A.** (2018). Heat distribution in material during fused deposition modelling. *Rapid Prototyping Journal*, 24(3), 615–622. <https://doi.org/10.1108/RPJ-04-2017-0062>
- Yin, J., Lu, C., Fu, J., Huang, Y., & Zheng, Y.** (2018). Interfacial bonding during multi-material fused deposition modeling (FDM) process due to inter-molecular diffusion. *Materials and Design*, 150, 104–112. <https://doi.org/10.1016/j.matdes.2018.04.029>
- Zhang, X., & Wang, J.** (2020). Controllable interfacial adhesion behaviors of polymer-on-polymer surfaces during fused deposition modeling 3D printing process. *Chemical Physics Letters*, 739(November 2019), 136959. <https://doi.org/10.1016/j.cplett.2019.136959>

Appendix A: printing parameters of overhanging PLA bridges

This appendix shows the findings of our research for printing overhanging parts. A paper of Mueller et al. (2014) was chosen as starting point. From this, we iterated the printing parameters to create a pattern of overhanging bridges.

A pattern with overhanging parts require different printing parameters than the regular layer-by-layer approach. Upon exiting the nozzle, the filament is still hot and thus viscous. So, when printing an overhanging part with regular parameters, the viscous filament will collapse.

Mueller et al. (2014) mention some parameters to be considered to allow wire printing. Since this has many touchpoints with our pattern, they are listed below.

The most relevant difference between the application of Mueller and this application is size and cooling capacity. Therefore, these parameters are considered a starting point and will be adjusted to match our application. Note, when said "increasing" or "decreasing" means in- or decreased in

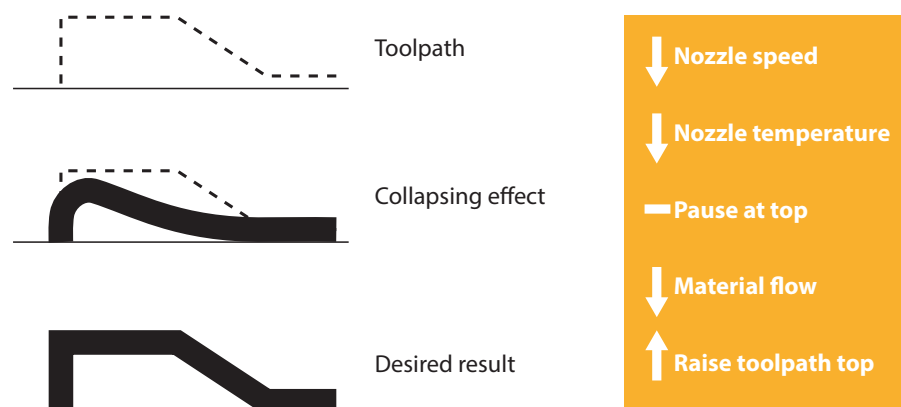


Figure 1: pattern printing parameters overview

comparison with print parameters of regular fusing mode (planar printing).

A way to keep the overhanging filament from collapsing is decreasing the nozzle speed to allow the filament to cool down when midair, i.e. when printing the overhanging part.

Another option is to pause after making an upward printing movement. This gives the filament of the vertical pillar the time to solidify in that particular position.

A parameter that could be tweaked as well is the nozzle temperature. Slightly decreasing this will improve solidification time and decrease drooling effect which is especially present when printing at low feed rates.

Fourthly, we can decrease the amount of material printed midair. Since the cooling process is, among other things, depended on the volume, decreasing the volume will decrease the solidification time.

Lastly, one could also try to circumvent these solutions by printing the pattern higher than required. When the pattern slightly collapses, the remaining pattern will be at the desired height. So here, the sagging effect is being calculated for rather than being solved.

Creating the desired structure will likely require tweaking more than one of the proposed parameters and solutions.

For a first experiment, feed rates from 100 to 800 mm/min with intermittent steps of 100 mm/min were tested. A pause of 100ms was introduced for each. Despite the proposal of Mueller suggesting 1800 mm/min, visual inspection of the results of the first experiment showed the lower feed rates, between 100 and 300 mm/min to be most promising. This difference could be because of the large geometrical difference. Where the height of Mueller's zigzag sections is 6 mm, these sections are only 1.2 mm high.

For the second experiment, feed rates from 150 to 250 mm/min with intermittent steps of 25 mm/min were tested including a pause of both 100 and 200ms. The results did not show major differences. All showed rather continuous patterns, uniform beads and no collapsing bridges.

Conclusions

For the PLA bridge pattern, a feed rate of 200 mm/min and pause of 100ms is chosen. Also, the nozzle temperature is adjusted to 200 d.C. and a volumetric flow of 75% is assigned to the overhanging parts to reduce collapsing of the bridges.

Appendix B: ideation phase

This appendix shows the findings of my ideation phase and is constructed in the following paragraphs:

Inspiration

Criteria – these are the most important specifications used to select the most promising idea to be developed into a concept.

Idea Matrix – delivers an overview where all ideas are clustered by their pattern type and extrusion mode. These clusters can contain more than one idea.

Ideas – shows more information of the ideas including an explanation for its given score, again arranged by its cluster.

Cluster Scores – shows the scores of the clusters. The scores are generated by rating the criteria on a 1-to-5 point scale.

Conclusion

Inspiration

I started by looking for generic ideas from engineering perspective. Different securing methods were analyzed for their workings and I analyzed how this geometry could be modelled for using it as an interlocking mechanism. A geometrically driven inspiration approach.

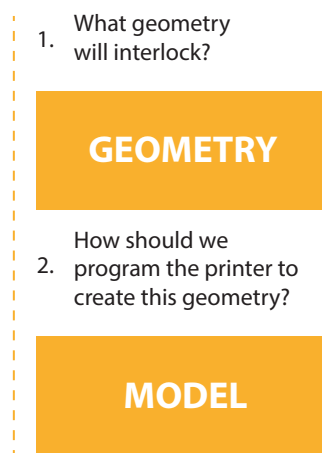


Figure 1: geometry driven approach



Figure 2: toolpath driven approach

Whereas the first brainstorm session was fueled by engineering securing methods, the second session was fueled by the basic workings of an FDM printer. In chapter FIXME, the workings of an FDM printer are explained and chapter FIXME its capabilities are explained by showing different extrusion modes. After analyzing possible toolpaths that can be created, I thought of ways to utilize these possibilities as an interlocking mechanism. This toolpath driven inspiration approach yielded interesting ideas, especially regarding the wish for increasing the knowledge of the FDM process.

Criteria

The first selection of ideas is based on 4 criteria. The scores indicate what ideas are most promising and worth further investigation. The criteria are explained below including an explanation for the desired outcome.

Pattern type – determines how strong the bond potentially could be. This can range from pure adhesive forces in case of butt-joined parts to an interlocked structure. Since the adhesive forces of non-compatible materials are very low, an interlocking structure is preferred. Here, its strength is determined by the minimum material strength of the two, since one of them must break to release the bond.

Toolpath – in general, a discontinuous production process is more difficult to regulate since input variables have to change much more in order to properly control the process. Inherently, this creates greater output uncertainty. Therefore, we prefer to change or optimize the bonding method to be a continuous

process as much as possible.

Applicability – to what extent can the pattern be applied to differently oriented split surfaces. Can range from simple vertical or horizontal planes to complex multi-curved freeform planes. Also, it is important at what size the pattern can be integrated and still function properly. The smaller the size, the higher its applicability.

New knowledge – one could base their geometry design on a well-developed extrusion mode and optimize this for the particular application. On the other hand, one could purposefully choose an extrusion mode with little previous development to increase the knowledge around that particular extrusion mode using an application as an example. The scientific nature of this project is more inclined to the latter. Do note, I think that either end of the scale has its focus misplaced too, it should be in balance.

Idea matrix

The generated ideas can be clustered according to their extrusion mode and pattern type. This allows us to score them more efficiently, since some ideas are only different in minor details. Such slightly differing ideas within one cluster will likely score very similar on the criteria mentioned so a score is given per cluster.

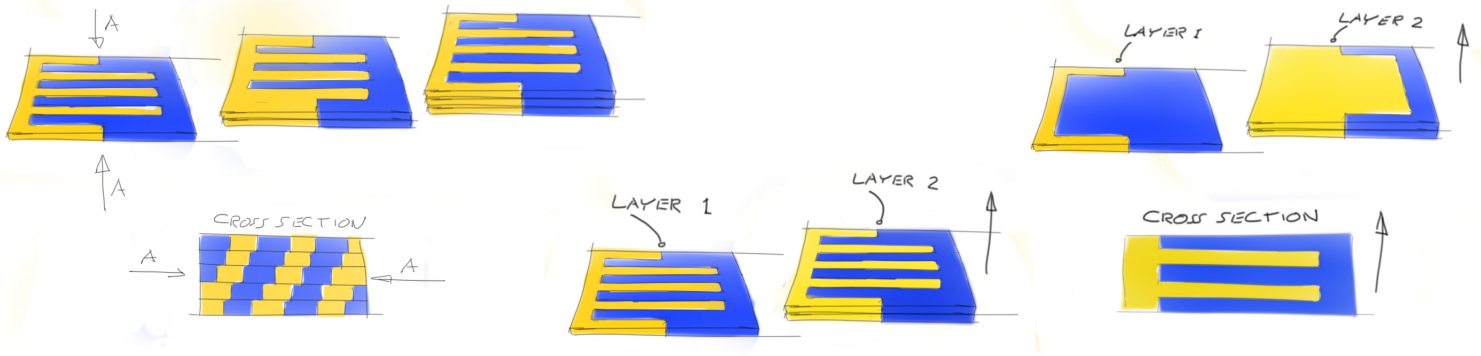
The table is an idea matrix with 'Extrusion Mode' as columns and 'Pattern Type' as rows. The 'Extrusion Mode' header is highlighted in orange, and the 'Pattern Type' header is highlighted in blue. The cells contain idea identifiers (A-J) and their total scores. The 'Continuous Multilayer Fusing' column is split into two sub-columns.

Pattern Type	Extrusion Mode						
	Fusing	Injection	Blobbing	Multilayer Extrusion	Continuous Multilayer Fusing	Mixing	Entangling
Friction	A Total score 7	B Total score 8					
Semi-interlocking		C Total score 10				D Total score 9	E Total score 8
Interlocking	F Total score 15	G Total score 13	H Total score 14	I Total score 17.5	J Total score 18		

Ideas

A - Anyone who's ever folded two phonebooks together has experienced this idea. The overlapping material together create more friction than gluing the side covers together. This might also work for bonding PLA and TPU.

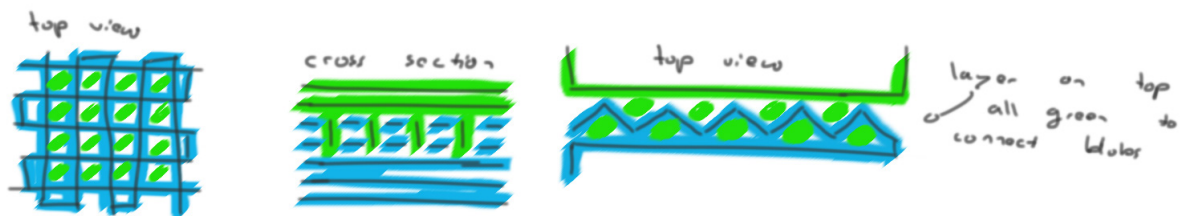
However, the larger the incompatibility of two materials the lesser the adhesion. The amount of friction will therefore be determined by its roughness. To create enough friction, a large amount of area is need. This frictional area could be optimized by dividing the overlapping material into fingers (Opt.1 and Opt.2).



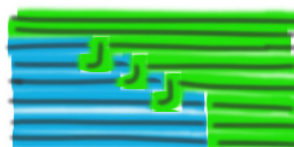
B - This idea is called Z-pinning, described by Duty (2019) and can be applied to horizontal splitting surfaces. The bottom object of material A holds cavities. Material B is extruded into these cavities. Subsequently, the remainder of the top object of material B is printed.

This idea also relies on friction. The larger the pins, the more frictional area available. The depth of the cavities is limited by its diameter and solidification rate of the injected material.

To apply this extrusion mode to a vertical splitting surface, an object of material A is printed having cavities near the boundary surface. This could be a zigzag shaped boundary line. These cavities are filled with material B. On top of this, a layer of material B is printed to connect the pillars with the object.

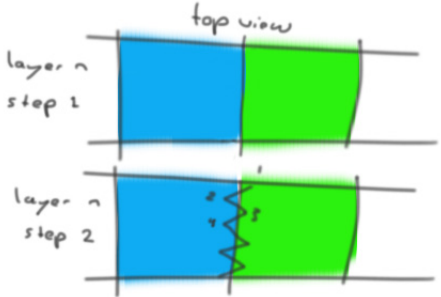


C - This idea could be used for sloped split surfaces. The bottom object of material A holds J-shaped cavities. Material B is injected into these cavities. A J-shaped injection would resist forces in both horizontal and vertical direction. This kind of shape places it in between a purely friction-based pattern and a fully form-interlocking pattern.



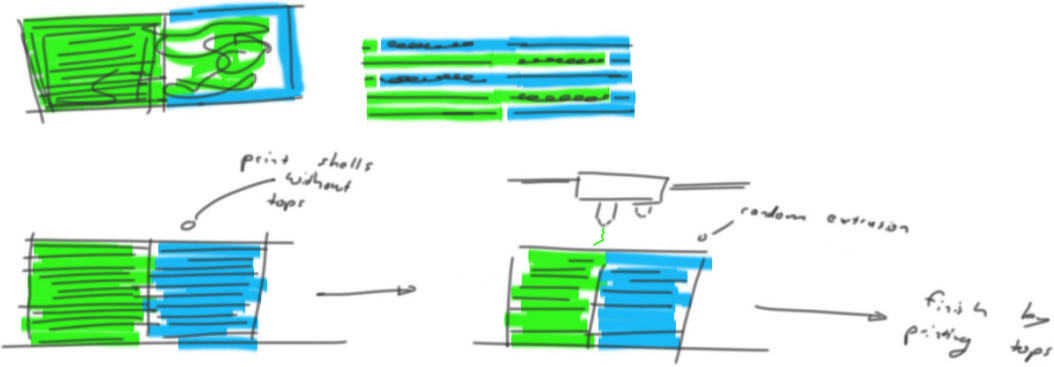
D – Planes of different materials are printed next to each other. By dragging the hot nozzle through both materials, the materials could be mixed at the boundary interface. The path could be something like a zigzag.

It is however questionable if this smearing movement would actually take with some green material to the blue part. Also, it seems a bit brusquely so it may decrease longevity of the printer hardware.

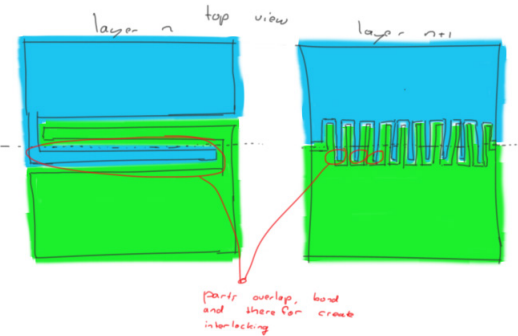


E – The bottoms and outer walls of two objects of dissimilar material are printed next to each other. Before printing the tops to closing the objects, semi-random lines are extruded with both materials so to entangle them. Alternatively to doing this for an almost finished object, this entanglement could be done for each layer.

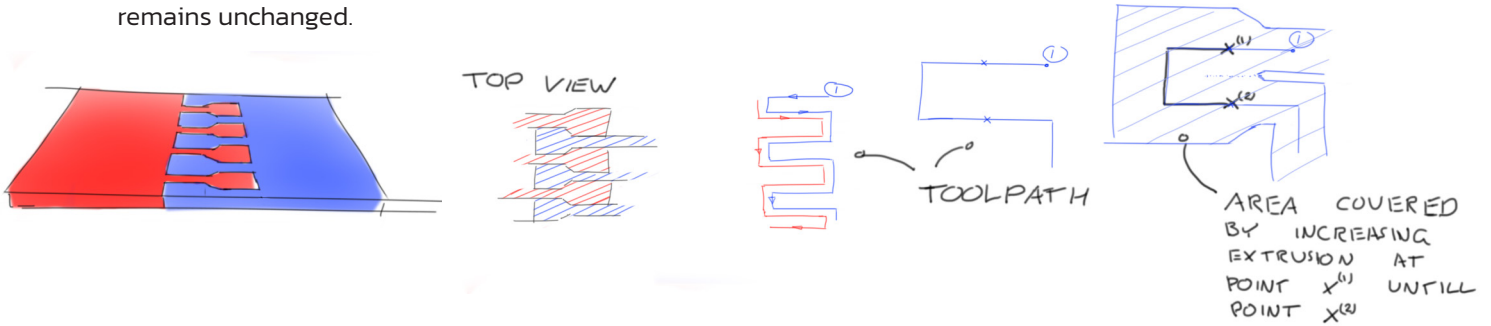
It is however questionable that entangling the two materials really interlocks. The rigidity will probably be low, e.g. an entangled ball of threads are interlocked with each other but can still be pulled and stretched easily.



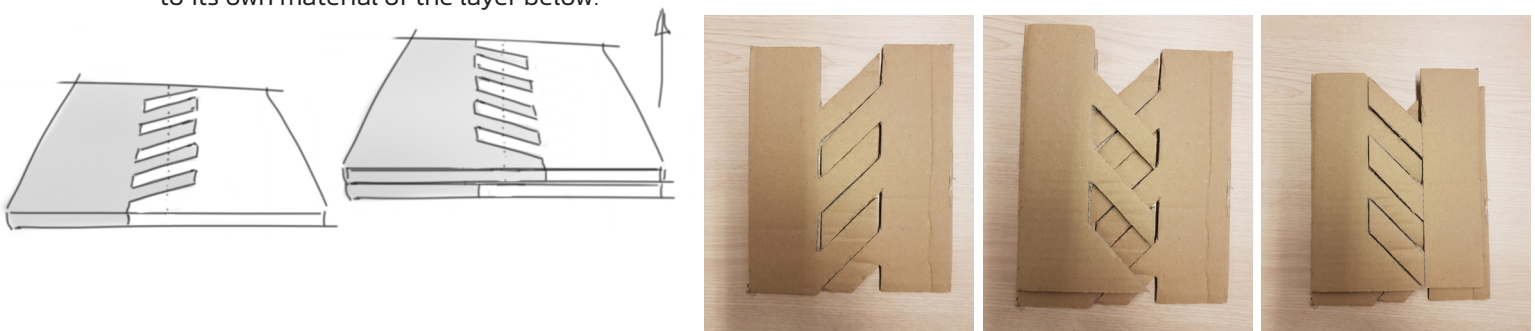
F – Every other layer, two planes of dissimilar materials are printed such that it sandwiches a beam of the other material. On top of that layer, planes are printed with fingers that fuse to the beam of its own material on the layer below.



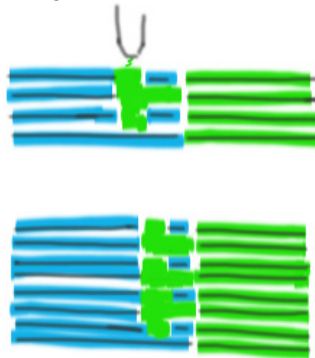
Its interlocking capabilities could be further increased by printing dovetail shapes instead of rectangular fingers. Reducing the printing speed at the tip would create this dovetail shape whereas the toolpath remains unchanged.



Every layer, two planes of dissimilar materials are printed. At the interface, these planes have fingers oriented at 45 degrees. This orientation is mirrored every layer. This connects the fingers of every layer to its own material of the layer below.



G – An object is printed of material A containing cavities that permeates from the top of its layer towards the boundary surface. At the top opening of these cavities, material B is extruded which should then fill the cavity and attach to the object of material B. It is however questionable whether injecting material into such a J-shaped cavity would really fuse with the object next to it.

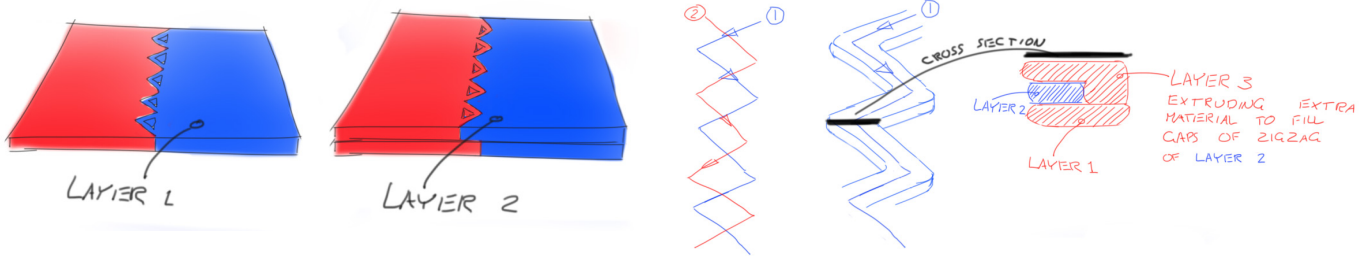


H – Blobs of material A are extruded near the boundary surface. Material B is extruded around it. This path could be something like a full circle or a repeated step-function pattern. The path is then continued into the object of material B. On top, a plane of material A is printed to secure the blobs to the object of material A.

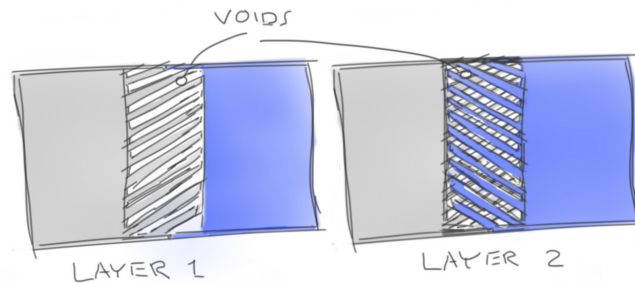
The blobbing feature is discontinues so rather difficult to control. Also, when depositing the blobs first and the step-function pattern second, this might create voids between the round blob and square zigzag.



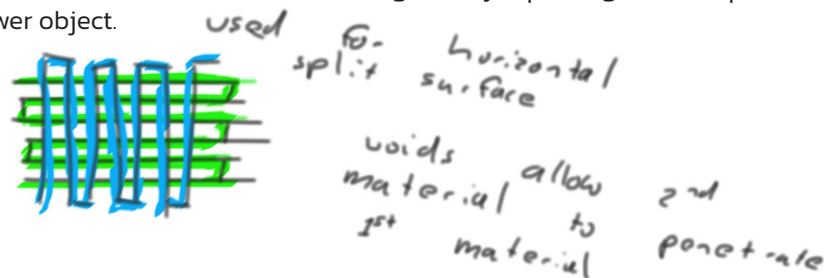
I – Every other layer, a zigzag pattern of material A is printed near the boundary surface. By doing so, cavities are created at every valley of the zigzag. On top of this layer, another zigzag is printed of material B but shifted half a period. By extruding enough of material B, this layer fills the cavities of the layer below and fuses to its own layer below that. Every two layers are now free of inter-material boundary layers around the boundary surface since they are extruded continuously.



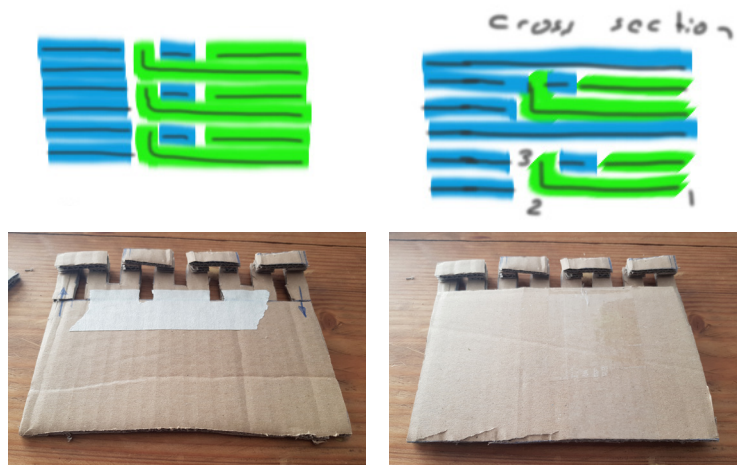
Every other layer, a plane of material A is printed having fingers oriented at 45 degrees. This leaves some room between the fingers. Creating the gaps between the lines could be by underextruding or by programming a wider path. On top, a similar plane is printed of material B but mirrored. By extruding enough of material B, the voids of the layer below will be filled and an interlocking is created.



Such patterns could also be used for horizontal splitting planes. A grid is printed of material A. On top, the same grid is printed of material B but rotated 90 degrees. By repeating these steps at least once will lock the upper and lower object.



J – A bridge pattern is printed of material A. This is a continuous bead throughout multiple layers. Material B is extruded around this geometry, filling the voids under the bridges and around it. This creates continuous beads throughout multiple layers for both materials and a form interlocking geometry.



Cluster scores

An overview of the scores given to each cluster is shown below. They are scored according to the earlier mentioned criteria. The scores are explained in more depth below the score overview.

A	Score	B	Score	C	Score	D	Score	E	Score
Pattern	1	Pattern	1	Pattern	1	Pattern	1	Pattern	1
Toolpath	4	Toolpath	2	Toolpath	2	Toolpath	3	Toolpath	2
Applicability	1	Applicability	2	Applicability	3	Applicability	1	Applicability	1
Knowledge	1	Knowledge	3	Knowledge	4	Knowledge	4	Knowledge	4
	7		8		10		9		8

F	Score	G	Score	H	Score	I	Score	J	Score
Pattern	5	Pattern	5	Pattern	5	Pattern	5	Pattern	5
Toolpath	4	Toolpath	2	Toolpath	2	Toolpath	5	Toolpath	5
Applicability	5	Applicability	3	Applicability	3	Applicability	3	Applicability	3
Knowledge	1	Knowledge	3	Knowledge	4	Knowledge	4,5	Knowledge	5
	15		13		14		17,5		18

A - criterium	Explanation	Score 1-5
Pattern	Friction strength is low due to low degree of material compatibility. Ribeiro et al. (2019) proved that a form interlocking structure creates a better bond than a structure based on friction.	1
Toolpath	Continuous within single layer.	4
Applicability	To create enough friction force, a large area is required. Applicable to vertical splitting planes only.	1
Knowledge	A lot is known about the regular fusing process already.	1
		7

B - criterium	Explanation	Score 1-5
Pattern	Friction strength is low due to low degree of material compatibility. Ribeiro et al. (2019) proved that a form interlocking structure creates a better bond than one based on friction.	1
Toolpath	A discontinuous toolpath creates challenges regarding controlling the process. Main challenges for this idea are controlling underfill and overfill of pillars.	2
Applicability	Applicable to horizontal splitting planes only. Also, to create enough friction force, a large area is required.	2
Knowledge	Injection using FDM has been studied by Duty ().	3
		8

C - criterium	Explanation	Score 1-5
Pattern	Friction strength is low due to low degree of material compatibility. Ribeiro et al. (2019) proved that a form interlocking structure creates a better bond than one based on friction.	1
Toolpath	A discontinuous toolpath creates challenges regarding controlling the process. Main challenges for this idea are controlling underfill and overfill of pillars.	2
Applicability	Applicable to horizontal, vertical and sloped splitting planes. To create enough friction force, a large area is required.	3
Knowledge	I have not found studies of FDM injection in such a J-shaped receptacle.	4
		10

D - criterium	Explanation	Score
Pattern	I am highly skeptical whether mixing materials would actually create (semi) form interlocking.	1
Toolpath	Non-extruding.	3
Applicability	Applicable to vertical splitting surfaces only. In theory, the smudging toolpath could be kept small.	1
Knowledge	Based on ironing mode which is available in Cura.	4
		9

E - criterium	Explanation	Score
Pattern	Highly skeptical whether this would actually interlock. Even when it does, it won't likely be rigid.	1
Toolpath	Continuous, semi random extrusion.	2
Applicability	It's unlikely to be able to keep the structure small.	1
Knowledge	Spaghettification mode, which is very related, is used to create artsy or decorative objects.	4
		8

F - criterium	Explanation	Score
Pattern	Interlocking so one material must break to release bond. Pattern can easily be extended to increase amount of interlocked foreign material.	5
Toolpath	Continuous within single layer.	4
Applicability	Applicable for horizontal and vertical splitting planes, both straight and single curved.	5
Knowledge	A lot is known about the regular fusing process already.	1
		15

G - criterium	Explanation	Score
Pattern	Interlocking so one material must break to release bond.	5
Toolpath	A discontinuous toolpath creates challenges regarding controlling the process. Main challenges for this idea are controlling underfill and overfill of pillars.	2
Applicability	Applicable to horizontal and vertical splitting planes.	3
Knowledge	Injection using FDM has been studied by Duty ().	3
		13

H - criterium	Explanation	Score
Pattern	Interlocking so one material must break to release bond.	5
Toolpath	A discontinuous toolpath creates challenges regarding controlling the process. Main challenge for this idea is creating steady standing pillars.	2
Applicability	Applicable to horizontal and vertical splitting planes.	3
Knowledge	Takahashi studied weaved structures which has similarities.	4
		14

I - criterium	Explanation	Score
Pattern	Interlocking so one material must break to release bond.	5
Toolpath	Continuous within multiple layers. Filament of second layer flows to first layer, creating a continuous bead. A continuous bead has superior strength over a discontinuous bead. Still relatively easy to control.	5
Applicability	Applicable to horizontal and vertical splitting planes.	3
Knowledge	I have found no studies regarding this method.	4.5
		17.5

J - criterium	Explanation	Score
Pattern	Interlocking so one material must break to release bond.	5
Toolpath	Continuous within multiple layers in two ways: 1) continuous bead through multiple layers created with one material. 2) Filament of second material flows from second to first layer, creating a continuous bead. A continuous bead has superior strength over discontinuous bead. Main challenge: creating a continuous bead through multiple layers.	5
Applicability	Applicable to horizontal and vertical splitting planes.	3
Knowledge	No studies found regarding this method.	5
		18

Conclusion

The ideas of category J scores highest. Particularly interesting is the toolpath with which this pattern is created. Since intralayer bonding is stronger than interlayer bonding, creating a continuous bead could potentially create a stronger multi-material bond. Also, from a scientific view this idea is very interesting since I have not found a similar study that combines these extrusion modes. Hence this idea will be developed further into a proper concept which can be tested afterwards. The main challenge regarding feasibility of this idea is creating a continuous bead through multiple layers.

Appendix C: literature review

This appendix holds an overview of the literature that we consulted. It is divided in three categories: Process parameter optimization, Addition of external energy or techniques, Mechanical interlocking.

Process parameter optimization

Multiple studies show the effects of process parameters (that can be adjusted within the slicer software) on interfacial bonding. The hardware of the particular FDM printer were unchanged. Slicer software allows (among other things) the orientation of the interfacial layers. Tamburrino et al. (2019) found that the Lines pattern created the highest bonding strength when joining PLA, TPU and CPE end-to-end, stacked on top of each other (horizontal interfaces). Also, other process parameters like the infill density were considered in this research. Increasing the infill density increases the bonding strength. Focus has been on temperature control as well. Yin et al. (2018), Khan (2019) and Lin et al. (2018) tested the effect of nozzle temperature, building stage temperature and printing speed on the bonding strength of their dual-material test specimens. The exact temperature outcome depends on the materials used but generally speaking the bonding strength increases by increasing temperature and printing speed, until a certain limit.

Addition of external energy or techniques

Another method for improving interfacial bonding is by adding external energy or including a different manufacturing method together with the FDM system. Changes in hardware were made. If possible, our proposed method should be backwards compatible and should not require changing the hardware. Rossing () proposed a method for overmolding silicon to a rigid material (PLA) printed with an FDM system. Here, mechanical interlocking of the silicon with PLA greatly improved bonding strength; up to 5.5 times higher compared to gluing the parts using a primer. Khondoker () demonstrated a method for bonding a rigid and a soft thermoplastic for the use of soft robotics by introducing a static intermixer just before the nozzle of an FDM system. Mixing SEBS (soft material) and HIPS (hard material) at the interface could increase the adhesion strength by 12 times compared with side-by-side printing (vertical interface). The show case, tendon-driven finger, withstood 10.000 cycles.

Mechanical interlocking

Lastly, some studies used mechanical interlocking as a tool to improve multi-material bonding, using an unmodified FDM system. Mechanical interlocking is the creation of a form interlocking shape at the interface. One of the two materials must fail to break the connection. Tamburrino et al. (2019) created a mechanical interlocking feature. They printed two parts of different materials on top of each other (horizontal interface). Instead of an end-to-end interface, the interface layer consisted of an outer ring of material A where the remaining part of the layer was made of material B. This interlocking feature doubled the peak tensile strength for PLA-TPU combination. Ribeiro et al. (2019) also experimented with different interlocking structures and their effect on the bonding of PLA to PLA and PLA to TPU. The materials were printed in XY-plane (vertical interface). They tested three different form interlocking shapes: a T-shape, an I-shape and a V-shape. The T-shape resulted in the highest Young's modulus and highest ultimate stress. Fernandez () tested the effect of material overlap for bonding PLA and TPU (vertical interface). They changed two variables: the orientation of extruded lines with respect to force direction and the amount of overlap. Applying a grid configuration (lines extruded at 0 and 90 degrees with respect to force direction) and a material overlap of either 1 or 2mm improved the tensile strength by 200% compared to side-by-side printing. A patent of Mosaic Manufacturing Ltd. describes a method for joining multiple materials on top of each other (horizontal interface) during additive manufacturing. The patent includes bulk deposition to form an anchor of material A into a receptacle in a body of material B. It also includes an anchor layer of material C deposited on top of the anchor of material A. A Technical disclosure common of Kuipers (2020) from Ultimaker describes a method for joining two parts of different materials during FDM through mechanical interlocking. Fingers and beams are printed that overlap into the other volume. These fingers and beams are part of the boundary of the first volume

so to make a continuous extrusion flow. The fingers and beams are rotated typically 90 degrees every X-number of layers to interlock the volumes in all directions

Interim conclusions

We have seen different methods for bonding chemically incompatible materials. Firstly, adding external energy or including a different manufacturing method together with the FDM system can improve the bonding strength of chemically incompatible materials. This requires changes in hardware. We want to create a joining method that does not require hardware changes to make it backwards compatible for every multi-material FDM printer. We therefore exclude solutions that require extra hardware.

Secondly, optimizing the printing parameters within the slicer software yields improvements for bonding chemically incompatible materials. These improvements are however mild compared with improvements yielded by introducing a form interlocking pattern for bonding chemically incompatible materials.

Appendix D: Hacksaw concept model

This appendix shows a calculation model of the Hacksaw pattern for predicting the peak force of the test specimen.

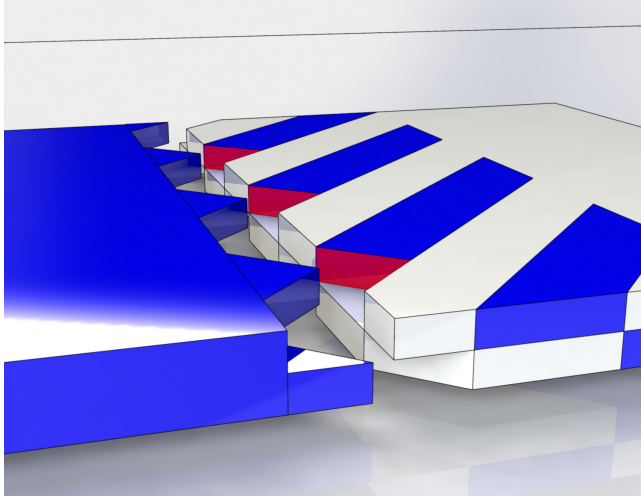


Figure 1: Hacksaw interface

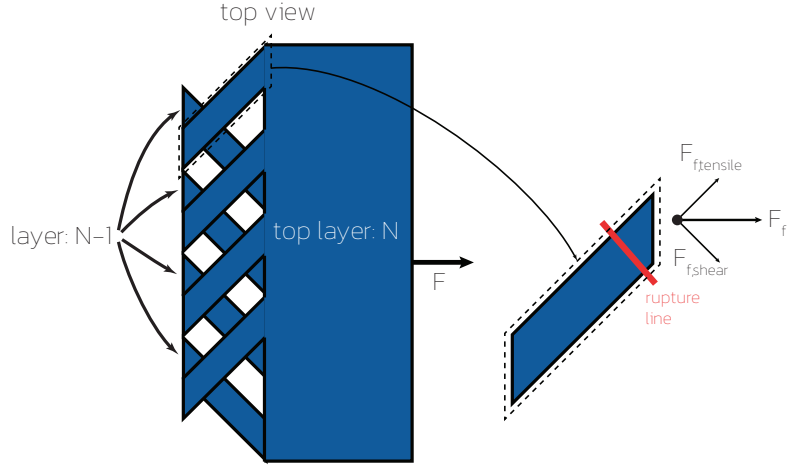


Figure 2: force decomposition of finger of Hacksaw concept

We expect that the Hacksaw specimens will break at the base of the TPU fingers, orthogonal to the length direction of the fingers.

A decomposition of the applied and reactant forces acting upon the finger can be found in figure 1. If designed with the correct finger length, the base of the PLA finger will break. F_f is the force applied to one finger. This force can be decomposed into a shear force $F_{f, shear}$ and a tensile force $F_{f, tensile}$. The maximum shear- and tensile force that the material allows is dependent on the cross-sectional area and the maximum shear- and tensile strength. This area is equal for both so the maximum force F_f that can be applied is limited by the minimum of either the shear or tensile strength. The maximum shear stress

$$F_{f, TPU, tensile} = A_{f, TPU} \times \sigma_{TPU, tensile} = \frac{1}{2} \sqrt{2} \times F_{f, TPU}$$

$$F_{f, TPU, shear} = A_{f, TPU} \times \sigma_{TPU, shear} = \frac{1}{2} \sqrt{2} \times F_{f, TPU}$$

$$\sigma_{tensile} > \sigma_{shear}$$

$$F_{f, TPU, max} = \frac{2 \times F_{f, TPU, shear}}{\sqrt{2}} = \frac{2 \times A_{f, TPU} \times \sigma_{TPU, shear}}{\sqrt{2}}$$

$$A_{f, TPU} = \text{cross - sectional area of one finger} = \text{layer height} \times 2 \times \text{layer width}$$

$$A_{f, TPU} = \frac{\sqrt{2}}{2} A_{TPU} \text{ where } A_{TPU} = \text{frontal area}$$

$$F_{max} = \sum_{i=1}^n F_{f, TPU, max} = \frac{2 \times \sum_{i=1}^n A_{f, TPU} \times \sigma_{TPU, shear}}{\sqrt{2}} = A_{TPU} \times \sigma_{TPU, shear}$$

$$A_{TPU} = 0.5 \times A_{total}$$

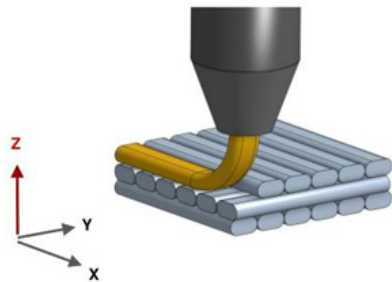
theory gives us a maximum shear stress of half the tensile strength, so $F_{f, max}$ is limited by the shear stress. Hence, the finger will break orthogonal to the length of the finger.

For the test specimen, this would give a maximum theoretical force of 780 N. Note that changing the ratio of TPU and PLA will change the maximum force. Appendix FIXME holds an optimization of this ratio.

Appendix E: extrusion modes

During the FDM process, polymers fuse together. This fusing is called an extrusion mode and enables the planar printing process. Other possible extrusion modes are described below. They are either not used during planar printing or undesirable for planar printing. This appendix shows an overview of different extrusion modes. They have been used as a form of inspiration for creating new ideas of an interlocking mechanism. The overview is based on the work of Doubrovski and Kuipers (n.d.).

Fusing – used for planar printing process. This is the basic idea of an FDM printer, i.e. the continuous extrusion of material that solidifies upon exiting the nozzle. Layers are stacked in vertical direction to create a 3D object.

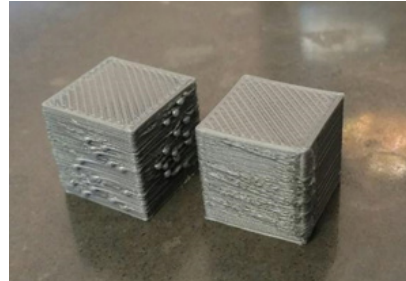


Retrieved from: <https://www.slideshare.net/ShuvomGhose/how-to-3d-print-right-now>

Under- and overextrusion – the idea of fusing remains the same for this extrusion mode but here, too little or too much material is extruded than required for forming a proper line. These terms are however mostly used to denote whether less or more material is extruded than intended. So these terms are more based on intention rather than the absolute width of a line.

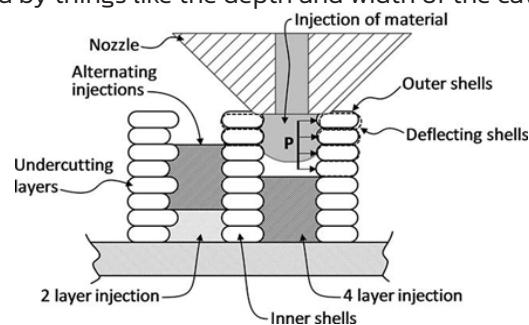


Retrieved from: <https://www.simplify3d.com/support/print-quality-troubleshooting/under-extrusion/>



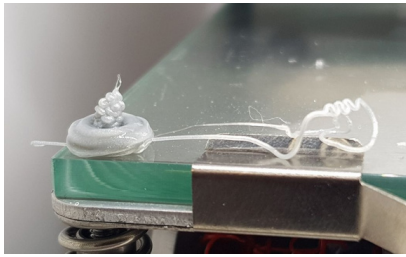
Retrieved from: https://www.reddit.com/r/FixMyPrint/comments/4b0qfk/over_extrusion_on_layer_change/

Injection – by creating an object containing cavities we can extrude material inside these cavities. This is called injection and creates a part that is not fabricated in a layer-by-layer fashion. Still, whether this is really homogeneous is debatable; this depends on things like extrusion speed and solidification time. These are then affected by things like the depth and width of the cavity relative to the nozzle diameter and more.

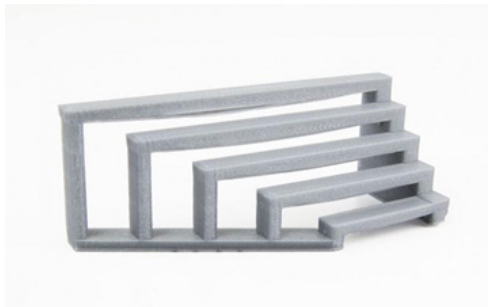


Kazmer, David O., and Austin Colon. (2020). Injection printing: additive molding via shell material extrusion and filling. *Additive Manufacturing* 36: 101469.

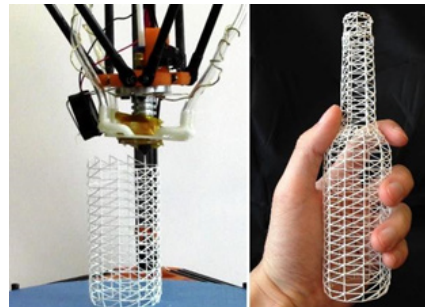
Blobbing – extruding material whilst sitting still in one spot creates a blob of material. Again, this creates a sort of pillar that is not fabricated layer-by-layer. Still, whether this is really homogeneous is debatable.



Bridging – spanning a line across a gap, between two pillars or objects. Increasing the span cause to bridge to sag and eventually collapse. A vast decrease in printing speed is necessary so to give the material time to solidify to reduce sagging.



Retrieved from: <https://support.ultimaker.com/hc/en-us/articles/360012112659-Bridging>



Mueller et al. (2014) WirePrint: 3D printed previews for fast prototyping.

Drooping – uses the sagging effect to create loops hanging from an object.



Spaghettification – mid-air semi random printing causing entangling of unfused material.



Ironing – remelting material by hovering over the layer to reduce the visibility of the line-based structure.



Retrieved from: https://www.reddit.com/r/3Dprinting/comments/cafw32/im_always_amazed_at_curas_experimental_ironing/

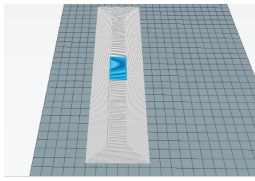
Engraving – creating an image or pattern by diving the heated nozzle into the printed object.



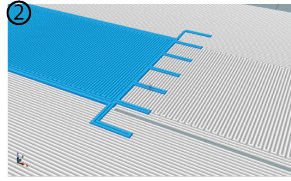
Conclusion

All of these extrusion modes are undesirable during planar printing. Since we want to investigate the non-planar printing process, these extrusion modes are of great help for creating new ideas. They have been used as a form of inspiration.

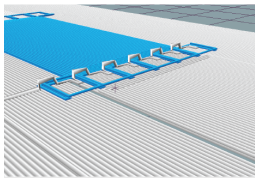
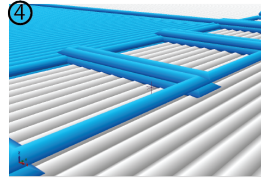
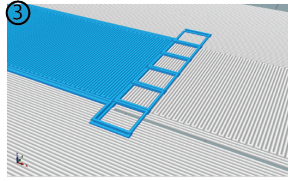
Appendix F: printing sequence



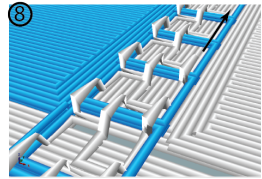
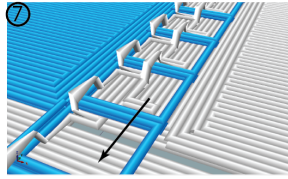
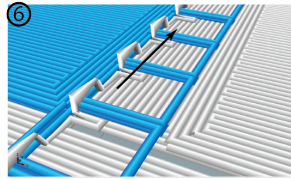
Start with PLA brim, PLA base planes and TPU base plane.



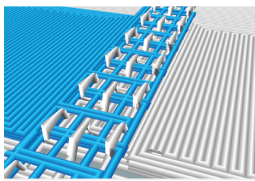
Step 2: TPU layer under PLA bridges. Please note that this step consists of two layers of TPU (layer 2 and layer 3) which are printed direction after one another. This pattern is then followed by a basic TPU and PLA plane.



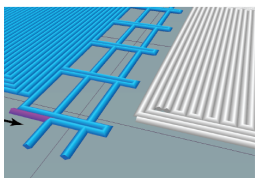
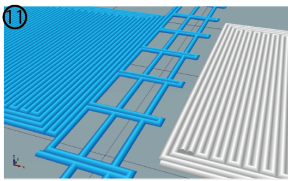
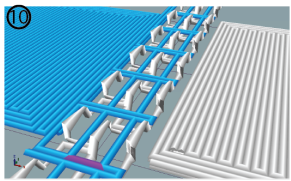
As bridges are printed over the already printed TPU. The arrow denotes the printing direction. Please note the connections between the parallel bridge patterns.



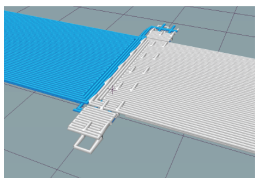
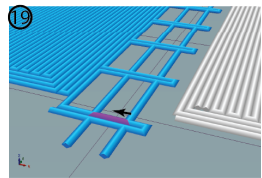
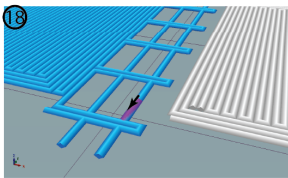
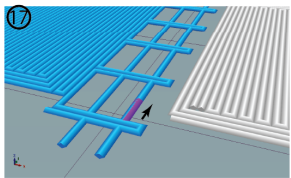
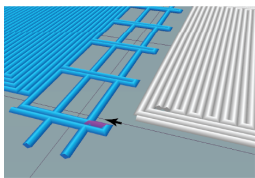
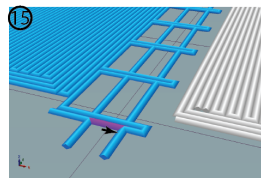
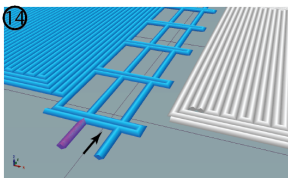
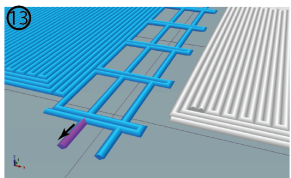
The middle pattern is printed in opposite direction so to keep the path continuous by going to and fro.



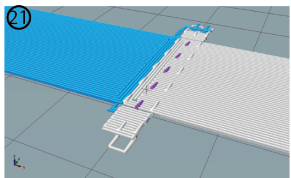
After printing the PLA bridges, TPU is extruded through the valleys of these bridges. Please note that these three pictures are of the same step. The right exclude earlier steps for convenience.



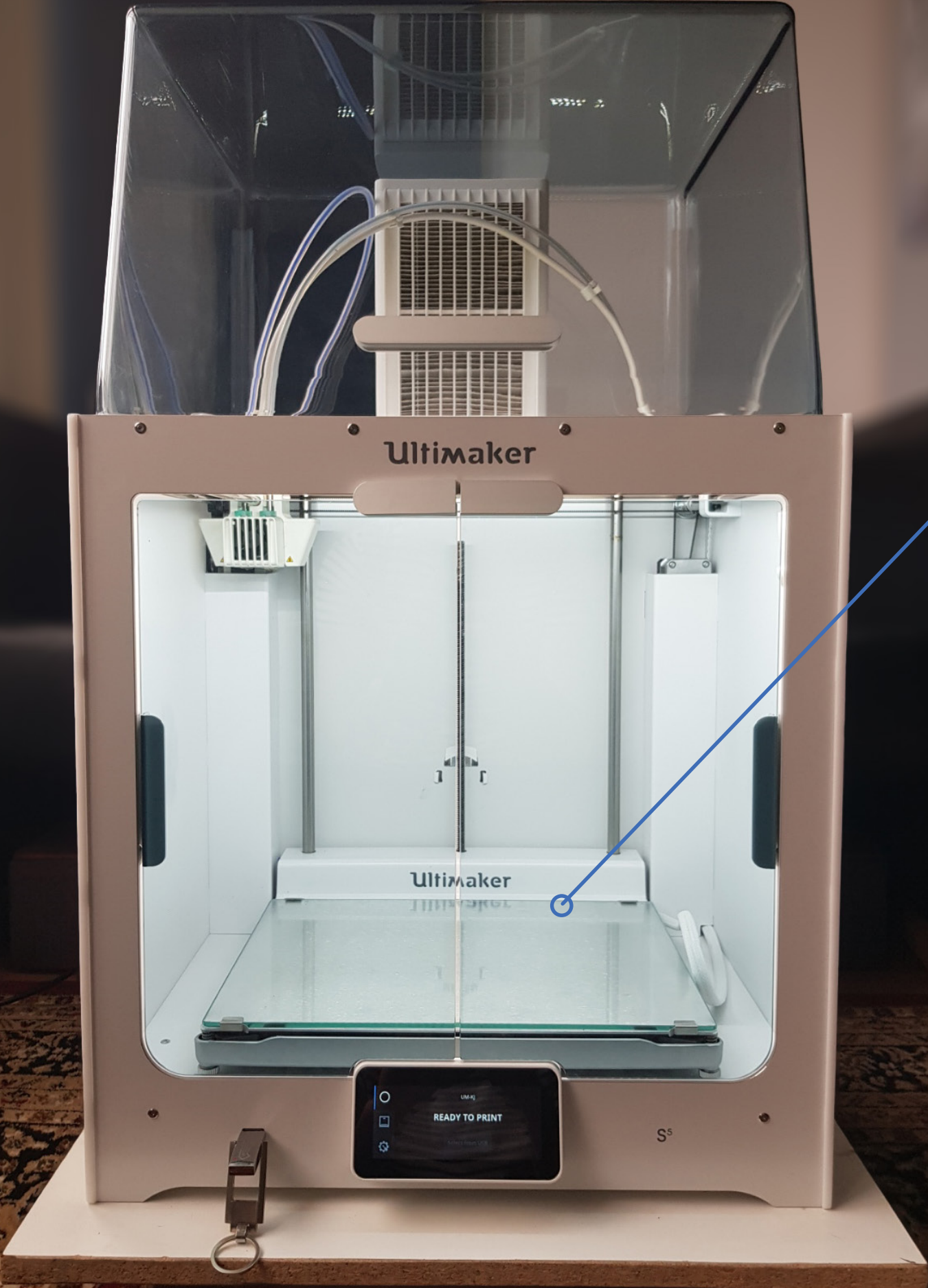
At the same layer, the purple section denotes the printed path. Please note that the outward and inward movement happens at the same height so to push the TPU under the bridges.



On top of this TPU pattern, a PLA plane is printed. The tops of the PLA bridges exactly match the top of this plane. They are highlighted in purple in the right picture.



When excluding the base plane and brim, this is a three-layer section that can be repeated according to the height of the object.



Ultimaker

Ultimaker

UM-4
READY TO PRINT

S⁵

Appendix G: FDM printing

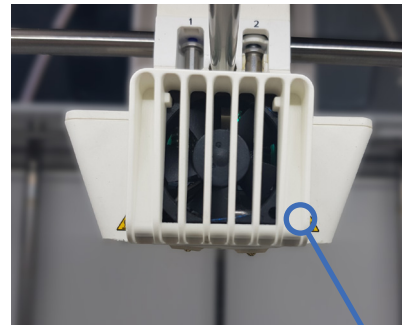
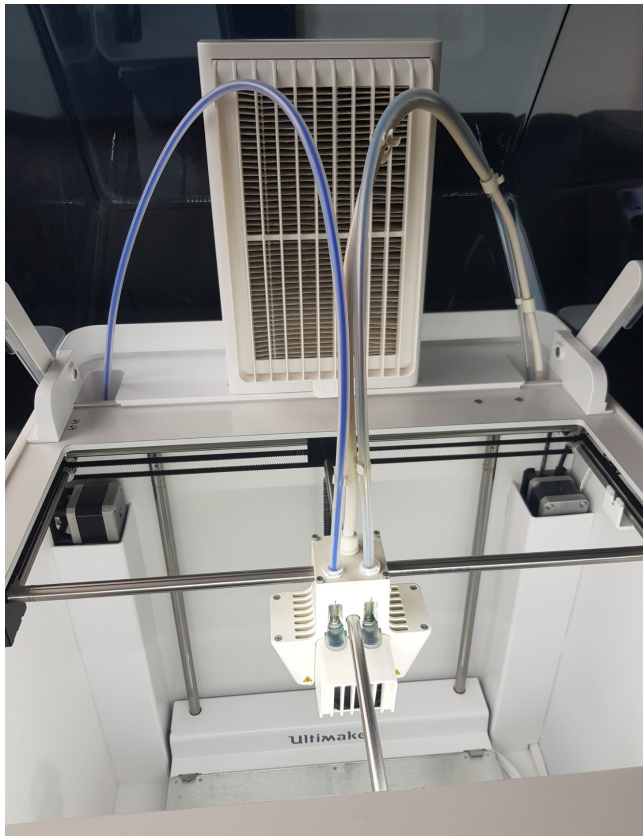
Fused Deposition Modeling

Fused Deposition Modeling (FDM) is an Additive Manufacturing (AM) technique that is used for producing 3-dimensional parts. An FDM printer melts a thermoplastic polymer filament and deposits this material from its printing head onto a building plate. The printing head can translate in 3 directions (X,Y, Z) relative to the building plate. Quickly after depositing the polymer, it solidifies at the desired location. An FDM printer stacks layers of material to create a 3D part.

1.2 - Printer components

The 3D part is created on top of this building plate. It can translate vertically (Z-direction). This FDM printer features a heated building plate to improve adhesion of the deposited layers to the building plate.

The printing head is attached to two rods to allow in-plane translation (X-direction and Y-direction). A printing head contains a nozzle which is heated. A thermoplastic polymer filament is inserted into the nozzle to melt the polymer. By controlling the movement of the printing head and the amount of material pushed through the nozzle, the FDM printer creates layers of material on the building plate. This particular printer features a printing head with two nozzles allowing multi-material printing (see paragraph 1.6).



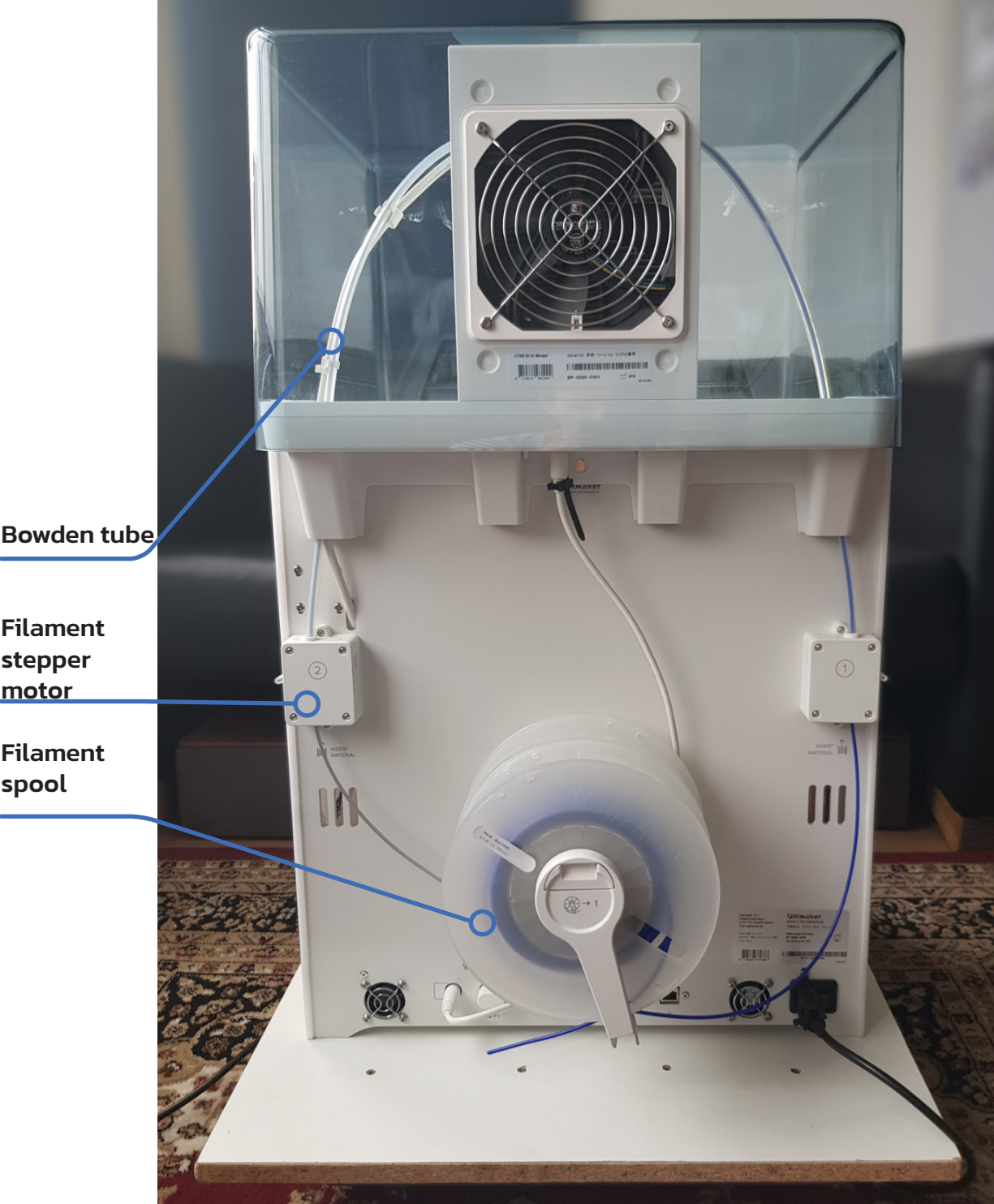
Printing head

Heating element

Nozzle

A gear attached to the stepper motor pushes the filament through the nozzle. The stepper motor is attached to the back of the printer. The filament comes on a spool. Since this particular printer is a multi-material printer it holds two filament spools and two stepper motors to push the filament.

The filament is pushed by the gear of the stepper motor (attached to the back of the printer) towards the nozzle through a Bowden tube.



Appendix H: Polymer bonding

This appendix shows three mechanisms that affect chemical bonding.

The FDM process relies on the bonding of polymers to create a 3D part. When creating a single-material part (e.g. PLA), the material extruded (PLA) from the nozzle bonds to material of its own kind (PLA). When creating a multi-material part (e.g. PLA and TPU), the extruded material (TPU) bonds to a different material (PLA). The face of contact when bonding materials is called an interface.

Bonding (or adhesion) is defined as the tendency of dissimilar particles to cling together. There are a variety of mechanisms affecting adhesion strength. This paragraph will describe three of those mechanisms: diffusion, chemical bonding and electrostatics. (Freund et al. 2019) An important thing to note is that these mechanisms should not be seen as additional items. These mechanisms all affect each other.

Diffusion

The mutual diffusion of molecules across the interface relies on the dynamics of polymer chains in that interfacial region and contribute significantly to the adhesion strength. Factors such as temperature, contact time, chemical nature and molecular weight affect these dynamics. The temperature of both materials should be higher than the glass transition to allow diffusion. As the molecular weight of a polymer increases, they are more likely to separate out into two phases. (Pizzi and Mittal, 1999) (Da Silva, 2011)

Chemical bonding

The fundament of chemical adhesion is the establishment of interatomic and intermolecular forces at the interface of the different materials. The magnitude of these forces depends on the chemical composition of the materials because this chemical nature defines what bonds are made and their magnitude. Chemical bonds can be ionic, covalent, intermediate, hydrogen and Van der Waals. (Tamburino, 2019) (Choempff, 2019) These chemical bonds are based on electrostatic interactions which are explained in the next paragraph.

Electrostatics

The two strongest forms of electrostatic bonding are based on dipole interactions and ion interactions where the latter is the strongest of the two.

Dipole interactions – a covalent bond is based on the attraction of electrons with two atomic nuclei. However, due to unequal sharing of electrons between two atoms, a polar covalent bond can occur. This creates dipole-dipole intermolecular forces and affects a number of physical properties including surface tension, solubility and melting and boiling points.

Ionic interactions – due to an electron transfer between two atoms, the atoms are charged positively and negatively. This net charge difference creates bonds between atoms. Ion interactions are stronger than dipole interactions due to the larger net charge difference. (Khan Academy, n.d.)

Chemical compatibility

A way to describe the chemical compatibility of materials is the Flory-Huggins interaction parameter. The interfacial tension, which is affected by electrostatic interactions, can be described as a function of the Flory-Huggins interaction parameter and the temperature (Stamm and Schubert, 1995). A smaller Flory-Huggins interaction parameter leads to a better solubility meaning a higher interfacial bonding strength (Yin et al., 2018).

Appendix I: Designing a prosthetic hand

The demonstrator should conform to the following criteria:

- *Must display the generated insights of this study.*
- *Must be made of TPU and PLA parts.*
- *Must display benefits of combining rigid and flexible materials.*
- *Should connect to short comings of current fabrication methods for products in that category.*

We chose to work on a prosthetic hand to demonstrate our findings of the joining method.

Designing prosthetic hand

We chose to replicate the hand by creating a rigid main body and rigid phalanges which are connected with flexible material to allow rotation. The rotating movement is actuated with a cable running through the phalanges.

Replicating a point rotation without using pin-hole connections provided the following challenge: when bending a material, it is subjected to tensional and compressional load, see Figure 76. Increasing the height (H) will increase the force required to bend it. On the other hand, decreasing the height will also decrease the tensional strength. The phalanges of the prosthetic hand are linked with a relatively small strip of TPU (compared to the dimensions of the phalanges). The height of the strip is 2 mm.

The TPU links are connected to the PLA phalanges only at the two ends of the TPU link (vertical interface). This allows the entire link to curve so to distribute the compression and tension forces along the length of the link (see Figure 77).

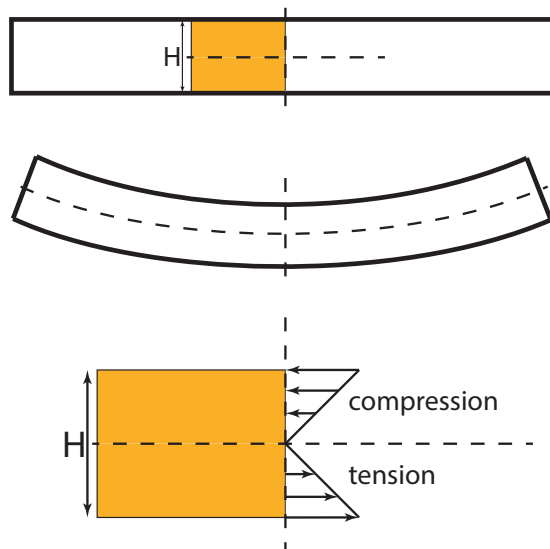


Figure 1: finger tension and compression under bending load.

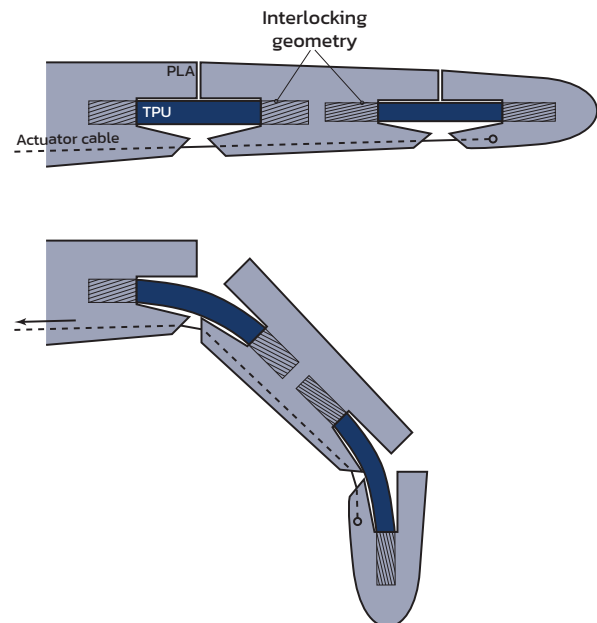
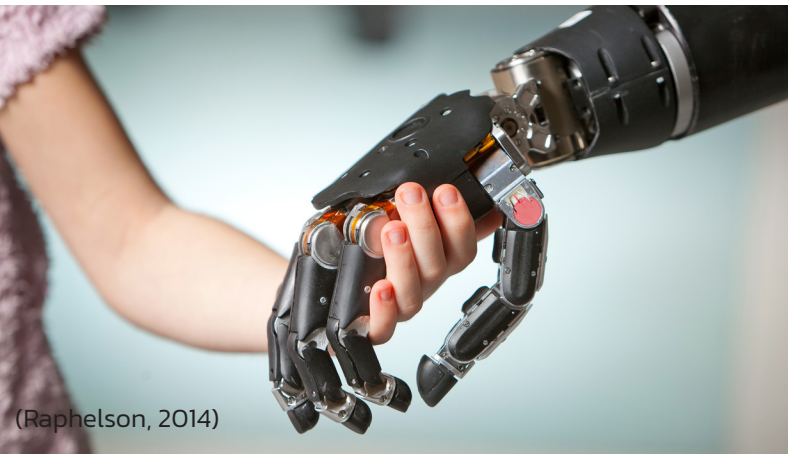
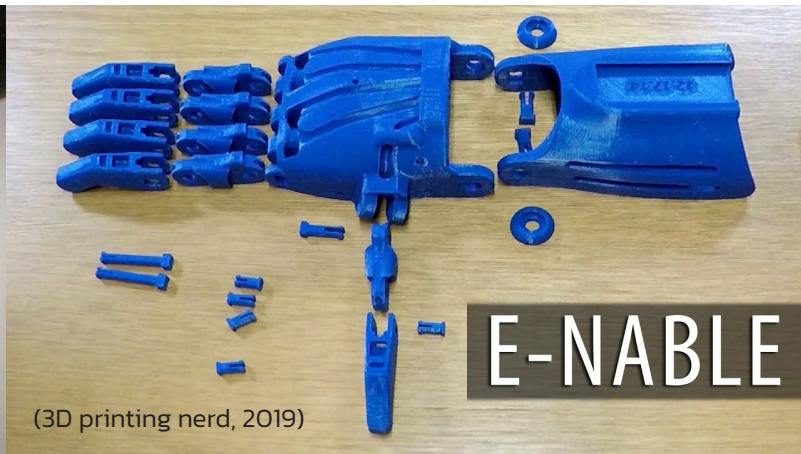


Figure 2: TPU links connecting PLA phalanges

In the PLA phalanges, relief cuts are created to prevent collision. Relief cuts are created of 90° since that is its rotation range for each phalange (see Figure 78). The TPU link is placed in the middle of the phalange. Although this is anatomically incorrect (the joint is more towards the top of the human finger), this decreases the chance of damaging the actuating cable which is vital for moving the finger.



(Raphelson, 2014)



(3D printing nerd, 2019)

State of art hand prosthetics and soft robotics

The finger joints of hand prosthetics mostly rely on the classic assembly technique of a pin-hole connection. In the more advanced prosthetics, metal pins or bolts act as the rotational axis between the phalanges. Hand prosthetics build using an FDM printer mostly use PLA snap pins for connecting the phalanges and acting as the rotational axis. Examples in soft robotic hands show hand-like devices that do not use a rotational axis between each phalange and/or hand main body. Instead, the finger is made of a flexible material and bends evenly along the entire finger.

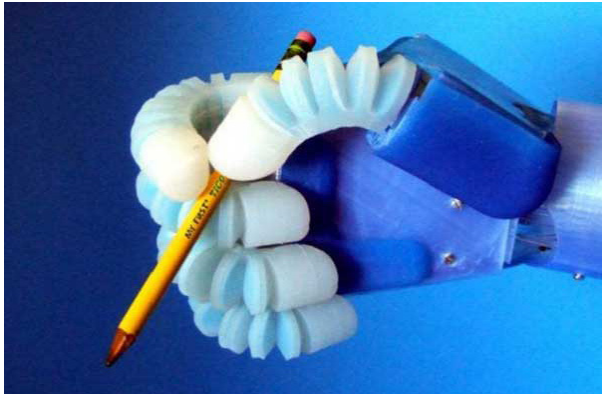


Figure 3: soft robotics – pneumatic hand (Rastogi, 2021)

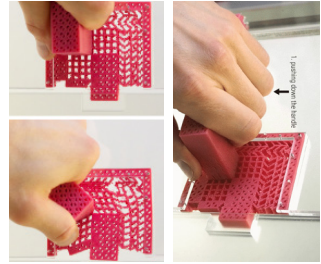


Figure 4: phalanges rotation range

Appendix J: Applications brainstorm



High degree of customization



Compliant mechanism



Flexible-to-rigid transition



BCN3D

Appendix K: Original project brief



IDE Master Graduation

Project team, Procedural checks and personal Project brief

This document contains the agreements made between student and supervisory team about the student's IDE Master Graduation Project. This document can also include the involvement of an external organisation, however, it does not cover any legal employment relationship that the student and the client (might) agree upon. Next to that, this document facilitates the required procedural checks. In this document:

- The student defines the team, what he/she is going to do/deliver and how that will come about.
- SSC E&SA (Shared Service Center, Education & Student Affairs) reports on the student's registration and study progress.
- IDE's Board of Examiners confirms if the student is allowed to start the Graduation Project.

! USE ADOBE ACROBAT READER TO OPEN, EDIT AND SAVE THIS DOCUMENT

Download again and reopen in case you tried other software, such as Preview (Mac) or a webbrowser.

STUDENT DATA & MASTER PROGRAMME

Save this form according to the format "IDE Master Graduation Project Brief_familyname_firstname_studentnumber_dd-mm-yyyy". Complete all blue parts of the form and include the approved Project Brief in your Graduation Report as Appendix 1 !



family name	<u>Van der Vlist</u>	<u>4652</u>	Your master programme (only select the options that apply to you):
initials	<u>K.J.</u>	given name <u>Klaas Jan</u>	IDE master(s): <input checked="" type="radio"/> IPD <input type="radio"/> Dfl <input type="radio"/> SPD
student number	<u>4291387</u>		2 nd non-IDE master: _____
street & no.	_____		individual programme: <u>- -</u> (give date of approval)
zipcode & city	_____		honours programme: <input type="radio"/> Honours Programme Master
country	_____		specialisation / annotation: <input type="radio"/> Medisign
phone	_____		<input type="radio"/> Tech. in Sustainable Design
email	_____		<input type="radio"/> Entrepreneurship

SUPERVISORY TEAM **

Fill in the required data for the supervisory team members. Please check the instructions on the right !

** chair	<u>Zjenja Doubrovski</u>	dept. / section: <u>SDE</u>
** mentor	<u>Tim Kuipers</u>	dept. / section: <u>SDE</u>
2 nd mentor	_____	
organisation:	_____	
city:	_____	country: _____
comments (optional)	: : :	

Chair should request the IDE Board of Examiners for approval of a non-IDE mentor, including a motivation letter and c.v..



Second mentor only applies in case the assignment is hosted by an external organisation.




Ensure a heterogeneous team. In case you wish to include two team members from the same section, please explain why.

Procedural Checks - IDE Master Graduation

APPROVAL PROJECT BRIEF

To be filled in by the chair of the supervisory team.

chair Zjenja Doubrovski date 15 - 01 - 2021 signature 

CHECK STUDY PROGRESS

To be filled in by the SSC E&SA (Shared Service Center, Education & Student Affairs), after approval of the project brief by the Chair. The study progress will be checked for a 2nd time just before the green light meeting.

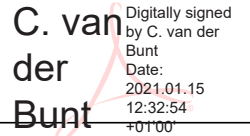
Master electives no. of EC accumulated in total: 27 EC

Of which, taking the conditional requirements into account, can be part of the exam programme 27 EC

List of electives obtained before the third semester without approval of the BoE

YES all 1st year master courses passed

NO missing 1st year master courses are:

name C. van der Bunt date 15 - 01 - 2021 signature 

FORMAL APPROVAL GRADUATION PROJECT

To be filled in by the Board of Examiners of IDE TU Delft. Please check the supervisory team and study the parts of the brief marked **. Next, please assess, (dis)approve and sign this Project Brief, by using the criteria below.

- Does the project fit within the (MSc)-programme of the student (taking into account, if described, the activities done next to the obligatory MSc specific courses)?
- Is the level of the project challenging enough for a MSc IDE graduating student?
- Is the project expected to be doable within 100 working days/20 weeks ?
- Does the composition of the supervisory team comply with the regulations and fit the assignment ?

Content: **APPROVED** **NOT APPROVED**

Procedure: **APPROVED** **NOT APPROVED**

- submission projectbrief very late by chair (has been explained)
- no abbreviation in title

comments

name Monique von Morgen date 02 - 02 - 2021 signature _____

Mechanical interlocking of non-compatible materials for FFF _____ project title

Please state the title of your graduation project (above) and the start date and end date (below). Keep the title compact and simple. Do not use abbreviations. The remainder of this document allows you to define and clarify your graduation project.

start date 07 - 09 - 2020 _____ 12 - 03 - 2021 _____ end date

INTRODUCTION **

Please describe, the context of your project, and address the main stakeholders (interests) within this context in a concise yet complete manner. Who are involved, what do they value and how do they currently operate within the given context? What are the main opportunities and limitations you are currently aware of (cultural- and social norms, resources (time, money,...), technology, ...).

This study is about multi-material additive manufacturing using fused filament fabrication (FFF) technique. The Ultimaker S3 and S5 feature a dual printing head making it possible to print items composed of two materials. This could increase the opportunities in prototyping and manufacturing such as printing items that consist of flexible and stiff parts or for instance an item that need a high wear resistant material at its contact points. However, the selection of combining materials is limited (Fig. 1) as most do not chemically bond making it easy to separate the materials or the print fails during production already. Combining non-compatible materials is sometimes still possible by gluing them post production but that increases labor thus is suboptimal. The aim of this study is therefore to propose a method to join incompatible materials by mechanical interlocking during only one production process which is FFF technique. This method could benefit the end users, i.e. the customers of Ultimaker, in two ways. For those that are already using alternatives like post production joining (gluing) it may highly decrease labor time and effort. For those that confine to current compatible materials it may vastly increase the combination of materials and so the possibilities in prototyping and manufacturing. A method for mechanical interlocking for FFF has been proposed by Kuipers (2020) to weave beams of both materials at the intersection of the parts. These beams fix displacement in three directions, thus gripping the other material. Although yield strength tests have not been performed to test its potential, the theory looks promising and will be investigated in this project. The main opportunities at this stage are investigating what pattern (possible such weaved beams), orientation and size would attain a proper yield strength whilst accounting for applicability to complex surfaces, printer and object properties and more. The method should be backwards compatible with current printers and slicing software. Ideally, a designer would assign a different material to different parts of a product upon which the slicer would generated the interlocking cell pattern and corresponding GCode for the 3D printer.

space available for images / figures on next page

Personal Project Brief - IDE Master Graduation

introduction (continued): space for images

	PLA	ABS	CPE	CPE+	Nylon	PC	TPU 95A	PP	PVA
PLA	✓	×	×	×	×	×	×	×	✓
ABS		✓	×	×	×	×	ⓘ	×	ⓘ
CPE			✓	×	×	×	×	×	✓
CPE+				ⓘ	×	×	×	×	×
Nylon					ⓘ	×	ⓘ	×	✓
PC						ⓘ	ⓘ	×	ⓘ
TPU 95A							ⓘ	×	ⓘ
PP								ⓘ	×
PVA									×

✓ Officially supported ⓘ Experimental × Not supported

Figure 1: compatibility Ultimaker filaments (Ultimaker, 2017)

image / figure 1: [Compatibility Ultimaker filaments \(Ultimaker, 2017\)](#)

TO PLACE YOUR IMAGE IN THIS AREA:

- SAVE THIS DOCUMENT TO YOUR COMPUTER AND OPEN IT IN ADOBE READER
- CLICK AREA TO PLACE IMAGE / FIGURE

PLEASE NOTE:

- IMAGE WILL SCALE TO FIT AUTOMATICALLY
- NATIVE IMAGE RATIO IS 16:10
- IF YOU EXPERIENCE PROBLEMS IN UPLOADING, COVERT IMAGE TO PDF AND TRY AGAIN

image / figure 2: _____

PROBLEM DEFINITION **

Limit and define the scope and solution space of your project to one that is manageable within one Master Graduation Project of 30 EC (= 20 full time weeks or 100 working days) and clearly indicate what issue(s) should be addressed in this project.

The amount of material combinations in FFF dual material 3D printing is limited because many materials do not chemically bond with another material, i.e. they are incompatible. This results in either a print failure or a product with poor yield strength at the juncture of the two materials.

This problem could potentially be solved by introducing a mechanical interlocking structure. Different shapes and sizes of such a structure can be investigated to create a proper yield strength between the two materials.

To keep this project manageable, the vast amount of material combinations will be narrowed down to two incompatible materials with high user demand. This could for instance be a rigid and a flexible material. Whether this method would be applicable for other incompatible combinations will be discussed.

In order to transform this production technique from proof of concept to a customer available product, the Cura slicer should be designed and programmed. However, given the time frame this will be out of scope for this study but should be addressed in a follow up or parallel study.

ASSIGNMENT **

State in 2 or 3 sentences what you are going to research, design, create and / or generate, that will solve (part of) the issue(s) pointed out in "problem definition". Then illustrate this assignment by indicating what kind of solution you expect and / or aim to deliver, for instance: a product, a product-service combination, a strategy illustrated through product or product-service combination ideas, In case of a Specialisation and/or Annotation, make sure the assignment reflects this/these.

This study will generate a method to allow dual material printing of two inherently incompatible materials, using a fused filament fabrication 3D printer. This method will include the use of a mechanical interlocking structure in order to create a single item made up of rigid and flexible sections.

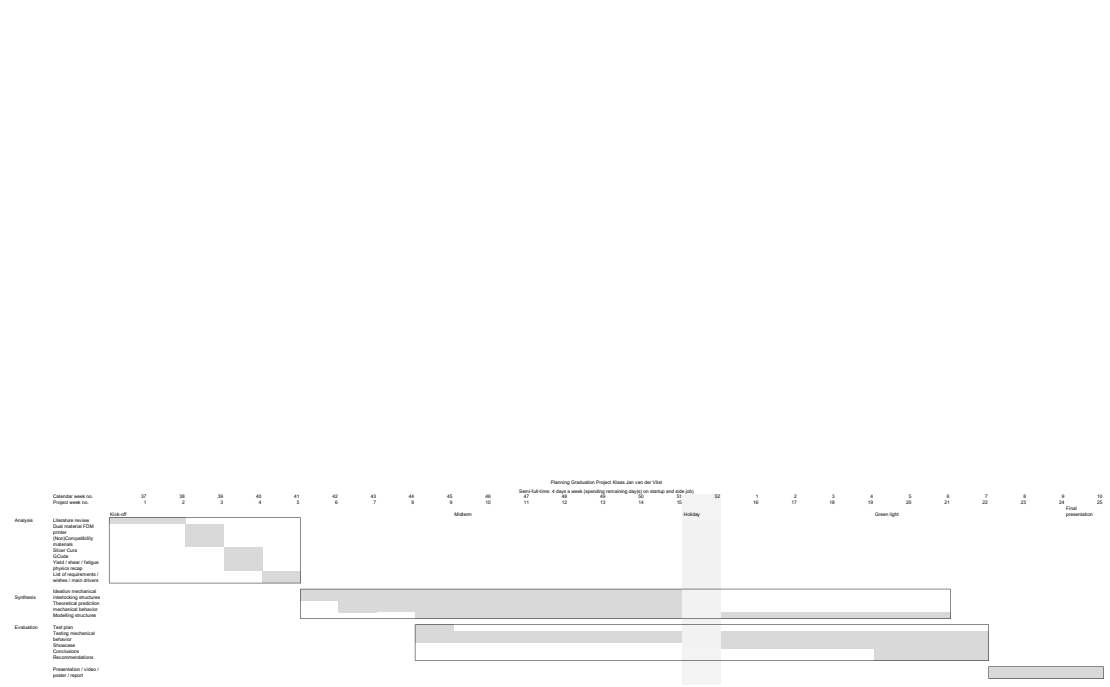
The study will deliver a show case to demonstrate the generated insights of the method.

Personal Project Brief - IDE Master Graduation

PLANNING AND APPROACH **

Include a Gantt Chart (replace the example below - more examples can be found in Manual 2) that shows the different phases of your project, deliverables you have in mind, meetings, and how you plan to spend your time. Please note that all activities should fit within the given net time of 30 EC = 20 full time weeks or 100 working days, and your planning should include a kick-off meeting, mid-term meeting, green light meeting and graduation ceremony. Illustrate your Gantt Chart by, for instance, explaining your approach, and please indicate periods of part-time activities and/or periods of not spending time on your graduation project, if any, for instance because of holidays or parallel activities.

start date 7 - 9 - 2020 12 - 3 - 2021 end date



Note: I will be spending 4 days a week on graduation. The other days will be spend on my startup company and side job. So including one week holiday the project will be taking 26 calendar weeks.

MOTIVATION AND PERSONAL AMBITIONS

Explain why you set up this project, what competences you want to prove and learn. For example: acquired competences from your MSc programme, the elective semester, extra-curricular activities (etc.) and point out the competences you have yet developed. Optionally, describe which personal learning ambitions you explicitly want to address in this project, on top of the learning objectives of the Graduation Project, such as: in depth knowledge a on specific subject, broadening your competences or experimenting with a specific tool and/or methodology, Stick to no more than five ambitions.

With this project I want to prove my competences in the field of embodiment design such as prototyping and production techniques.
 I have always been interested in the production techniques of any product. It fascinates me to see how different parts build up to a product not only by its particular function but also by its production technique. Production techniques determine how a product is made and vice versa; a desired form or function of a product pushes production techniques to change. Therefore, I enjoy this topic around 3D printing and its possibilities for functional prototyping and manufacturing.
 I have a fair amount of knowledge of the workings of an FFF 3D printer which is a necessity for starting this project. Also, I finished the bachelor Mechanical Engineering where I learned about material characteristics and material testing.
 So the main learning goal of this project is gaining in depth knowledge in FFF 3D printing and becoming an expert on dual material printing.
 As an addition I aim to broaden my set of modeling tools. So far I have always modeled with either SolidWorks, AutoCAD or Catia in which I modeled by hand. In this graduation project I would like to take the opportunity to learn about parametric modeling as well, which I will be doing with Grasshopper as a plugin of Rhinoceros.

FINAL COMMENTS

In case your project brief needs final comments, please add any information you think is relevant.